National Library of Canada
Canadian Theses Service
Ottawa, Canada
K1A 0N4

Bibliothèque nationale du Canada
Services des thèses canadiennes

CANADIAN THESES

THÈSES CANADIENNES

NOTICE

The quality of this microfiche is heavily dependent upon the quality of the original thesis submitted for microfilming. Every effort has been made to ensure the highest quality of reproduction possible.

If pages are missing, contact the university which granted the degree.

Some pages may have indistinct print especially if the original pages were typed with a poor typewriter ribbon or if the university sent us an inferior photocopy.

Previously copyrighted materials (journal articles, published tests, etc.) are not filmed.

Reproduction in full or in part of this film is governed by the Canadian Copyright Act, R.S.C. 1970, c. C-30. Please read the authorization forms which accompany this thesis.

AVIS

La qualité de cette microfiche dépend grandement de la qualité de la thèse soumise au microfilmage. Nous avons tout fait pour assurer une qualité supérieure de reproduction.

S'il manque des pages, veuillez communiquer avec l'université qui a conféré le grade.

La qualité d'impression de certaines pages peut laisser à désirer, surtout si les pages originales ont été dactylographiées à l'aide d'un ruban usé ou si l'université nous a fait parvenir une photocopie de qualité inférieure.

Les documents qui font déjà l'objet d'un droit d'auteur (articles de revue, examens publiés, etc.) ne sont pas microfilmés.

La reproduction, même partielle, de ce microfilm est soumise à la Loi canadienne sur le droit d'auteur, SRC 1970, c. C-30. Veuillez prendre connaissance des formules d'autorisation qui accompagnent cette thèse.

THIS DISSERTATION
HAS BEEN MICROFILMED
EXACTLY AS RECEIVED

LA THÈSE A ÉTÉ
MICROFILMÉE TELLE QUE
NOUS L'AVONS REÇUE

NL 339 (r. 86/01)

Canada

National Library of Canada
Bibliothèque nationale du Canada

135

Ottawa, Canada
K1A 0N4

TC –

IS 0-315-23332-X

CANADIAN THESES ON MICROFICHE SERVICE – SERVICE DES THÈSES CANADIENNES SUR MICROFICHE

PERMISION TO MICROFILM – AUTORISATION DE MICROFILMER

• Please print or type – Écrire en lettres moulées ou dactylographier

AUTHOR – AUTEUR

Full Name of Author – Nom complet de l'auteur

STEVEN CRAIG HARDING

Date of Birth – Date de naissance	Canadian Citizen – Citoyen canadien
MAY 18/1959	☒ Yes / Oui ☐ No / Non
Country of Birth – Lieu de naissance	**Permanent Address – Résidence fixe**
CANADA	636 15 AVE S.W. (APT 11) CALGARY ALTA.

THESIS – THÈSE

Title of Thesis – Titre de la thèse

SEDIMENTOLOGY OF THE SWIFT FORMATION, SOUTHEASTERN ALBERTA.

Degree for which thesis was presented Grade pour lequel cette thèse fut présentée	Year this degree conferred Année d'obtention de ce grade
MASTER OF SCIENCE	1985
University – Université	**Name of Supervisor – Nom du directeur de thèse**
UNIVERSITY OF ALBERTA	DR. FRANCIS J. HEIN

AUTHORIZATION – AUTORISATION

Permission is hereby granted to the NATIONAL LIBRARY OF CANADA to **microfilm** this thesis and to **lend** or **sell copies of the film.**

The author reserves other publication rights, and neither the thesis nor extensive extracts from it may be printed or otherwise reproduced without the author's written permission.

L'autorisation est, par la présente, accordée à la BIBLIOTHÈQUE NATIONALE DU CANADA de **microfilmer** cette thèse et de **prêter** ou de **vendre des exemplaires du film.**

L'auteur se réserve les autres droits de publication; ni la thèse ni de longs extraits de celle-ci ne doivent être imprimés ou autrement reproduits sans l'autorisation écrite de l'auteur.

ATTACH FORM TO THESIS – VEUILLEZ JOINDRE CE FORMULAIRE À LA THÈSE

Signature	Date
[signature]	October 4/1985

NL-91 (r. 84/03)

Canada

UNIVERSITY OF ALBERTA

THE SEDIMENTOLOGY OF THE SWIFT FORMATION, SOUTHEASTERN ALBERTA

BY

© STEVEN CRAIG HARDING

A THESIS

SUBMITTED TO THE FACULTY OF GRADUATE STUDIES AND RESEARCH

IN PARTIAL FULFILMENT OF THE REQUIREMENTS FOR THE DEGREE

OF MASTER OF SCIENCE

DEPARTMENT OF GEOLOGY

EDMONTON, ALBERTA

FALL 1985

THE UNIVERSITY OF ALBERTA

RELEASE FORM

NAME OF AUTHOR STEVEN CRAIG HARDING

TITLE OF THESIS SEDIMENTOLOGY OF THE SWIFT FORMATION, SOUTHEASTERN ALBERTA

DEGREE FOR WHICH THESIS WAS PRESENTED MASTER OF SCIENCE

YEAR THIS DEGREE GRANTED Fall, 1985

Permission is hereby granted to THE UNIVERSITY OF ALBERTA LIBRARY to reproduce single copies for private, scholarly or scientific research purposes only.

The author reserves other publication rights, and neither the thesis nor extensive extracts from it may be printed or otherwise reproduced without the author's written permission.

(SIGNED) .....

PERMANENT ADDRESS:

#11 636 15 AVE S.W.

CALGARY, ALBERTA

CANADA

DATED Oct. 1 1985

THE UNIVERSITY OF ALBERTA

FACULTY OF GRADUATE STUDIES AND RESEARCH

The undersigned certify that they have read, and recommend to the Faculty of Graduate Studies and Research, for acceptance, a thesis entitled "Sedimentology of the Swift Formation, Southeastern Alberta" submitted by Steven Craig Harding in partial fulfillment of the requirements for the degree of Master of Science.

Frances J. Hein

Supervisor

Date Oct. 14/85

Abstract

The uppermost Jurassic Swift Formation in southeastern Alberta can be divided into 6 lithofacies. A complete succession of facies from stratigraphic bottom to top includes: a) basal mudstone-shale facies b) lenticular to silt-streaked dark ribbon facies c) wavy-irregular dark ribbon facies d) wavy light ribbon facies e) capping silty-sandstone facies and f) an interbedded coarser grained stringer sandstone facies. The absence of individual facies in some sections may result from erosional or depositional processes.

The Swift Formation is a coarsening-upwards, shallowing-upwards sequence, deposited in an epicontinental seaway. Sediments were deposited from suspension, primarily under low energy conditions. An offshore to onshore regressive cycle is suggested by the sedimentary structures which is further supported by the transition in authigenic iron compounds and clay mineral assemblages. Paleo-shoreline reconstruction of the Oxfordian Sea, suggests that a shoreline to the north penetrated the study area during latest Oxfordian times.

Porosity and Permeability are both depositionally and diagenetically influenced. Depositional controls include the abundance of interbedded mudstone, burrow density, and coarser sandstone (Facies 6). Organic detritus within the lower facies has chemically influenced diagenesis of the Swift Formation. Diagenetic controls include solution, authigenesis and microfracturing. These features are most commonly associated with the sandstone stringers (Facies 6).

Reservoir development of the Swift Formation is dependent upon locating sand accumulations (Facies 6), which may develop on the lee side of offshore shoals.

Acknowledgments

The writer wishes to express his gratitude to his supervisor, Dr. F.J. Hein, who has assisted and encouraged the writer throughout the duration of this thesis. Her instruction and insight were invaluable to the completion of this project.

Many thanks are extended to Shell Resources in Calgary for the use of their technical facilities. Special thanks to Dr. B.J. Hayes, Dr. A. Rupp and Mr. A. Polischuk for their co-operation and assistance. Additional thanks are extended to Home Oil in Calgary for providing a technical report of interest to this study.

The writer thanks Dr. F. Longstaffe and Mrs. Diane Caire for their assisatnce in x-ray diffraction preparation and interpretation. Addition thanks to Dr. G. Pemberton for assistance with ichnofacies classification.

Thanks are also extended to Jennifer Gall and Shannon Wahler for their technical assistance is compiling this project.

Financial support for this project was provided by a National Research Council Grant to Dr. F.J. Hein, Shell Resources and the Sigma XI Research Society.

Thank-you Laurie.

TABLE OF CONTENTS

Chapter		Page
I.	Introduction	1
	A. Scope of Investigation	1
	B. Depositional Synopsis	2
II.	Facies Descriptions	8
	A. Introduction	8
	B. Facies 1	11
	C. Facies 2	13
	D. Facies 3	14
	E. Facies 4	16
	F. Facies 5	18
	G. Facies 6	19
III.	Petrography	20
	A. Introduction	20
	B. Facies 2	28
	C. Facies 3	29
	D. Facies 4	30
	E. Facies 5	31
	F. Facies 6	32
IV.	X-ray Diffraction Results	33

V. Depositional Processes..... '41
A. Introduction..... 41
B. Mudstone-Shale..... 41
C. Light and Dark Ribbon Sediments..... 43
D. Structureless Sediments..... 44
E. Stringer Sandstones..... 45

VI. Regional Analysis..... 52

VII. Facies Model..... 71

VIII. Depositional Controls on Porosity and Permeability..... 82

IX. Diagenetic Processes in the Swift Formation..... 119
A. Introduction..... 119
B. Clay Minerals..... 120
C. Quartz..... 122

X. Diagenetic Controls or Porosity and Permeability..... 124

XI. Interpretations and Conclusions..... 127

XII. Plates..... 129

XIII. References..... 155

XIV. Appendix..... 168

List of Tables

Tables		Page
1	Swift mineralogy.....	24
2	Petrographic characteristics.....	25
3	Swift clay mineralogy.....	35
4	Kaolinite/Illite ratios.....	36

List of Figures

Figure		Page
1	Lithostratigraphic nomenclature	4
2	Structural elements	6
3	Representative section (Swift Formation)	9
4	Ternary diagram	22
5	Grain size distribution	26
6	X-ray diffractograms (Facies 2 to 5)	37
7	X-ray diffractograms (Facies 6)	39
8	Density current mechanism	48
9	Current velocity profiles	50
10	Swift Formation Isopach	53
11	Facies 2 & 3 Isopach (pre-erosional)	55
12	Facies 4 Isopach (pre-erosional)	57
13	Facies 5 Isopach (pre-erosional)	59
14	Detailed Facies 2 & 3 Isopach	63
15	Detailed Facies 4 Isopach	65
16	Detailed Facies 5 Isopach	67
17	Facies 6 accumulation, Section 29	69
18	Middle Oxfordian Paleography	78
19	Late Oxfordian Paleography	80
20	Grain size distribution - Chondrites without Facies 6 access	86
21	Grain size distribution - Chondrites with Facies 6 access	88

Figure		Page
22	Macroscopic factors vs Por./Perm. (6-29-5-5W4).....	93
23	Macroscopic factors vs Por./Perm. (16-21-5-5W4).....	95
24	Macroscopic factors vs Por./Perm. (16-29-5-5W4).....	97
25	Macroscopic factors vs Por./Perm. (6-28-5-5W4).....	99
26	Macroscopic variables vs Por./Perm. Crossplots...	101
27	Macroscopic variables vs Por. (6-29-5-5W4).....	103
28	Macroscopic variables vs Perm. (6-29-5-5W4).....	105
29	Macroscopic variables vs Por. (16-21-5-5W4).....	107
30	Macroscopic variables vs Perm. (16-21-5-5W4).....	109
31	Macroscopic variables vs Por. (16-29-5-5W4).....	111
32	Macroscopic variables vs Perm. (16-29-5-5W4).....	113
33	Macroscopic variables vs Por. (6-28-5-5W4).....	115
34	Macroscopic variables vs Perm. (6-28-5-5W4).....	117

1. Introduction

A. Scope of Investigation

The Manyberries oil field is located in southeastern Alberta, approximately 65 km south of Medicine Hat. This study deals with the sedimentology of the Swift Formation, the uppermost component of the Upper Jurassic Ellis Group. The region of study extending from Townships 1-10 to Ranges 1-16, encompasses the Manyberries Field in Townships 4-5 to Ranges 4-5W4M. Thirty-two wells have been logged in detail from this area, representing most of the available core of the Swift Formation. Most stratigraphic sections were described using slabbed 3.5 inch (9 centimetre) exploration core. A few wireline cores were also logged.

A variety of marine environments, from estuarine to offshore shelf, have been interpreted to describe the depositional setting for the Swift sediment any rocks in this study area (Reimer, 1982). Post-Swift erosion which has removed the Swift lithologies has further obscured the stratigraphic record (Hayes, 1983). The purpose of this study is threefold: (1) to develop a workable facies model for the Swift Formation; (2) to ascertain the relationships between the reservoir properties (porosity, permeability) and the facies distribution; (3) to determine the diagenetic history of the Swift deposits and the influence of diagenesis on the reservoir properties. This investigation deals with the interlaminated-interbedded sandstones, siltstones and mudstones, commonly called the "ribbon sands" of the Swift Formation. Because of the complex sediment relationships involved and the often near absence of sandstone, these sediments will be called the "ribbon sediment" in this thesis.

B. Depositional Synopsis - Upper Jurassic to Lower Cretaceous

Various workers have discussed the stratigraphy of the Upper Jurassic and Lower Cretaceous of Southern Alberta (Cobban, 1945; Weir, 1949; Glaister, 1959; Pocock, 1962; 1970; Brenner and Davies, 1974; Herbaly, 1974; Hayes, 1982). The lithostratigraphic nomenclature used in this project will be that of Hayes (1982), modified from Cobban (1945)(Figure 1). The region of study lies to the east of the north-south trending Sweetgrass Arch, locally in Alberta referred to as the Bow Island Arch (Herbaly, 1974). The strata dip eastward across the study area towards the Williston Basin, which lies further to the east (Christopher, 1980)(Figure 2).

During the Middle Jurassic, marine sedimentation resumed after a substantial period of erosion (Imlay, 1957; Peterson, 1972). To the west of the Bow Island Arch, outside of the study area, the Sawtooth Formation (the lowermost component of the Ellis Group) was deposited in a shallow epicontinental sea. To the east of the Bow Island Arch, the Shaunavon Formation (within the study area) was laid down under shallow marine conditions, unconformably overlying Mississippian strata. The Shaunavon has not traditionally been classified as a component of the Ellis Group, yet represents the stratigraphic equivalent of the Sawtooth Formation.

During further advancement of the broad shallow sea in early Callovian times, the shaly, calcareous Rierdon Formation was deposited. Deposition continued until the Late Callovian, when a slight regression of the sea resulted in a period of exposure and regional erosion. Renewed subsidence characterised early Oxfordian times, during which the transgressive basal shale member of the Swift Formation was deposited.

The interbedded sandy-siltstones and mudstones of the ribbon sediment resulted from a progressive shallowing of the sea as the shoreline advanced seaward. By the end of the Oxfordian, subaerial exposure dominated the midwest of North America, a condition which would prevail until Aptian time in southeastern Alberta. Within this time frame, intense erosion took place, with deep incision of the Jurassic strata.

The Morrison Formation lies unconformably on the Swift Formation in Montana, as noted by Cobban (1945). This continental deposit appears to represent uppermost Jurassic sedimentation (Peterson, 1980). Its presence in southeastern Alberta has not been observed and, therefore, it will not be discussed here.

Accumulation of the Blairmore Group began in Early Cretaceous Aptian time, commencing with deposition of the coarse, fluvial Cut Bank Formation, unconformably overlying the Swift Formation. These sediments were only deposited west of the Bow Island Arch and are not found in the study area. Prevailing fluvial conditions produced a second, more widespread continental deposit, the Gladstone Formation, characterised by finer-grained channel, floodplain and lacustrine sediments (Christopher 1974), which unconformably overlie the Swift Formation in southeastern Alberta. The Beaver Mines Formation, a continental sandstone of Albian age, caps the sequence, concluding Blairmore sedimentation.

Figure 1: Lithostratigraphic nomenclature in southern Alberta and northern Montana. (Modified from Hayes, 1982).

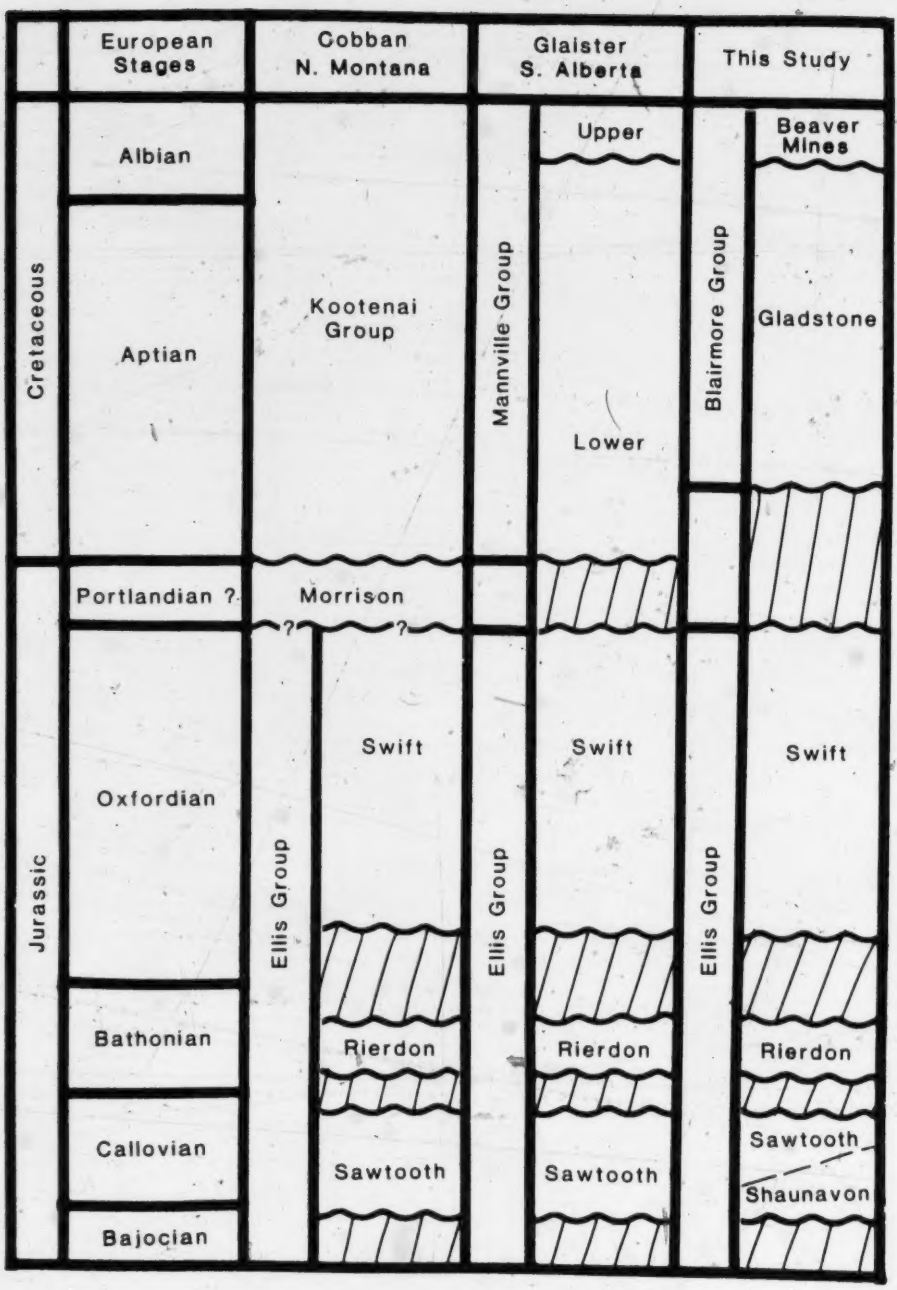
European Stages
Cobban N. Montana
Glaister S. Alberta
This Study
Cretaceous
Albian
Aptian
Kootenai Group
Mannville Group
Upper
Lower
Blairmore Group
Beaver Mines
Gladstone
Jurassic
Portlandian ?
Morrison
Oxfordian
Ellis Group
Swift
Rierdon
Sawtooth
Bathonian
Callovian
Bajocian
Shaunavon

Figure 2: Structural elements influencing the study area (boxed).

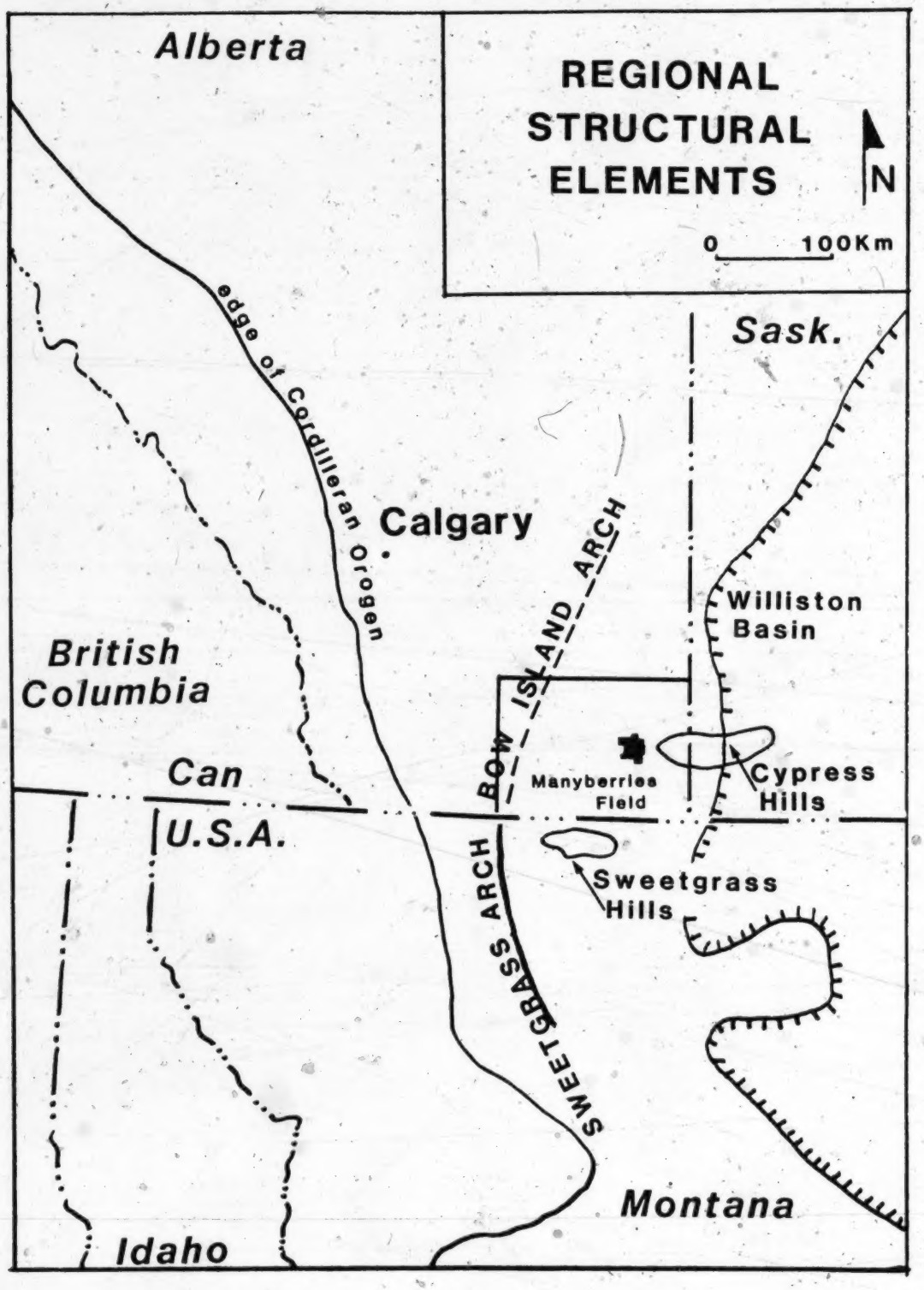

FIGURE 2 Structural elements influencing the study area (boxed).

II. Facies Descriptions

A. Introduction

After careful examination of the available core of the Swift Formation, it became apparent that six representative facies could successfully describe the entire sequence (Figure 3). Facies were primarily subdivided on the basis of lithology and sedimentary structures (including bioturbation). Careful note was taken of the iron compounds present in the sediments (siderite, pyrite and glauconite), as well as presence and abundance of organic detritus. These divisions were chosen strictly for descriptive purposes and bear no relation to any pre-existing stratigraphic subdivisions. The facies described below are listed in ascending stratigraphic order, throughout the study region. The uniformity in superposition of individual lithofacies allows this approach to be consistent throughout the region.

Figure 3: Representative section of the Swift Formation - well 14-5-6-5W4M

a. Relative sediment percentages determined from core
b. Sedimentary structures within facies
c. Resistivity log response in Ohm-metres

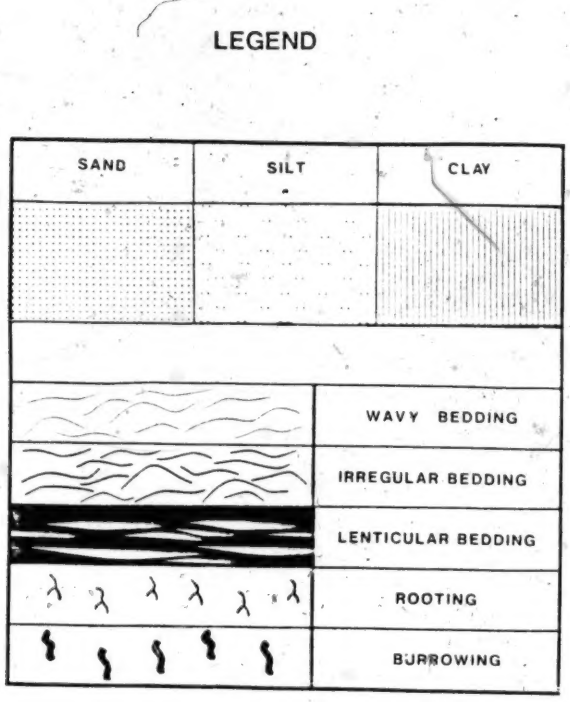

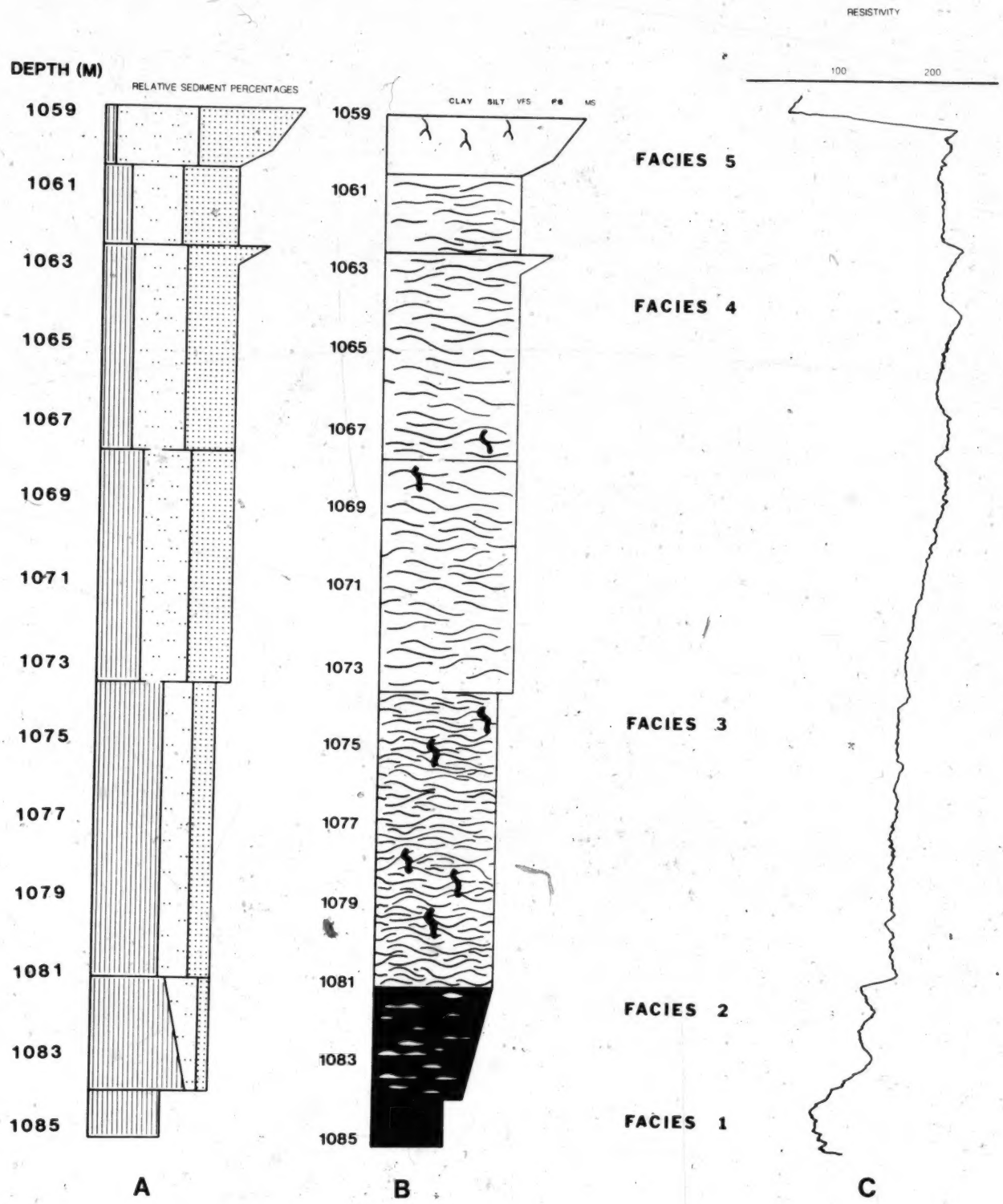
DEPTH (M)
RELATIVE SEDIMENT PERCENTAGES
1059
1061
1063
1065
1067
1069
1071
1073
1075
1077
1079
1081
1083
1085
A
CLAY SILT VFS FS MS
1059
1061
1063
1065
1067
1069
1071
1073
1075
1077
1079
1081
1083
1085
B
FACIES 5
FACIES 4
FACIES 3
FACIES 2
FACIES 1
RESISTIVITY
100
200
C

B. Facies 1

Mudstone-Shale Facies

The lowermost facies of the Swift Formation consists of friable mudstones and splintery shales. This facies was elevated to member status (Shale Member) by Cobban (1945) from outcrop work in Montana. Hayes (1982) recognized the lithological continuity of the shales northwards through Montana and into southeastern Alberta (including this study area).

The facies is primarily structureless mudstone and shale, with a minor silt component, occurring as lenses or as individual grains dispersed within the finer-grained mudstone and shale. The silt fraction seldom exceeds .025 mm in diameter. Detrital carbonaceous fragments are a common matrix accessory. Small silt to sand size glauconitic particles are commonly disseminated throughout this lithology; less commonly glauconite is concentrated in thin laminations. Nodular authigenic pyrite occurs sporadically.

The basal contact of Facies 1 is often poorly represented in cores from the study area, due either to lack of coring or poor core recovery. At the type locality (Montana, NE 1/4, Section 27, Twp 28N, Rge. 10W) a basal chert-belemnite conglomerate disconformably overlies shales of the Rierdon Formation. In southeastern Alberta this conglomeratic contact is preserved solely in the McColl-Frontenac Union 9A-22-3-8W4 well at 704.3 metres (2290 feet). The disconformable contact with the underlying Rierdon Formation would appear to prevail as indicated by an abrupt kick in the resistivity, gamma and

sonic logs (Hayes, 1982). Regionally this "Rierdon Shoulder" is not always consistent with the basal Swift contact (Peterson, 1957). In the study region, however, it appears to be a useful marker.

The upper contact of the Mudstone-Shale Facies appears to be somewhat less uniform. In outcrop, at the type section, a second chert-belemnite conglomerate occurs at the upper contact of the Swift shale (Facies 1). However, this was not observed in cores examined in this study. In core, the contact may be sharp or less commonly gradational into the overlying ribbon sediments (Facies 2 or 3). Rarely, the light ribbon sediments (Facies 4) sharply overlie the massive shale (Facies 1).

C. Facies 2

Lenticular - Silt-streaked Dark Ribbon Sediments

The lenticular - silt-streaked shale (Facies 2) of the dark ribbon sediments is characterised by silty, millimetre-to centimetre-thick intercalations within a shaly mudstone (Plate 1). The silt fraction seldom exceeds 15% of the total sediment mass, with this facies dominated by a dark, cohesive mudstone, rich in organic matter. Laminated sediments range from mudstone to siltstone. Silt laminae commonly display single to double grain thicknesses, but may extend up to 1.4 centimetres thick. Laminations are sub-parallel; rarely they occur as unidirectional low-angle cross-stratified beds, with mud and organic drapes.

Silt bands are lenticular and may be isolated into pod-like discs within the mudstone. Minor soft sediment deformation on a centimetre scale was observed in some cores. Burrowing is observed throughout the facies, although the burrow density is commonly low.

Glauconite is dispersed throughout the facies and is commonly concentrated as burrow infill. Pyrite is frequently observed, typically as nodules ranging between 1-8 centimeters in diameter.

The upper contact of Facies 2 is gradational with the overlying irregularly to wavy bedded dark ribbon sediments of Facies 3. In some cores Facies 2 interfingers with Facies 3 in zones up to 40 centimetres thick.

D. Facies 3

Wavy-Irregular Dark Ribbon Sediments

This facies consists of interlaminated sandy-siltstone and organic-rich mudstone (Plate 2). The coarser layers are generally composed of coarse grained silt-size material, but may contain an admixture of silt and very fine sand-sized grains. Facies 3 is generally of sublitharenite composition. The percent of interbeds of detrital clays and organic matter decrease upsection, while the sandy-siltstones become thicker and more continuous towards the top of the unit. Thickness of the coarser interbeds is not constant, with laminae ranging from less than 0.1 cm to 1.8 cm in thickness and pinch-outs commonly occurring across the width of a core (9 centimetres). In most cores examined, a slight coarsening-upwards sequence is detected within this facies, as well as a decrease in the proportion of detrital clay upsection.

Glauconite persists as the major iron-bearing mineral constituent, commonly associated with burrow infill; less commonly concentrated as thin laminae within the silts. These glauconite particles are the alteration product of an illitic precursor, which became iron and potassium enriched at or below the sediment-water interface. Pyrite is abundant, occurring as microcrystalline aggregates and nodules.

Sedimentary structures are more complex in this facies and are not necessarily consistent regionally or even within an individual core. Much of this reflects grain size variation. Bedding tends to be irregular, although it may become wavy or cross-stratified. Burrow density varies considerably throughout the facies. A complete spectrum is found to exist between total

bioturbation and an absence of burrows (Plate 2). Burrow structures are dominated by branching, meandering Chondrites. Additional burrow structures present within Facies 3 include Skolithos, Planolites, Paleophycos, Teichichnus, and possibly Asterosoma. Burrows typically penetrate and interconnect the sandy-siltstone laminae, giving the lithology a very mottled appearance.

Reactivation surfaces are found within this facies and commonly exhibit easily identifiable characteristics. The first type of reactivation surface is characterised by a break in sedimentation, apparently induced by a period of non-deposition. Frequently a slight colour change occurs across the boundary, with darker muds typifying the upper contact. Intense bioturbation may also be seen in the region 2-5 cm below the reactivation surface. Nodular pyrite is also commonly observed just below the reactivation boundary within the bioturbated sediments. These features associated with the reactivation surfaces are best observed in core from the 15-12-5-5W4 well, between 1119 m and 1124 m. A second type of reactivation surface is produced by change in the apparent depositional direction. In a few cores apparent bidirectionality occurs in the low-angle cross-stratified sandstones. This is best observed in the 6-2-4-7W4 well at 892.3 m, but may also be found in the 10-34-2-7W4 well (927 m) and the 9-22-3-8W4 well (879 m).

These dark interlaminated sediments are overlain by the more oxidized, organic-poor, light ribbon sediments (Facies 4). The contact is gradational, marked by a progressive loss of organic matter in the mud laminae, as indicated by a lighter colouration in the sediments upsection.

E. Facies 4

Light Ribbon Sediments

The light ribbon sediments of Facies 4 are very comparable to the underlying dark ribbon sediments, but differ by the absence of organic matter within the mud laminae, which are now very light grey (Plate 3). Lamination thicknesses are slightly greater (Range 0.1 cm to 2.4 cm), and the facies contains a greater proportion of silt and sand.

Glauconite occurs throughout most of the facies, but decreases upsection and disappears near the top. Pyrite no longer appears to be a stable authigenic iron compound, as it was observed only rarely near the basal contact of the facies. Siderite, appears midway upsection within the light ribbon sediments occurring as small spherulites which are dispersed or preferentially concentrated in the sandy laminae. These small concretions increase both in size and number towards the upper contact. In some cores siderite becomes radially spherulitic towards the top of the facies.

The light ribbon sediment is irregular to wavy bedded, generally becoming more wavy towards the upper contact. Small scale cross-bedding is slightly more frequent in this facies, relative to Facies 3. Flaser bedding rarely occurs. Minor soft-sediment deformation has been recorded in Facies 4 of some cores, as well as a few scour-and-fill structures. Burrow density is generally lower in the light ribbon sediments than in Facies 3, although local bioturbation zones do exist.

A variety of contacts are observed at the top of this facies. The greatest difficulty in the interpretation of the upper contact occurs where post-Swift erosion has taken place. Fluvial processes have created pre-Gladstone topography, resulting in removal of significant proportions of the Swift Formation. The upper facies are greatly affected, with the frequent loss of this original depositional contact. A second complication stems from variation in the uppermost facies. Regional differences in the depositional environment results in lithological contact differences. A gradational contact seems to represent the general case. The gradational interval, however, ranges in thickness from a few centimetres to greater than 2 metres.

F. Facies 5

Massive Silty Sandstone

The uppermost facies of the section is predominantly a massive unit, displaying a range in lithology from siltstone to medium-grained sandstone. Bimodal lithologies of silty sandstones are most commonly observed, with the constituent sands in the medium-sand grain size (Plate 4). This facies is the most difficult to distinguish within the Swift Formation, because of its resemblance to the overlying Gladstone Formation. The gradational contact with the underlying light ribbon sediment is often necessary for accurate identification, as the basal Gladstone contact is erosional. Detrital clays vary in abundance from core to core. The unit generally coarsens upsection, but local fining-upward sequences occur.

Glauconite was not observed in Facies 5. Siderite occurs as disseminated spherulites, which diminish in abundance upsection. Carbonaceous detritus is uncommon in these sediments.

Carbonized rootlets are visible in several cores, but this is not diagnostic of this facies. Minor soft sediment deformation occurs in the siltier cores, but is only locally a typical structure. In two cores 6-28-5-5W4 and 5-14-5-5W4 possibly altered rootlets containing clay and calcium carbonate were found towards the middle of the unit. Clay intraclasts occur within this lithology, particularly near the basal contact.

The upper contact of the silty-sandstones is erosional, and the facies is commonly absent, owing to the post-Swift fluvial erosion and the fact that the depositional thickness of the sediment was originally quite thin.

G. Facies 6

Stringer Sandstone

Facies 6 consists of stringer-like medium grained sandstones which interfinger at irregular intervals into the Swift ribbon sediments (Facies 2,3 and 4). This facies does not occur stratigraphically above Facies 5, but is listed last because of its interfacies relationship with the ribbon sediments. The reservoir quality of the Swift Formation, as will be shown later, is largely dependent upon the occurrence of this facies. The sandstone lenses vary in thickness from a few millimetres to greater than a metre (average thickness of 1.8 cm). The basal contacts of the coarser ribbon sandstones are commonly loaded into the ribbon sediments (Plate 5A).

Pyrite is not as common in this facies, as compared with Facies 3. It occurs in nodular form solely in those stringer sandstones which occur within the dark ribbon sediments (Facies 2 and 3). Glauconite is disseminated throughout the lithology or concentrated in burrows.

These stringer-sandstones are commonly massive and occasionally graded. Less commonly, the thicker units have low-angle cross-stratification. Burrowing is frequently associated with this facies resulting in much of the sand-size component being redistributed by organisms into the underlying and overlying sediments. Possible biogenic escape structures were also observed in some cores.

III Petrography

A. Introduction

Thirty-six thin sections, representing the various facies of the Swift Formation were examined petrographically and 13 samples were studied with the scanning electron microscope. All specimens from which thin sections were cut were impregnated with a blue epoxy-plastic to enhance recognition of the pore spaces within the lithologies. Staining for potassium feldspar was done in several samples.

All particles were classified by the phi grade scale introduced by Krumbein (1934). Determination of particle size by thin section techniques may inaccurately depict the distribution of the grain population (Blatt et al., 1980). In a randomly oriented section, the largest grains of the population are most likely to be cut. Additionally, a preferred grain orientation may bias against the maximum grain size, if the largest grain axes are not in the plane of the section. Since only the maximum grain size observed will correspond to the true size of the parent population (Blatt et al., 1980), the longest axis was measured on point counted particles.

Sorting coefficients were assessed using the graphical methods of Inman (1952). Sediment roundness was determined by visual comparison of grains with the Powers (1953) standard images. Using the classification scheme of Dapples (1972), particle framework and matrix associations were interpreted for individual facies. Mineral percentages were assessed using a grain counting method along incremented traverses across various thin sections. All thin

section counts exceeded 400 grains (Figure 4; Table 1). Textural and diagenetic interpretations of SEM images was based on the work of Dapples (1972), Hayes (1979), Schmidt and McDonald (1979) and Pittman (1979)(Table 2).

Figure 4: Ternary diagram of framework constituents for Swift Formation Facies 2 to 6 Folk (1968).

Fields: a. Quartz arenite

b. Subarkosic arenite

c. Sublithic arenite

d. Arkose

e. Lithic arkose

f. Feldspathic lithic arenite

g. Lithic arenite

(Individual points were produced from grain counts in excess of 100 grains. Four cores were examined.)

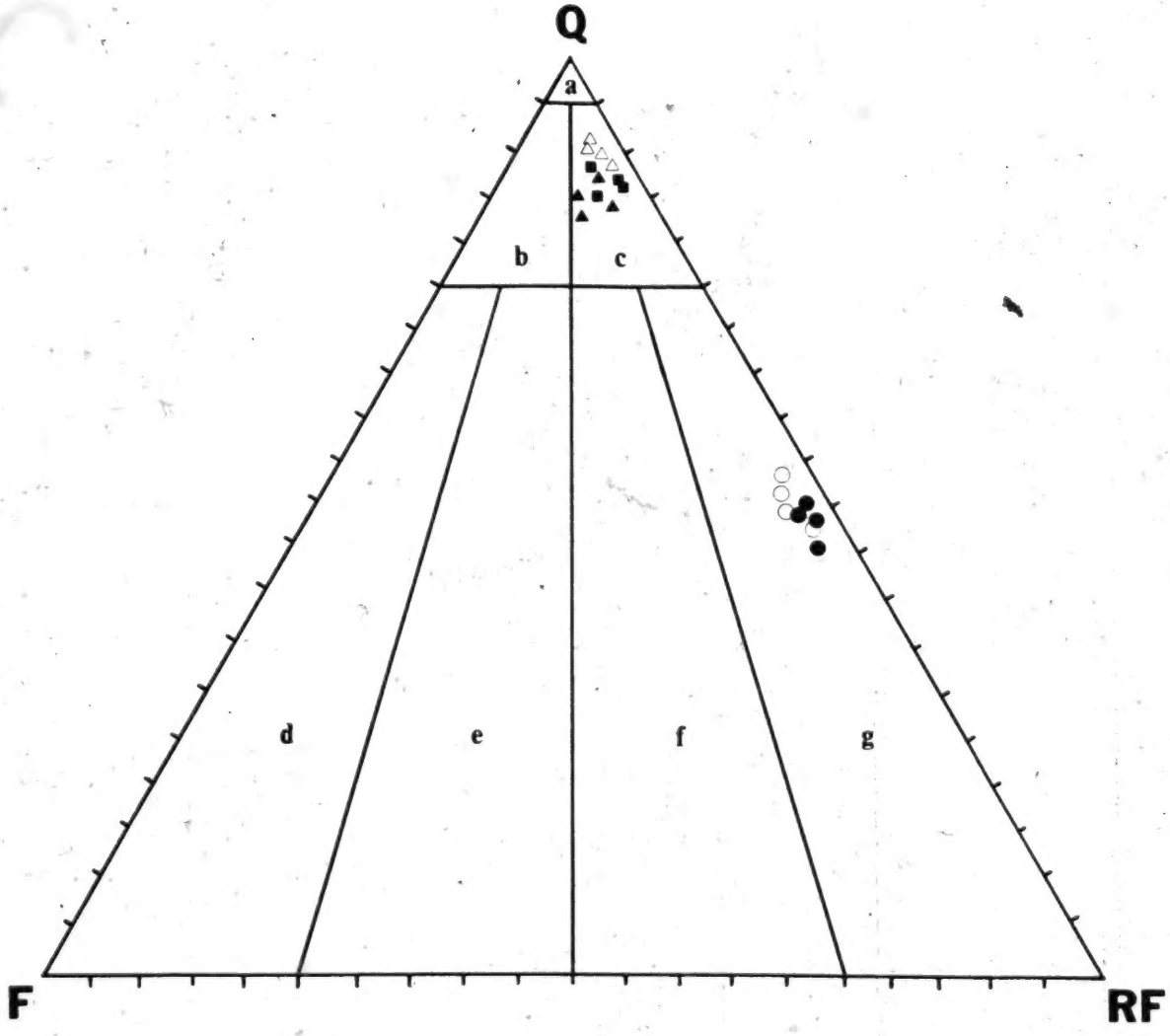
Q
a
b
c
d
e
f
g
F
RF

TABLE 1

MINERAL	FACIES				
	2	3	4	5	6
QUARTZ	55-60	60-70	70-75	40-50	40-45
ORTHOCLASE	4-7	6	5	1	1-3
PLAGIOCLASE	1	2	1	1	0-1
ROCK FRAGMENTS (CHERT)	3-5	3-7	4-7	35-45	40-45
BIOTITE	3-8	4-7	2-4	TRACE	0-2
MUSCOVITE	7-12	4-7	3-7	TRACE	1-2
SIDERITE	-	0-5	0-15	0-10	-
GLAUCONITE	3-7	2-5	0-5	-	0-7
PYRITE	3-5	4-5	-	-	0-5
ACCESSORIES	1	1	1	1	1

*NOTED ACCESSORY MINERALS INCLUDE: HORNBLENDE, ZIRCON, APATITE, CALCITE, DOLOMITE, BARITE AND EPIDOTE.

Percentages for each facies were determined from grain counts exceeding 400 grains (4 to 6 thin sections/facies)

TABLE 2

FACIES	FRAMEWORK CLASS	GRAIN SIZE (mm)	ROUNDNESS	CEMENT*
2	SUBLITHAR.	.035	SUBROUNDED	K/I/S/H
-	-	-	-	-
3	SUBLITHAR.	.07	SUBROUNDED	K/I/H/S
-	-	-	-	-
4	SUBLITHAR.	.081	SRND.-SANG.	K/H/I
-	-	-	-	-
5	LITHAR.	.235	SUBANGULAR	K/H/S
-	-	-	-	-
6	LITHAR.	.24	SUBANGULAR	K/I/H/S

*CEMENTS: K - KAOLINITE
I - ILLITE
S - SMECTITE
H - HEMATITE

LISTED IN DECREASING ORDER OR IMPORTANCE

Figure 5: Grain size distribution for Swift Formation Facies 2 to 6 (framework constituents). Histograms for each facies were derived from 4 to 5 thin sections (grain counts in excess of 400 grains/thin section).

a)

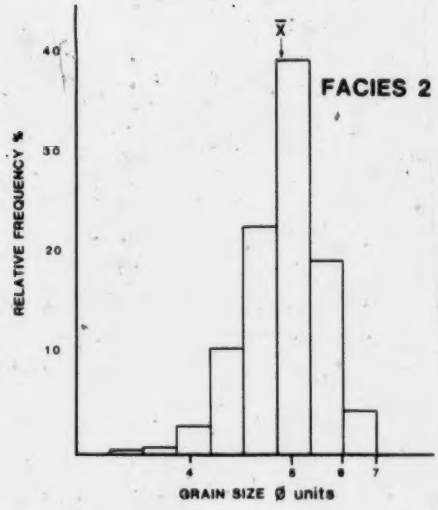
FACIES 2
RELATIVE FREQUENCY %
40
30
20
10
4
5
6
7
GRAIN SIZE Ø units

b)

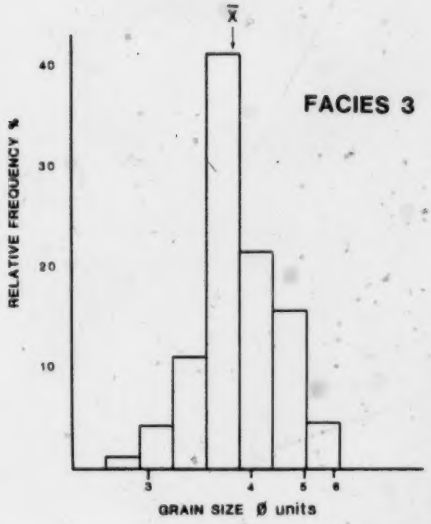
FACIES 3
RELATIVE FREQUENCY %
40
30
20
10
3
4
5
6
GRAIN SIZE Ø units

c)

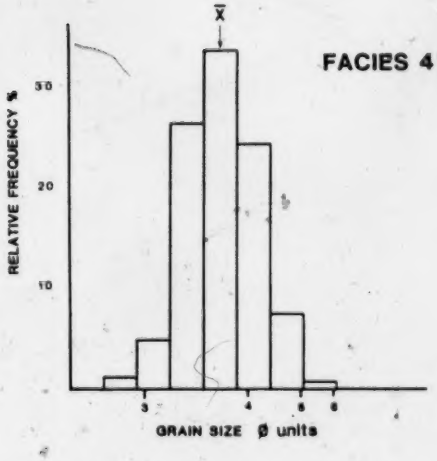
FACIES 4
RELATIVE FREQUENCY %
30
20
10
3
4
5
6
GRAIN SIZE Ø units

d)

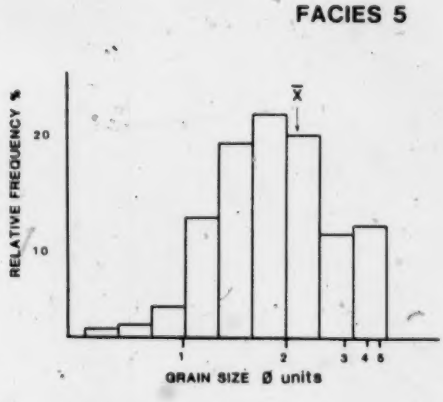
FACIES 5
RELATIVE FREQUENCY %
20
10
1
2
3
4
5
GRAIN SIZE Ø units

e)

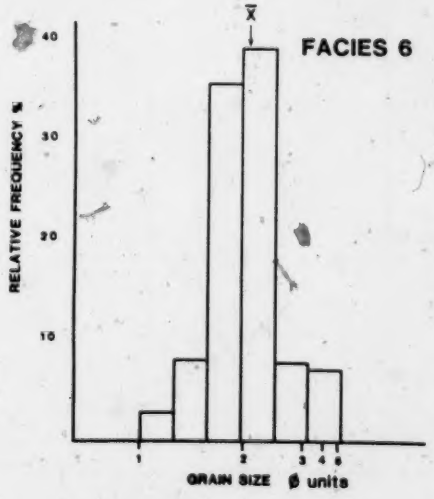
FACIES 6
RELATIVE FREQUENCY %
40
30
20
10
1
2
3
4
5
GRAIN SIZE Ø units

B. Facies 2

The lenticular silt-streaked shales of Facies 2 are composed of laterally discontinuous siltstone laminae enclosed in dark organic-rich mudstone (Figure 5). The framework constituents of this facies are dominated by quartz, which ranges from 55 to 50 percent of the silt fraction. Phyllosilicate minerals, particularly muscovite, are most abundant in this facies, many of which show alteration. Hematite coatings are commonly present on biotite. Grain orientation is most notable for these platy minerals, with orientation parallel with bedding planes.

Orthoclase feldspar is commonly observed, with only minor amounts of plagioclase present. Scanning electron microscopy reveals extensive etching and secondary solution of much of the potassium feldspar. Mosaic solution patterns are commonly observed, controlled by crystallographic constrictions (Heald and Larese, 1973). Solution in some cases was so intense that only fragmented outlines of grains are preserved.

Identification of chert fragments is often complicated by the fine grain size of the framework constituents and diagenetic alteration. Glauconite occurs throughout the sediments of this facies in varying proportions and particle sizes. Glauconite particles are commonly elliptical and slightly larger than the framework constituents (0.12 - 0.22 mm). This component is often associated with burrow fill (Plate 8A). Additional accessories include hornblende, apatite, zircon, calcite and siderite.

C. Facies 3

The dark ribbon sediments of Facies 3 have an increase in average grain size and a decrease in mud content relative to Facies 2 (Plate 6A; Figure 5), although a rhythmic interbedding of coarse and fine layers, similar to Facies 2, is maintained.

Monocrystalline quartz is the dominant framework component, with its percentage varying between 60 to 70 percent. A variety of solution textures are seen with the scanning electron microscope. Etching and pitting occur on quartz surfaces with pore access. Close examination of pitted surfaces generally reveals a preferred orientation for solution scours, reflecting the orientation of cleavage planes (Subramanian, 1975). Quartz grains also have minor overgrowth development, with most of the grains lacking typical quartz crystal morphology.

The major supplementary minerals are similar to those of Facies 2, occurring in comparable percentages (Table 1). Partial solution of orthoclase feldspar also occurs with several spectacular examples illustrating crystallographic control on secondary texture (Plate 16). Hematite coatings on biotite also appears to prevail throughout the facies.

Pyrite is the most abundant iron compound in these dark ribbon sediments. As with Facies 2, this component occurs randomly in nodular form and may also be found dispersed within the argillaceous laminae. In thin section this amorphous-microcrystalline phase is often observed engulfing detrital grains. Accessories similar to those found in Facies 2 are also observed. Apatite, zircon, calcite and siderite are present with the additional occurrence of dolomite and barite, established by X-ray diffraction bulk analysis (Reimer, 1982; Home Oil).

D. Facies 4

As indicated by its light colour, the more highly oxidized light ribbon sediment displays a much cleaner petrographic appearance (Plate 6B). This primarily reflects the near absence of organic detritus and a slightly varied clay mineralogy. The rhythmic interlamination of mudstones and quartz-rich sediment continues in this facies, with a minor increase in the mean detrital grain size (Figure 5). The coarser sediment within the laminae are fine-skewed, very fine-grained sandstones. The mudstone laminae, enriched in silt-sized particles, may be classified as a "wacke" framework (Dapples, 1972).

The framework mineralogy is dominated by quartz. Although this constituent has increased in abundance only marginally from the dark ribbon sediments (now representing 70 to 75 percent of the siltstone and sandstone) it now appears more dominant because of the absence of organic constituents. Quartz overgrowths on grain boundaries are more common and generally display better crystal development than in Facies 2 or 3. Surface solution is a common feature associated with the quartz surfaces, most readily observed on diagenetic overgrowths. This agrees with Dapples (1959) claim that quartz solution will take place after major overgrowth development.

The mineralogy of the additional framework constituents is similar to the previously discussed facies, displaying comparable phases and phase abundances (Table 1). Glauconite is a persistent mineral within most of the light ribbon sediment (range 0 to 5 percent of the mineral components), but tends to decrease upsection disappearing towards the top of this facies. Although siderite may be observed within the dark ribbon sediments, this mineral is characteristically associated with the upper portion of the light ribbon sediment.

Siderite concretions range in size from 0.1 mm to 1.8 mm, with mineral diameters generally increasing towards the upper contact of the facies. In many cores, the siderite in the uppermost portion of the facies is radially spherulitic (Plate 7A). These concretions typically engulf primary framework constituents, but may also be observed "pushing" adjacent grains aside, suggesting in situ development. Thin iron oxide halos may be observed around the concretions.

E. Facies 5

The uppermost facies of the Swift Formation is very different petrographically than the underlying ribbon sediments. Grain-size distributions of framework constituents are less consistent, with sediment sizes varying between very fine siltstone and medium-grained sandstone (Figure 5).

The mineralogy of this facies is dominated almost entirely by detrital quartz grains and chert fragments. The framework quartz is quite diverse in terms of crystallinity ranging from monocrystalline to polycrystalline, with a complete spectrum between these two end-members. The majority of detrital chert fragments display a typical microcrystalline quartz fabric. Some chert fragments are composed of a combination of microquartz and megaquartz in mosaic patterns. Rarely the chert fragments exhibit a variety of fibrous chalcedonic textures. Argillaceous rock fragments also occur, but they

represent only a small percentage (less than one percent) of the framework components. Authigenic siderite is commonly present near the base of Facies 5.

F. Facies 6

The coarser stringer sands of Facies 6, are well sorted, highly porous sediments (Plates 11A, B and C). They are not enriched in organic material, yet do contain fragments of carbonaceous matter, particularly when these stringers occur amidst Facies 2 or 3 (Plate 7B). The sandstones are predominantly clay cemented, but appear to have been cemented earlier by calcium carbonate which has since undergone secondary solution. This earlier cement is indicated by the occurrence of interstitial calcite, encased in sealed pores.

The compostion of the framework constituents is similar with that of Facies 5, with only minor exceptions (Table 1). Chert fragments and quartz grains are the dominant constituents, with textural and crystalline variety similar to the uppermost Facies 5. Quartz overgrowths are most common in this facies, displaying the best crystal morphology (Plate 12). Minor framework constituents include orthoclase, plagioclase, muscovite, biotite, glauconite and pyrite.

IV X-ray Diffraction Results

X-ray diffraction analyses of the clay minerals (less than 2um fraction) were performed on the major facies within the Swift Formation (with the exception of Facies 1). Shale from the lowermost lithology (Facies 1) was not available for analyses. Samples were taken from the most clay-rich zones within individual facies (i.e. shale laminae). Clay analyses were performed on the Shell 14-5-6-5W4 well, because it best represented a typical succession of lithofacies. Mineral identification was based on diffractograms produced from Ca-and K-saturated samples and auxillary X-ray scans of Ca-saturated glycol clay samples and heated K-saturated samples. Samples were irradiated with CoK radiation, which is typically used for identifying iron-rich minerals. Cok radiation is most effective in clay mineral identification due to greater resolution at low angles (F.J. Longstaffe, pers. comm.; Ignasiak et al., 1983). The results of these procedures are listed in Table 3 and the glycolated charts are presented in Figures 6 and 7.

The clay mineralogy varies systematically from stratigraphic bottom to top. The lowermost ribbon sediment facies contains the greatest relative percentage of illite as well as smectite (Table 4). Both components decrease volumetrically upsection, with the disappearance of smectite in the light ribbon sediment and the loss of illite in the uppermost Facies 5. Correspondingly, kaolinite systematically increases upsection, becoming overwhelmingly dominant within the upper facies (Table 4). A mixed-layer illite/smectite prevails throughout much of the ribbon sediment, also decreasing in abundance from bottom to top. This constituent is best

developed in the porous stringer facies within the lower dark ribbon sediments (Facies 2 & 3). Quartz is present throughout all of the facies and minor chlorite is observed within the lowermost ribbon sediments (Facies 2).

TABLE 3

FACIES	KAOL	ILL	IN	SM	QTZ
2	+	+	+	+	+
3	+	+	+	+	+
4	+	+	-	-	+
5	+	-	-	+	+
6	+	+	+	+	+

*PRESENT (+)

NOT PRESENT (-)

KAOL - KAOLINITE

ILL - ILLITE

IN - MIXED - LAYER ILLITE/SMELTITE

SM - SMELTITE

QTZ - QUARTZ

TABLE 4

FACIES	ILLITE PEAK INTENSITY	KAOLINITE PEAK INTENSITY	RATIO K/ILL
2	440	1500	3.41
3	380	3280	8.63
4	360	6500	17.1
5	0	5900	0.00
6	250	4200	16.8

Figure 6: X-ray diffractograms (Ca-saturated glycol) for Facies 2 to 5, listed in ascending order from stratigraphic bottom to top.

SM - SMECTITE

IN - MIXED - LAYER ILLITE/SMECTITE

IL - ILLITE

K - KAOLINITE

Q - QUARTZ

FACIES 5

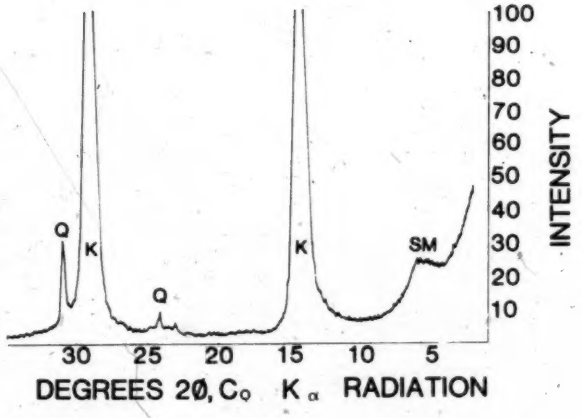

FACIES 4

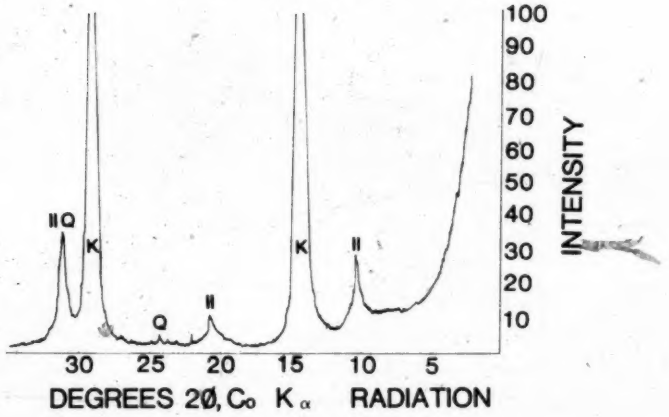

FACIES 3

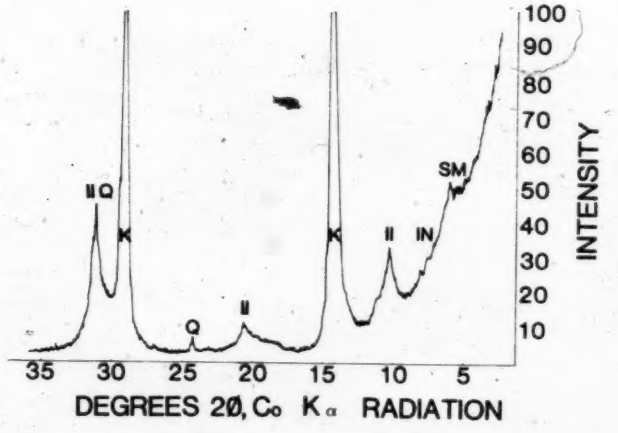

FACIES 2

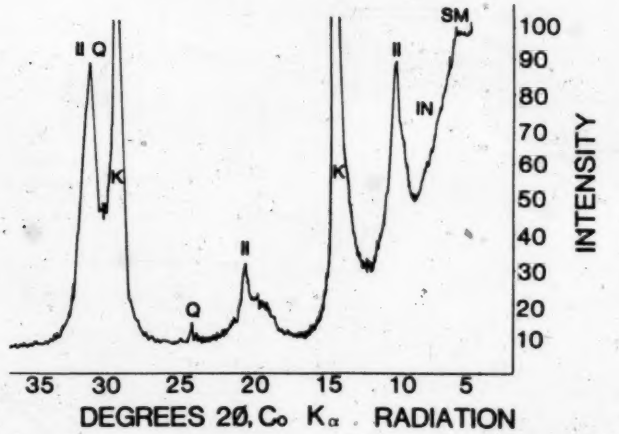

Figure 7: X-ray diffractograms (Ca-saturated glycol) for Facies 6.

SM - SMECTITE

IN - MIXED - LAYER ILLITE/SMECTITE

IL - ILLITE

K - KAOLINITE

Q - QUARTZ

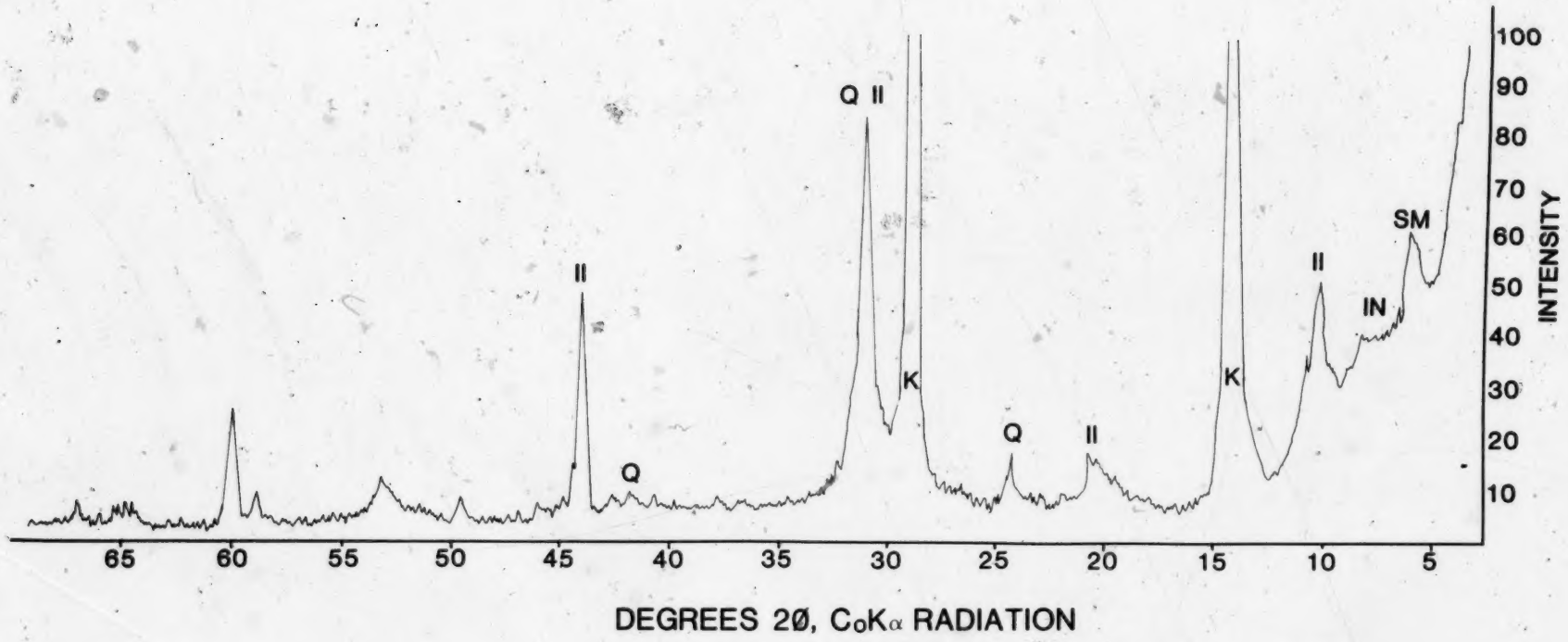
Q II
II
Q
K
Q
II
K
II
IN
SM
100
90
80
70
60
50
40
30
20
10
INTENSITY
65
60
55
50
45
40
35
30
25
20
15
10
5
DEGREES 2Ø, CoKα RADIATION

V. Depositional Processes

A. Introduction

The sequence of Facies with the Swift Formation is lithologically simple. Development of a Facies Model for this coarsening upwards sequence may be evaluated primarily on the basis of sedimentary structures. Additional support for environmental interpretation may be drawn from authigenic iron compounds, trends in clay mineral assemblages and regional facies distribution.

B. Mudstone-Shale Facies

The fine-grained sediments of Facies 1 were deposited under low energy conditions. Suspension sedimentation is suggested by the lack of sedimentary structure and the very fine grained nature of the sediment. Minor lenses of silt and glauconite imply deposition under slightly higher energy conditions.

Cross-shelf transport of fine-grained sediment may be accomplished by eddy diffusion or advection in semi-permanent currents (McCave, 1972). Advective transport involves the net horizontal movement of suspended material in a moving water mass. Advective transport is most effective off the mouths of rivers (residual current). Sediment plumes, observed off deltas, carry sediment well offshore, most evident at times of flood stage river discharge (Kulm et al, 1975).

Water mixing by wave action and tidal currents along coastlines may also transport fine-grained sediment offshore through processes of diffusion. Diffusion moves sediment from areas of high concentration to areas of low concentration in an attempt to maintain a uniform particle distribution; since areas of highest concentration are nearshore diffusive transport is directed offshore (McCave, 1972). This mechanism is of far less significance to offshore sediment transport, compared with the advective processes.

Offshore dissipation of transporting currents results primarily in suspension settling of the entrained sediment (Whitehouse et al, 1960; Edzwald and O'Melia, 1975; Gibbs, 1977). Settling will begin when the competency of the diminishing current can no longer hold the particle in suspension. Particle size should decrease seaward for sediments deposited from an offshore moving water mass. Although bioaggragation is a recognized process influencing clay sedimentation, it does not dominate the process and pattern of deposition on continental shelves (Carder et al, 1971; McCave, 1972). Therefore, specific clay minerals are not selectively influenced by organic aggragation.

The occurrence of thin silt and glauconite lenses within the shale facies may have resulted from either increased competence of seaward moving water masses or the development of a storm induced density current (Brenner, 1980). The latter will be discussed in the following sections.

C. Light and Dark Ribbon Sediments

The dark ribbon sediments (Facies 2 and 3) are heterolithic lithologies of interlaminated siltstones/sandstones and shales. Low depositional energy is suggested by these predominantly structureless fine grained sediments, with periodic increases in current strength for deposition of the small-scale, low angle cross-stratified coarser laminae.

In the light ribbon sediments of Facies 4 the grain size and percentage of framework constituents has increased from Facies 3. Lamination within the light ribbon lithology is wavier and the occurrence of small-scale low-angle trough cross-stratification has increased slightly relative to Facies 2 or 3. This suggests a more proximal depositional environment (Clifton, 1983).

In the modern setting, transport of coarser silts and very fine sands across continental shelves is accomplished during the higher energy winter season (Kulm et al., 1975). Strong winds blowing onshore cause surface waters to be directed towards the coast. This results in the downwelling of surface water adjacent to the shoreline. An alternative mechanism for offshore sediment transport has been offered by Walker (1984). Under the influence of gravity, sediment laden currents may flow down the sloping shoreface and dissipate across the shelf. Descending water masses are directed away from the coast by an onshore pressure gradient, induced by the upward sloping shoreface (Smith and Hopkins, 1972). These large-scale descending water masses are referred to as geostrophic currents. Current velocities are proportional to the pressure gradient induced by onshore water accumulation (hydraulic head). Geostrophic current velocities may exceed the critical shear velocity (40 cm/sec) required to entrain sand-sized particles (Smith and Hopkins, 1972).

Sediment transported offshore will be deposited systemically as the current energy decreases. The resulting particle fractionation shows a decreasing grain size distribution in the seaward direction. The upward coarsening sequence within the Swift Formation suggests a similar fractionation.

D. Structureless Sediments

Facies 5 represents the most lithologically diverse unit within the Swift Formation, with lithologies ranging from silty mudstones to medium-grained sandstones. Most of the sediments are structureless and become coarser grained upward. These features imply that depositional energy has varied both stratigraphically and regionally, suggesting that Facies 5 has accumulated by more than one process.

The deposition of massively bedded sediments is not clearly understood. Very rapid deposition from turbulent suspension or deposition from very highly concentrated sediment dispersions, can result in structureless beds (Blatt, et al, 1980). Sediment-laden currents experiencing deceleration, deposit their suspended load very rapidly. Particles become buried and effectively immobilised before significant bedload movement can take place (Collinson and Thompson, 1981).

High-energy currents are most easily generated during storm events. In some cores, faint bedding distinguished by sediment variation, suggests successive depositional events of varying intensity. Depositional processes for Facies 5 will be further examined in section 6.

E. Stringer Sandstones

The medium grained sandstone stringers of Facies 6 are found throughout the Swift ribbon sediments. The frequency of this lithology decreases downsection, becoming near absent within Facies 2 of the dark ribbon sediments. As discussed in section 3, the petrography differs from the enclosing ribbon sediments. The petrography of the Facies 6 sandstones is most similar to the petrography of the uppermost Facies 5. The dramatic grain size difference between the coarser lenses of Facies 6 and the silty facies suggests that the Facies 6 sands were emplaced under higher energy conditions. Rapid deposition is suggested by the occurrence of loaded basal contacts, the lack of sedimentary structures, graded bedding and biogenic escape structures, implying deposition from sediment gravity flows.

On most modern day continental shelves, sands are deposited offshore during storms (Stubblefield et al., 1975). Coarser grained sands are transported across the shelf by density currents. Current generation appears to be controlled by strong onshore winds and the development of a two layer circulation system on the inner shelf. High velocity winds approaching the coast at near perpendicular angles will effectively shear large volumes of surface waters landwards. This phenomenon is referred to as "wind forcing" (Morton, 1981) and initiates the two layer circulation system. In counterbalancing the piling up of water in the onshore direction, a return current is generated flowing in the offshore direction. This sinking water mass entrains and transports shoreface-derived sediments in an offshore direction (Figure 8). Bottom current dynamics and duration are controlled by several variables. These include the shelf slope, shoreline orientation,

geographic orientation relative to the storm centre, and storm characteristics such as surge height, wind velocity and duration, forward speed of the storm and its angle of approach to the shoreline (Morton, 1981).

Deposits similar to the medium grained sand lenses of the Swift Formation have been observed on modern day continental shelves. These sediments were eroded from the shoreface and transported seaward during high energy storms. Storm deposits are generally composed of fine grained sands, with grain size and bed thickness decreasing offshore. Grain size may indicate the competency of the storm currents, or reflect the sediment sizes available in the source area.

Sands eroded from the shoreline during high energy storms have been deposited as far as 40 kilometres offshore (Reineck and Singh, 1972), and generally range from a few centimetres to a few decimetres in thickness (Hayes, 1967; Murray, 1970, Forristall et al, 1977). Sediments deposited during Hurricane Carla extended further than 24 kilometres offshore and covered approximately 800 square kilometres (Hayes, 1967). Bed thickness and lateral extent are primarily controlled by nearshore bottom gradients and local channelization across the shelf (Morton, 1981). Storm deposits may be graded and are frequently sharp-based.

During storm conditions, strong unidirectional bottom flows have been monitored. Murray (1970) measured current velocities as high as 1.6 metres/sec, 1.5 metres off the bottom in 6.3 metres of water, 360 metres offshore, in the Gulf of Mexico (approximately 160 kilometres from the storm centre). In a similar study from offshore Galveston Island during Tropical Storm Delia, currents directed seaward exceeded 0.75 metres/sec, 3 metres off the bottom in 20 metres of water, 40 kilometres from the shoreline (Forristall

et al, 1977) (Figure 9). Currents of these magnitudes produce bed shear velocities in excess of the critical velocity required for entrainment and transport of most sand-sized particles (as predicted using Hjulstrom and Shields diagrams the critical shear velocity U* 1.3 cm/sec is approximately generated by current velocities in excess of 40 cm/sec in the water column, 3 metres above the shelf bottom (Smith and Hopkins, 1972). Morton (1981) suggests that graded sequences are a function of water depth and distance from the coast. There are limited data available on the generation of graded beds in offshore shelf settings (Hayes, 1967; Reineck and Singh, 1972; Nielson, 1978). Burrowing, if present, is generally associated with the uppermost layer of the storm-sand deposit. However, escape structures do originate from the base of storm-sand layers in the North Sea (Reineck and Singh, 1972); an additional indicator of rapid deposition.

Figure 8: Mechanism proposed for the generation of offshore moving sediment gravity flows. The density current in the bottom layer of the water column flows offshore in response to shoreward wind forcing of the surface water layer.

STORM SEDIMENT TRANSPORT - OFFSHORE MECHANISM

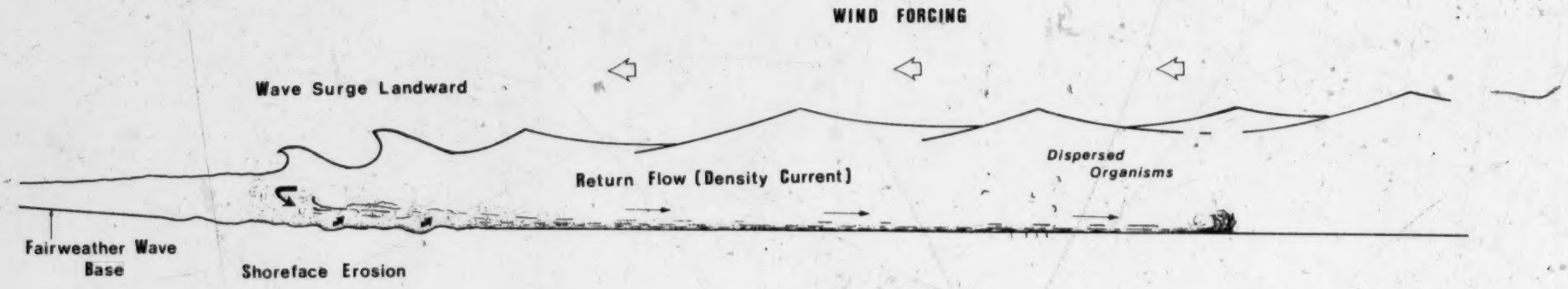

Figure 9: a. Wind and current velocity profiles during Hurricane Camille (16-18 August, 1969 - after Murray, 1970).

b. Current velocity profiles during Tropical Storm Delia (3-5 September, 1973 - after Forristall et al., 1977).

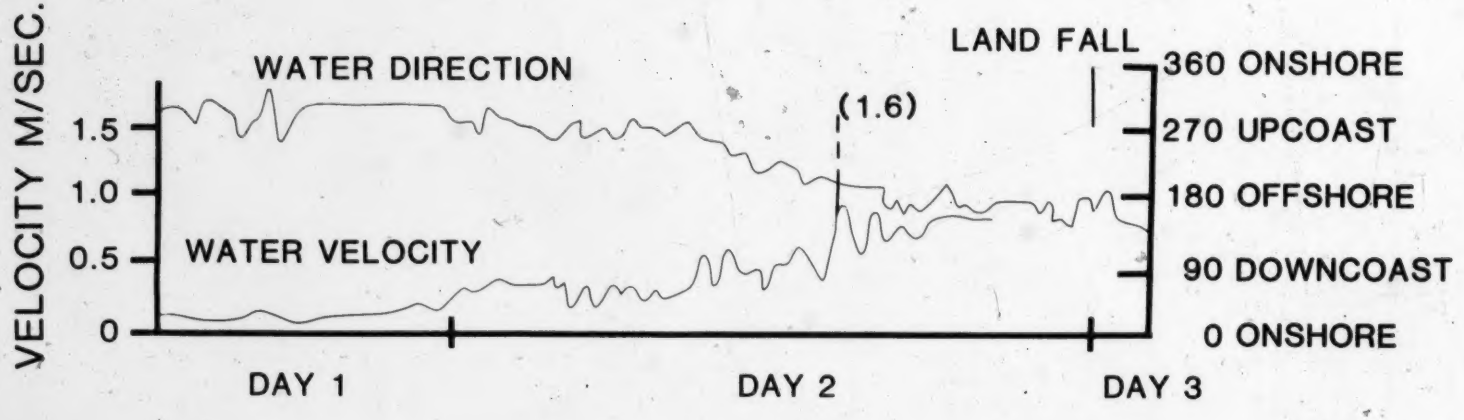
VELOCITY M/SEC.
1.5
1.0
0.5
0
WATER DIRECTION
WATER VELOCITY
(1.6)
LAND FALL
360 ONSHORE
270 UPCOAST
180 OFFSHORE
90 DOWNCOAST
0 ONSHORE
DAY 1
DAY 2
DAY 3

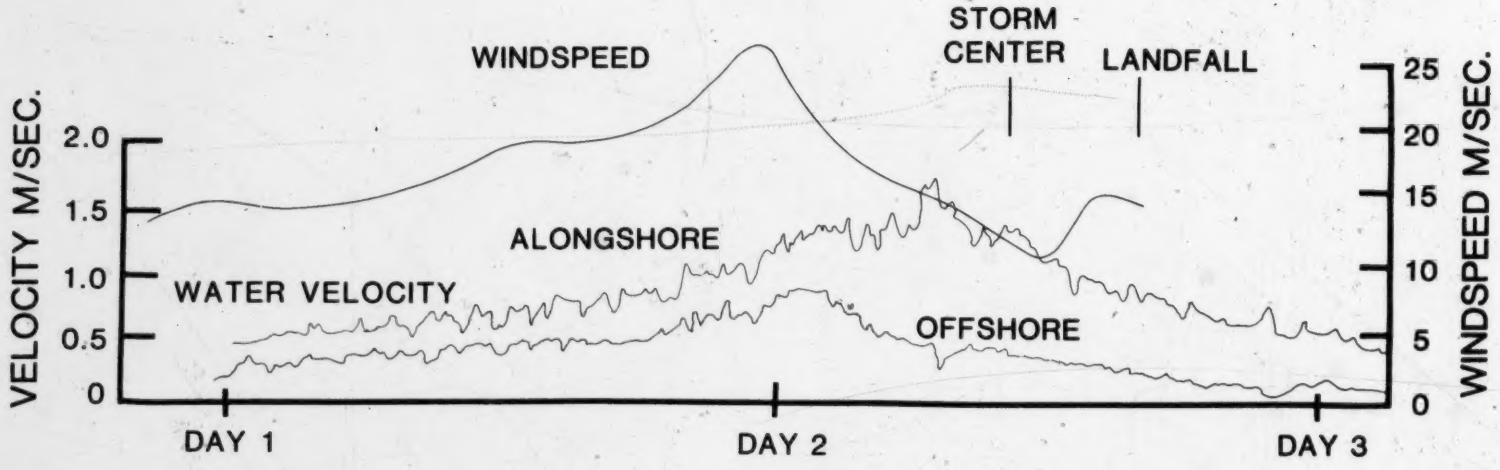
VELOCITY M/SEC.
2.0
1.5
1.0
0.5
0
WINDSPEED
STORM CENTER
LANDFALL
ALONGSHORE
WATER VELOCITY
OFFSHORE
25
20
15
10
5
0
WINDSPEED M/SEC.
DAY 1
DAY 2
DAY 3

VI. Regional Analysis

The major facies of the upper Swift sediments were examined regionally within the study area (Figures 11 to 13). Depositional trends were assessed by constructing isopach maps of facies thicknesses. In some areas poor core control and variations within the facies do not favour the accurate reconstructions of depositional thicknesses. Additionally, a discontinuous subcrop has complicated regional correlation. Post-Oxfordian erosion is well illustrated in an isopach map of the total Swift Formation (southeastern Alberta and northern Montana; Hayes 1983) (Figure 10).

Both the dark and light ribbon sediments pinch out to the north and west. This corresponds with a relative increase in thickness of the non-marine uppermost Facies 5 (with its near absence in the southeastern quadrant of the study area). The direction of thinning of the marine facies or units can be used to interpret a sediment source-shoreline direction. This corresponds to the thickening trend of the non-marine Facies 5.

Figure 10: Isopach map of total Swift Formation, illustrating post-Swift erosion. Note complete removal of the Swift Formation in the Cut Bank and Whitlash Valleys (after Hayes, 1983).

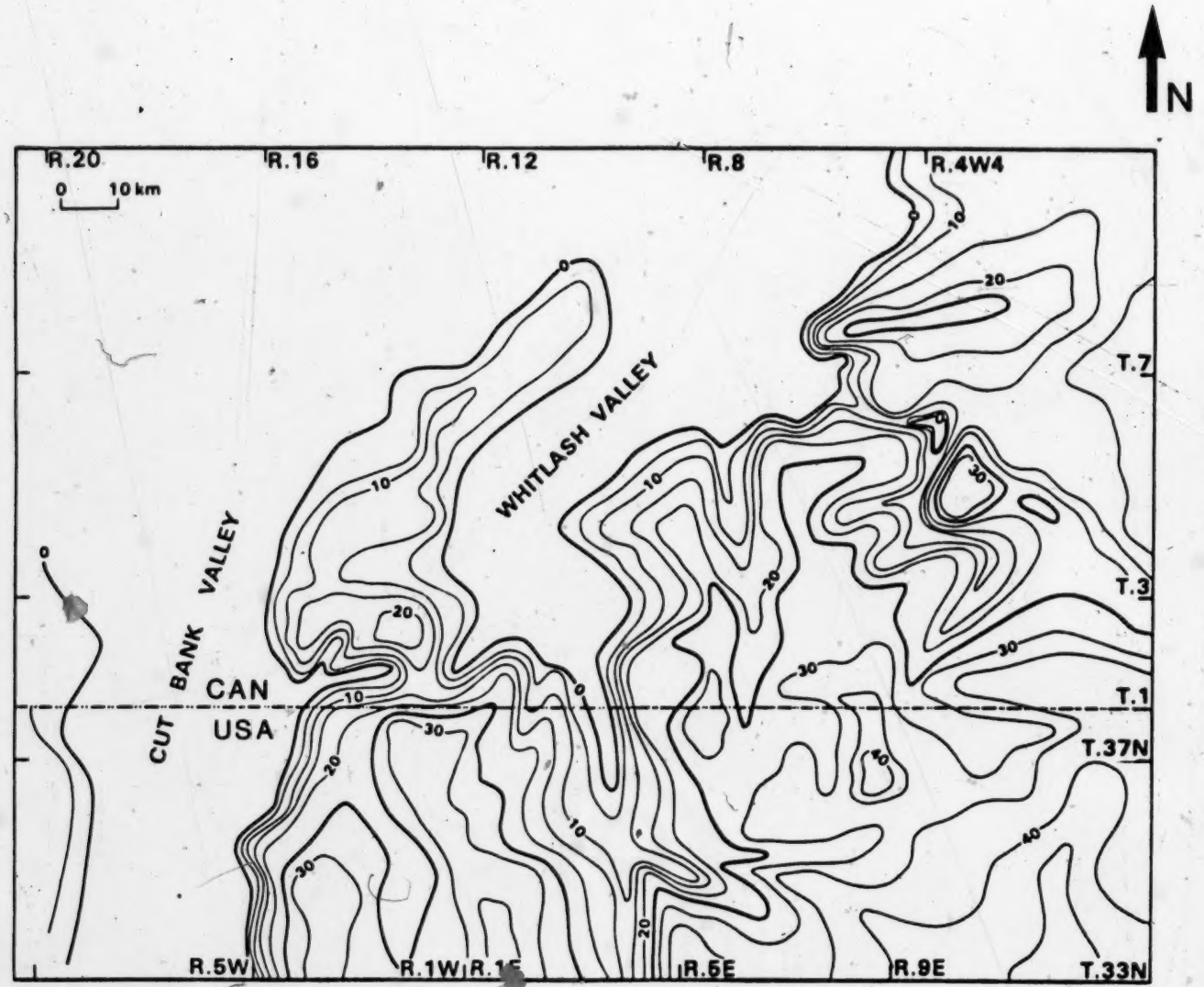
N
R.20
R.16
R.12
R.8
R.4W4
0 10 km
WHITLASH VALLEY
CUT BANK VALLEY
CAN
USA
T.7
T.3
T.1
T.37N
T.33N
R.5W
R.1W
R.1E
R.5E
R.9E
0
10
20
30
40

Figure 11: Regional isopach map estimating pre-erosional thicknesses of the Swift Facies 2 and 3.

Contour interval = 5 metres.

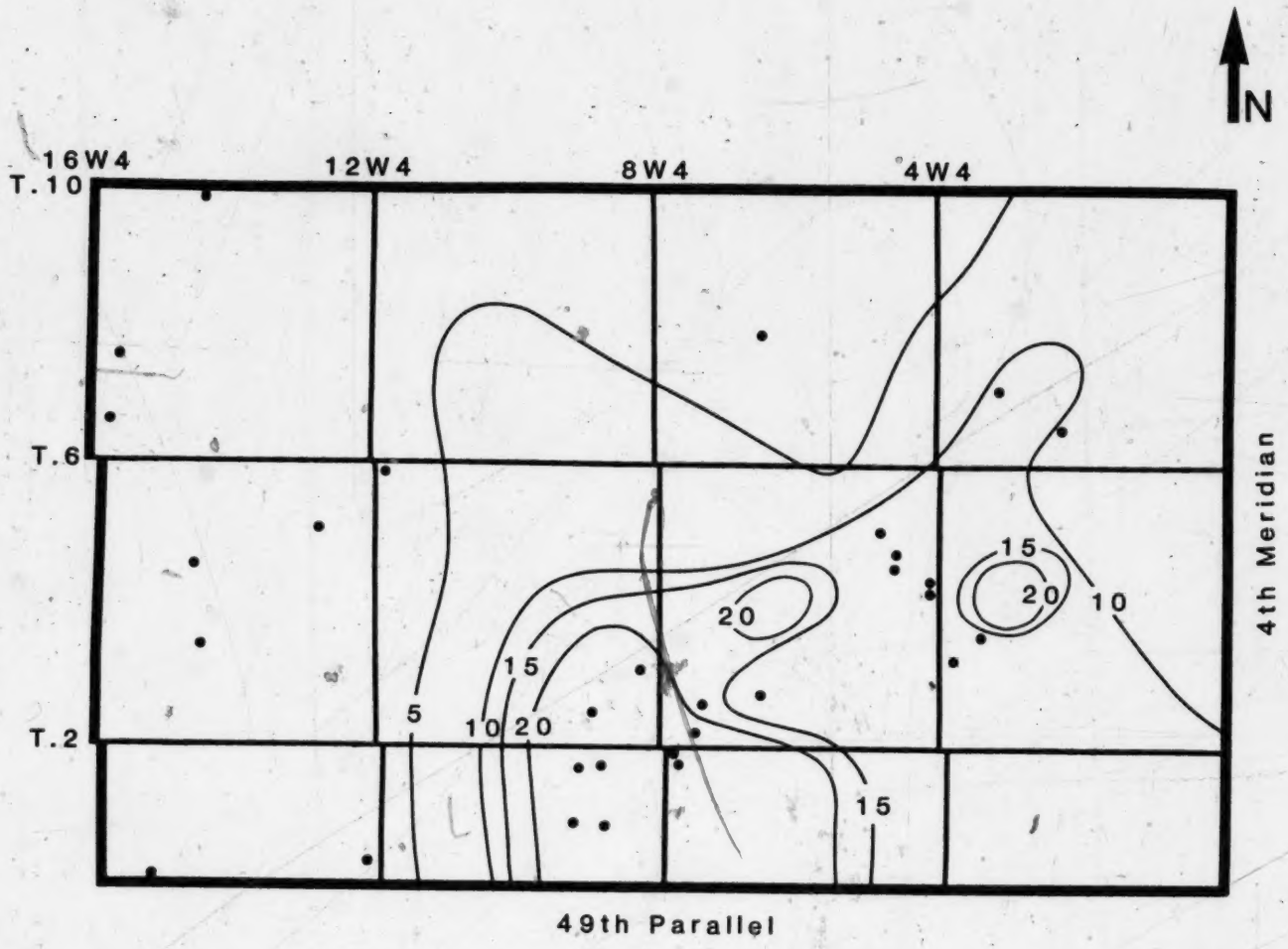
N
16W4
12W4
8W4
4W4
T.10
T.6
T.2
4th Meridian
49th Parallel
5
10
20
15
20
15
20
10
15

Figure 12: Regional isopach map estimating pre-erosional thicknesses of the Swift Facies 4.

Contour interval = 2 metres

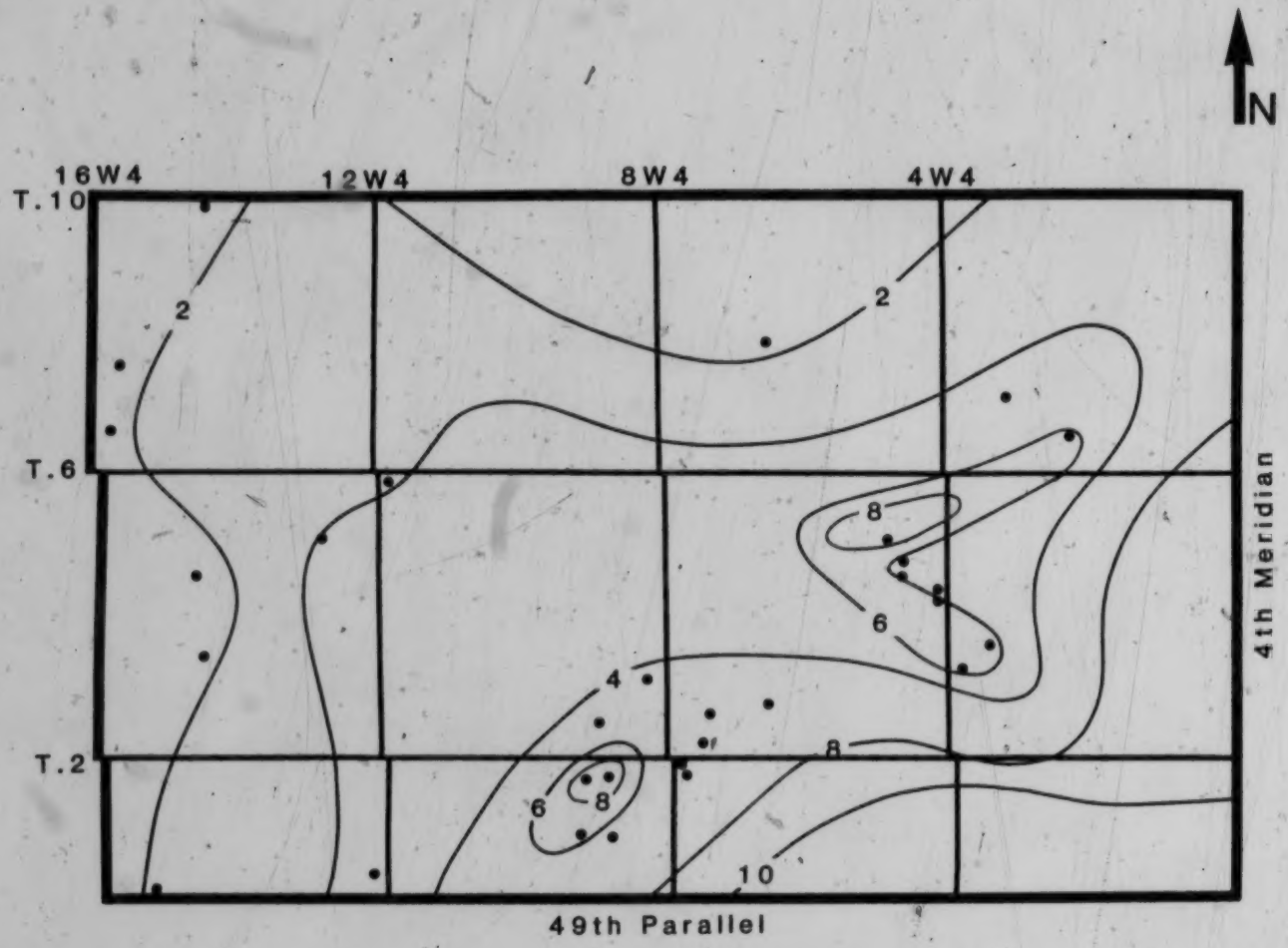
N
16W4
12W4
8W4
4W4
T.10
T.6
T.2
2
2
8
6
4
8
6
8
10
4th Meridian
49th Parallel

Figure 13: Regional isopach map estimating pre-erosional thicknesses of the Swift Facies 5.

Contour interval = 2 metres

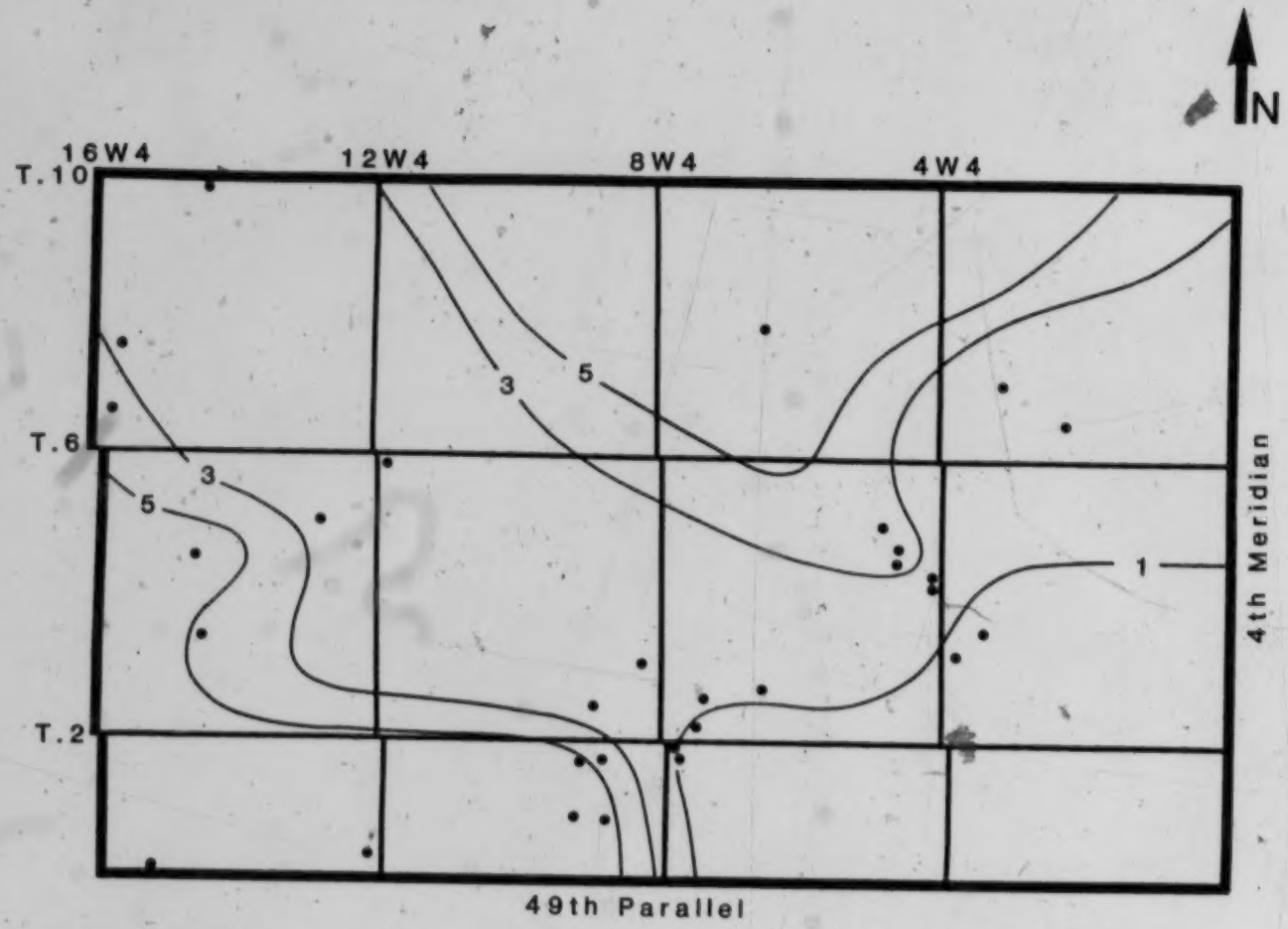
N
16W4
12W4
8W4
4W4
T.10
T.6
T.2
3
5
3
5
1
4th Meridian
49th Parallel

More detailed isopach maps were constructed for Range 5, Township 5, where core and well control are quite good (Figure 14 to 16). These maps clearly illustrate the greater detail present in thickness variation existing in the Swift facies. Thinning of all three facies occurs near the centre of Township 5. This cannot be attributed to post-Swift erosion, nor to a paleotopographic anomaly; consequently it must represent a depositional phenomenon. The absence of Facies 2 and 3 (dark ribbon sediments) in wells 6-28-5-5W4M and 8-29-5-5W4M suggests sediment deposition in a more oxygenated setting. The zero isopach in Figure 14 is surrounded by relatively thick deposits of dark ribbon sediment and is closely coincident with a thicker elliptical accumulation of light ribbon sediment (Figure 15). These features correspond to the position of a topographic high (ridge or shoal) within the shelf regime.

Of related interest and additional reservoir importance, is the accumulation of medium-grained sandstone (Facies 6) to the northwest of this feature. Correlating diagonally across section 29 of Township 5, Range 5W4M, two distinct sandstone bodies are observed, both approximately 0.75 - 1.00 metre in thickness (Figure 17). In well 6-29-5-5W4M good planar tabular cross-stratification is observed in the sandstone build-ups, which may suggest incipient bar development. Sand accumulation may have been controlled by current deflection or convergence around the topographic rise of light ribbon sediment to the southeast. Recognition of such topographic

features from geophysical control (seismic lines) might provide a means for predicting reservoir accumulation.

Figure 14: Detailed isopach map of Facies 2 and 3 in Township 5 Range 5W4M (within the Manyberries Field)

Contour interval = 10 feet = 3.28 metres

TOWNSHIP 5 RANGE 5W4

Figure 15: Detailed isopach map of Facies 4 in Township 5 Range 5W4M (within the Manyberries Field)

Contour interval = 5 feet = 1.65 metres

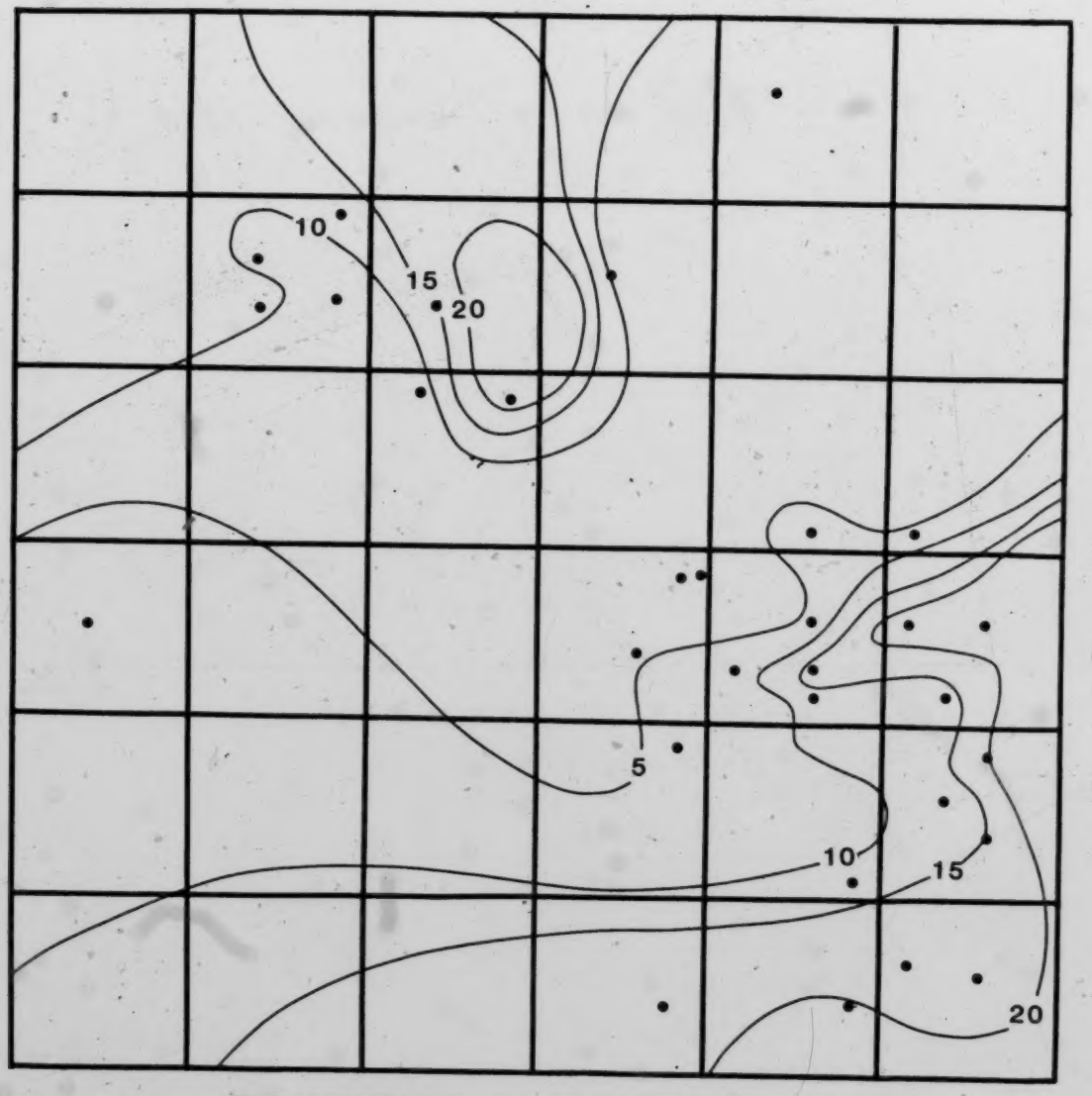

TOWNSHIP 5 RANGE 5W4

Figure 16: Detailed isopach map of Facies 5 in Township 5 Range 5W4M (within the Manyberries Field).

Contour interval = 2 feet = .66 metres

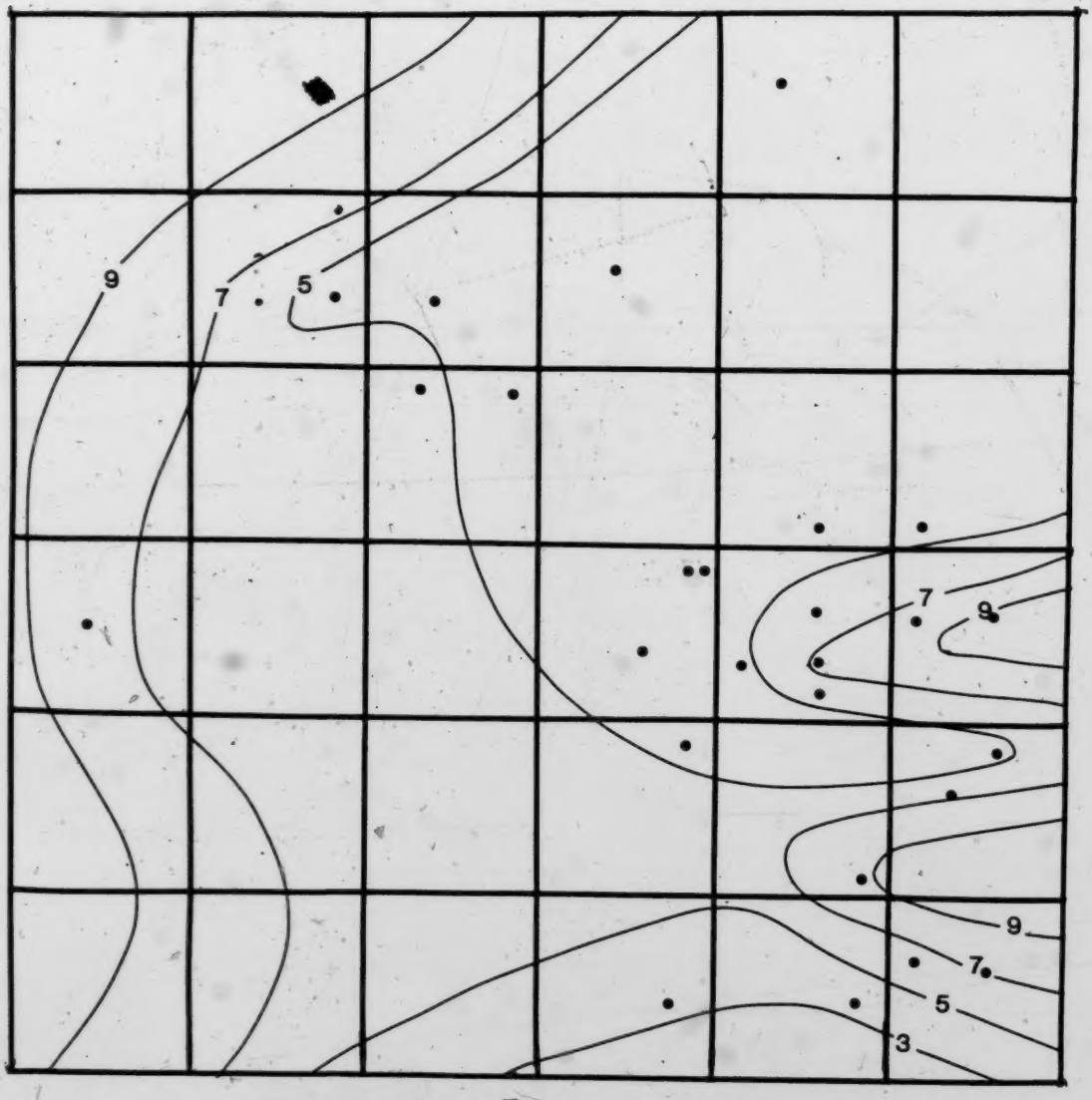

TOWNSHIP 5 RANGE 5W4

Figure 17: Accumulation of Facies 6 noted in section 29 of Township 5 Range 5W4M; sand build-ups located to the northwest of an apparent offshore shoal. Correlation line drawn in Figure 14. (Datum = Rierdon Unconformity)

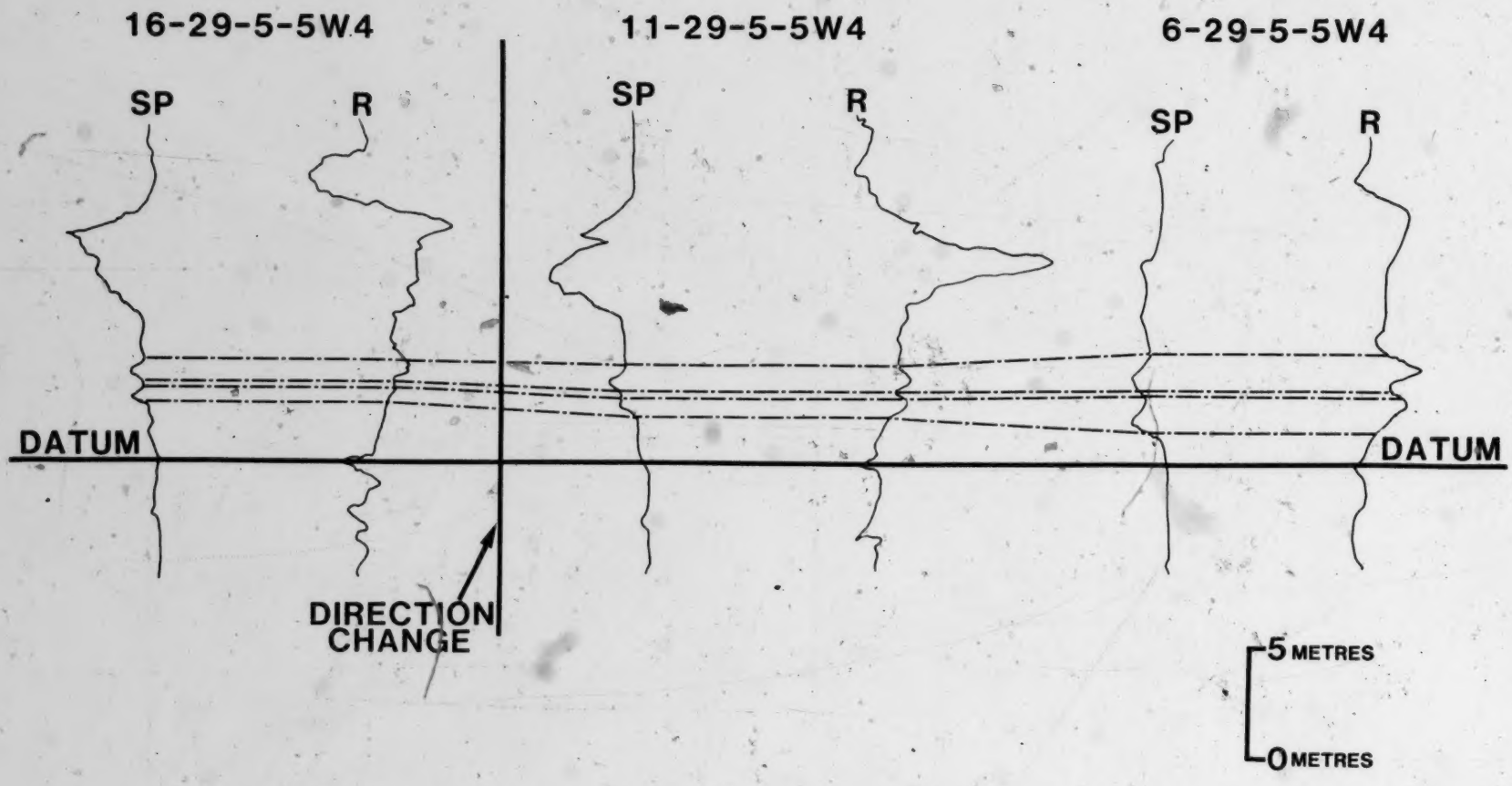

SAND BUILD-UP: CORRELATION SECTION 29

VII. Facies Model

Deposition of the Swift Formation began during the early Oxfordian when a large epicontinental seaway flooded the Western Interior of North America, marking the third Jurassic transgression (Brenner, 1980). The coarsening-upwards Swift sequence suggests an increasing energy gradient from bottom to top. This will be shown to correspond to a shallowing sequence upsection.

Facies 1,2 and 3 appear to have been deposited in an offshore marine setting. The lowermost shale unit was deposited offshore during the transgressive phase of marine inundation. The transition to ribbon sedimentation records the onset of the regressive cycle with its characteristic coarsening-upwards signature. Deposition of the dark ribbon sediment was dominated by suspension sedimentation, with minor marine and tidal current reworking (inferred from low-angle crossbedding). The presence of mud laminae which appear continuous and thin coarser storm deposits support a subtidal depositional environment (Clifton, 1983).

Burrow densities are unusually low for an offshore environment. Howard and Reineck (1972) suggest that burrow density should increase with increasing water depth, hence distance from nearshore/storm influence. Trends in burrow density similar to those of the Swift Formation are described by Hill (1985) in the N.W. Gulf of Mexico. A decrease in diversity and abundance of biogenic sedimentary structures is observed with increasing water depth across an interlaminated size-graded shelf. He attributes this primarily to seaward increasing sedimentation rates and an under consolidated substrate serving to preclude preservation. Similar conditions may have prevailed during the

deposition of the Swift Formation. This may further suggest a very shallow offshore setting within the Oxfordian Sea, which could enhance the influence of nearshore processes.

Further support for an offshore depositional setting may be drawn from evidence missing from a nearshore or intertidal environment. Neither rooting nor mudcracks were observed within the dark ribbon lithologies, both of which are commonly diagnostic of intertidal settings (Clifton, 1983). The absence of channel sequences and associated current bedding further complicates a nearshore model. Typically along present day macro to meso-tidal coasts, a complex sequence of current-generated bedforms in nearshore sediments is observed. Horizontal and cross-stratification are typically absent within the upper Swift lithologies, suggesting that strong tidal processes were not of depositional importance.

Lithofacies 4 was deposited nearer shore. Laminae are wavier and the percentage of detrital mud is notably less. Tidal circulation is suggested in some cores by the presence of apparent bimodal trough cross-stratification. The gradational loss of organic matter with the dark-light ribbon sediment transition, may be a function of oxygen supply to the sediment-water interface. Preburial oxygenation of organic detritus in the light ribbon sediment is supported by the absence of authigenic pyrite. In most cases, the uppermost segment of Facies 4 was deposited in a very nearshore setting. Nearshore sedimentation is suggested by the gradational upper contact with the rooted Facies 5. An offshore shoal in section 28 of Township 5, Range 5W4M, was identified from isopach construction of the light ribbon Facies 4 sediments and the dark ribbon Facies 2 and 3 sediments. In this instance,

light ribbon deposition has occurred on an offshore topographic high on the shelf bottom, suggesting that oxidation of the light ribbon sediment occurred in shallower water.

The use of clays as a paleoenvironmental indicator has attracted some interest (Weaver, 1959; 1960; Wilson and Pittman, 1977). An upward shallowing sequence for ribbon sedimentation is supported by clay mineral trends noted with the interbedded shale laminae. As discussed in Chapter 4, kaolinite, the dominant clay mineral, increases in relative abundance upsection. Illite decreases upsection, disappearing near the top of Facies 4. Detrital smectite also decreases upsection, disappearing near the top of Facies 6. In modern environments similar trends have been observed in shelf sediment progressing from a nearshore to an offshore location. With increasing distance from an active fluvial/estuarine system the clay mineral suite changes from a kaolinite-dominated assemblage to a smectite dominated one (Powers, 1957; Nelson, 1960; 1972; Parrenga, 1966; Bigham, 1973; Edzwald and Omelia 1975; Gibbs, 1977; etc). This is primarily a function of differential settling velocities for the clay minerals, which in turn is controlled by relative tendancy to flocculation, bioaggradation and organic complexing. The increase in detrital kaolinite upsection associated with a decrease in smectite, in the Swift Formation supports a shift to more nearshore deposition.

The predominantly structureless sediments of Facies 5 do contain indicators that may be used to interpret paleoenvironment. Carbonized rootlets are sporadically observed, suggesting a coastal-onshore depositional setting. Glauconite is absent. Radially spherulitic siderite is often observed in the base of the unit. This variety of siderite is believed to be exclusively precipitated in sediments with fresh to hyposaline pore waters, such as would occur in a brackish embayment or stagnant phreatic zone.

Much of the coarser sediment of Facies 5 accumulated along a prograding coastal plain, while the fine-grained sediment was deposited in low-energy embayments. Sedimentation was controlled by coastal processes of varying intensity. Facies complexity stems from the sub-environments associated with the prograding coastal system. Lithology may be a function of fluctuation in sediment supply, environment variation or a combination of both.

Coastal chenier complexes may have represented a facies sub-environment. Chenier stratifaction is typically poor and deposits are often nearly structureless (Byrne et at, 1959; Curray et al, 1969). Grain size generally ranges from fine to medium sand and deposits are well sorted. Authigenic siderite has also been observed in chenier ridges along the western Louisiana coast (Byrne et al, 1959). These characteristics are very analogous to the coarser sediments of the uppermost Swift facies.

Strand-plain development is poorly understood, however a prograding shoreline appears essential. A mechanism proposed by Curray et al (1969) suggests that cheniers develop in response to high sand supply and low wave energy. If tidal conditions are favourable, longshore bars may become attached to the shoreline and act as the new beach. The internal stratification of Facies 5 does not resemble that of bar complexes and no evidence for longshore bars is observed in cored Swift sequences. A second model for chenier development involves transgressive and regressive pulses during a dominantly progradational cycle (Gould and McFarland, 1959; in Curray et al, 1969). During periods of high sediment influx, mud/sand flats prograde seaward and the coastal plain undergoes little change. During periods of low sediment influx, linear sand complexes develop in response to wave reworking of previously poorly sorted nearshore sediments. It should be noted that onshore sediment accumulation would best be accomplished during storm surges.

Storm events would also account for the abraded clay rip-up intraclasts observed within Facies 5 of several cores.

Bimodal lithologies composed of silt and sand within Facies 5 may also develop in the coastal plain environment. Curray et al (1969) observed a silty-sand facies around the seaward periphery of the Nayarait chenier plain. The sediment is interpreted as a transitional deposit between the beach sands and the shelf silts, which developed from wave reworking. This may be consistent with the coastline model proposed for the uppermost Swift facies. Alternately, this lithology could have developed as a washover deposit in a low energy embayment or as a flood deposit reworking chenier sediment. This is suggested by the presence of rooting in some cores, which favours onshore deposition. This facies, however, appears restricted to a coastal plain setting.

In several locations within the study area the Swift ribbon sediments are capped by a fine graind argillaceous lithology suggesting a low-energy shoreline. Clastic sequences developed along low-energy shorelines, however, are often not unlike those generated along a high energy coastline, although depositional thickness is typically reduced (Reineck and Howard, 1981). Sediment size increase towards the coast with shoreline sediment within the sand-sized fraction. A more specialized type of shoreline environment should be considered for the uppermost Swift lithology.

Fine-grained clastic sediment predominantly accumulates in marshy embayments and on mudbanks in coastal settings. These deposits may be found alongside and overlapped by the chenier-plain facies (Byrne et al, 1959). Fine-grained clastic shorelines do not require barrier bar development with tidal inlet circulation, as was once thought. Non-barred mud-dominated coastlines have been documented in southeast India, central Surinam and

western Louisiana (Nair, 1976; Wells and Coleman, 1977, 1981; Byrne et al, 1959; Beall 1968). Mudflat development is dependent upon the existence of broad shallow shelves and exceptionally high fine-grained sediment concentrations in coastal waters (Postma, 1961; Beall, 1968; Nair, 1976; Wells and Coleman, 1977; 1981). Greatest turbidity occurs near rivers with high suspended sediment discharge (Beall, 1968; Wells and Coleman, 1977), or along shorelines after storm events (Buss and Rodolfo, 1972; Nair, 1976). In both cases the influx of fresh water lowers salinity which initially inhibits mud settling. Wave action and longshore currents act to retain some of the sediment within the nearshore regime. Entrapment of this sediment is also enhanced adjacent to the coast, owing to the greater tide settling lag effect in very shallow water (van Straaten and Keunen, 1957). Under conditions of high turbidity, the settling lag effect should become enhanced (Beall, 1968). Fresh water dispersion increases salinity, which catalyses flocculation and promotes mud sedimentation by settling. This fine-grained sediment then becomes trapped within marshy embayments, or deposited on nearshore mudbanks. Within the study area fine-grained clastic shorelines may have dominated the Oxfordian sea. It is possible that swampy embayments may have acted as traps for storm entrained sands. The sandstones of Facies 5, therefore, may have accumulated on a marshy coastline, as opposed to the earlier suggested Strand Plain environment.

The stringer sandstones of Facies 6 were deposited during high energy storms. Sediment derived from the shoreface and coastline (Facies 5 sediment) was transported in seaward-flowing density currents onto the shelf. The sands were deposited offshore in thin (millimetre-centimetre) beds, loaded into the ribbon sediments (Facies 2,3 and 4). Thicker shelf-sand accumulations occurred within incipient bars on the lee-side of topographic highs or

"shoals" on the shelf. These sand build-ups likely in response to additional current reworking of storm deposits.

During maximum transgression, the middle Oxfordian shoreline was north of the study area. This is supported by the distribution of the lowermost shale Facies 1, which occurs throughout much of southeastern Alberta, except where removed by post-Swift erosion. Minor thinning of the Swift basal shale occurs across the Sweetgrass Arch (Hayes, 1982; 1983). The paleoshoreline has been estimated using additional data from Hayes (1983) (Figure 18). The late Oxfordian shoreline occupied a more southerly position, possibly penetrating the north-central region of the study area. Shoreline position is based primarily on the facies trends in the regional isopach maps, and cannot be confirmed in subcrop, due to erosion of the Swift Formation in this region. Additionally, shoaling was taking place in the southwest quadrant of the study area, across the Sweetgrass Arch, and possibly, to a minor extent in the northern portion of Township 5, Range 5W4M (Figure 19).

Figure 18: Shoreline reconstruction at maximum Swift sea transgression (middle Oxfordian)(modified from Hayes, 1983).

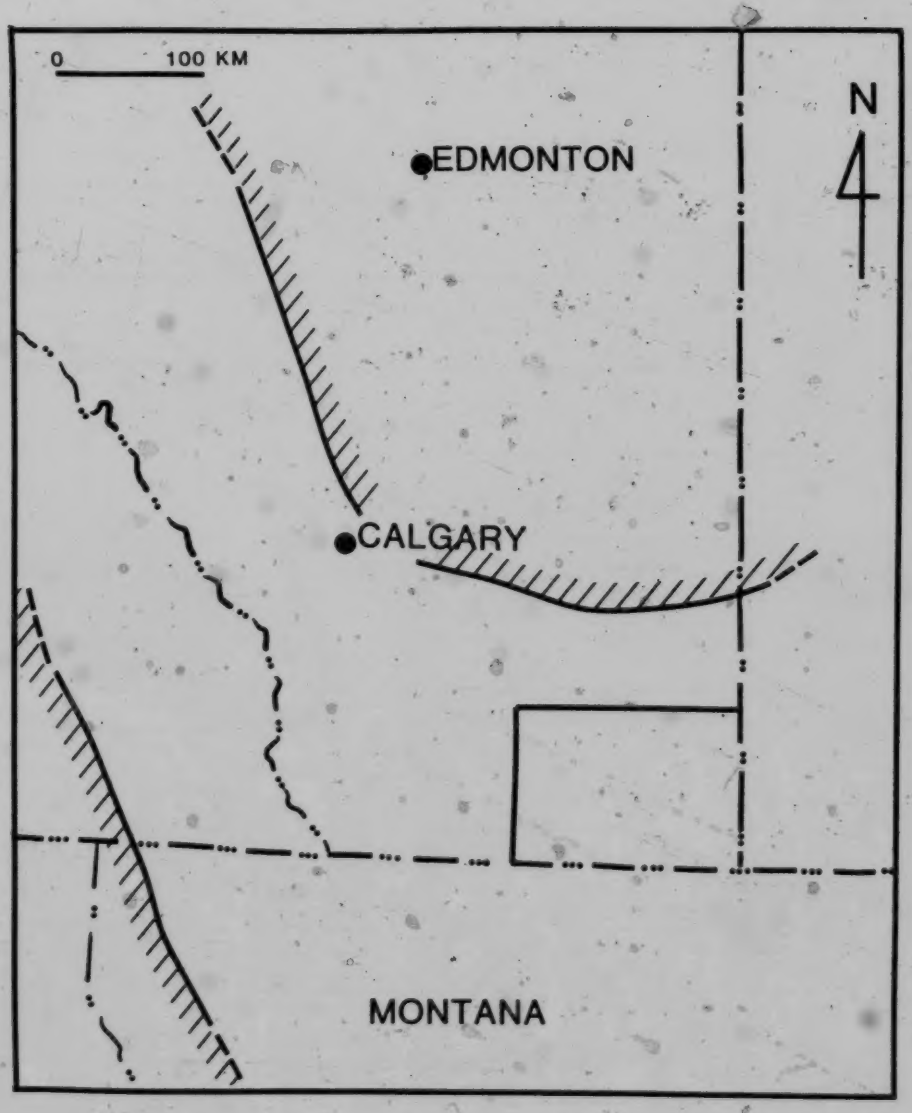
0
100 KM
N
EDMONTON
CALGARY
MONTANA

Figure 19: Shoreline reconstruction during regression of the Swift sea (late Oxfordian)(modified from Hayes, 1983).

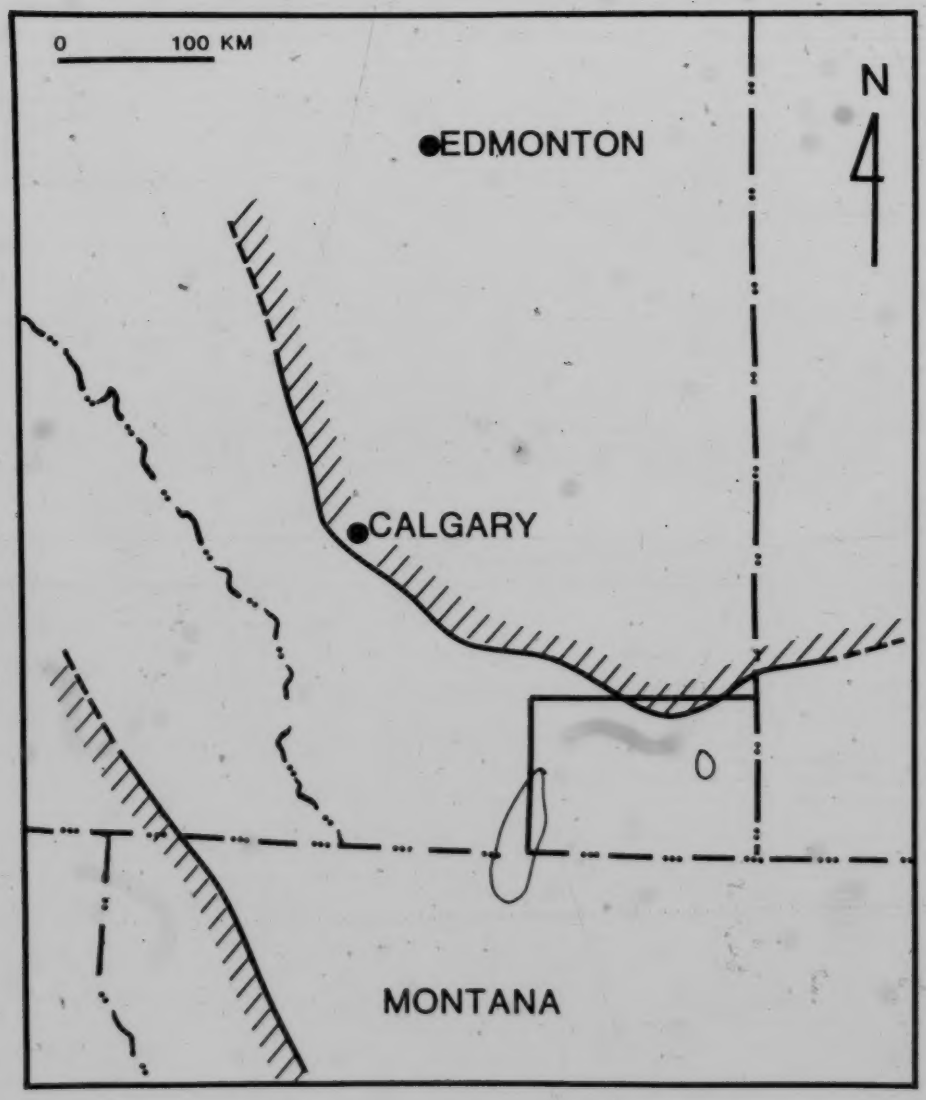
0 100 KM
N
EDMONTON
CALGARY
MONTANA

VIII. Depositional Controls on Porosity and Permeability

The heterogeneity of the Swift Formation is expressed by the wide range of porosity and permeability within the lithologies. Typical porosities of 13-18 percent for reservoir-quality wells in the Swift sediments may drop below 3 percent or reach upwards of 27 percent. Similarly, permeability may change by as much as 700 millidarcies within one metre of section.

The ribbon sediments of Facies 2,3 and 4 do not have characteristics commonly associated with oil reservoirs. Although well sorted, the fine-grained argillaceous nature of these units greatly restricts the pore size within the sediments. In addition, the abundance of detrital and authigenic kaolinite has further restricted pore throats, limiting the transmissive potential of the sediments (Plate 10B). Without the influence of other primary variables this heterolithic sequence could not have attained reservoir status.

Factors influencing fluid transmissibility of the various facies can be subdivided into two classes. Macroscopic factors are sedimentary characteristics which are readily observable in core, and include the percentage of coarser sand (Facies 6), detrital mud, and the burrow density. Microscopic factors account for the internal texture of the rock, and are controlled diagenetically.

Prior to discussing the effect of diagenesis on porosity and permeability within the Swift facies (Chapter 10), it is essential first to identify the depositional factors favouring the enhancement of porosity and permeability in these fine-grained argillaceous deposits. Important sedimentary characteristics include the occurrence of mud drapes, the distribution of Facies 6 sandstones, and the effects of burrowing.

Firstly, a somewhat irregular local seafloor topography produced discontinuous mud drapes on a macro-scale (centimetre-decimetre scale). In this situation, the coarser silty-sandstone laminae were allowed to come into contact with one another, which is an important aspect for porosity/permeability enhancement in heterolithic sediments (Polesek and Hutchinson, 1967).

Secondly, the distribution of Facies 6 is of major importance to potential reservoir development in the Swift Formation. This medium grained sandstone which is irregularly interfingered with the light and dark ribbon sediments, represents the best oil reservoir facies, and the volumetric percentage of which is a good basic indicator of reservoir potential.

Thirdly, reworking by burrowing organisms was very common within the coarser grained sediments. The influence of burrowing on the transmissability of clastic sediments has received little attention. Pettijohn et al. (p.525) states that "Biogenic structures destroy depositional fabric and bedding and thus drastically reduce permeability and cause minimal, if any, horizontal anisotropy of permeability. Effect on porosity is unknown, but may be negligible." This concept may accurately infer ideal fluid flow response to sediment with intense bioturbation. Bioturbated heterolithic sediment possessing a mud fraction will exhibit clay dispersion, which upon early compaction and subsequent dewatering, will "squeeze" the fines into the pore

throats between grains. This condition rapidly decreases porosity and permeability and may also promote early clay cementation.

The effect of less intense burrowing may not be detrimental to rock transmissibility. Burrowing enhances both the porosity and permeability within the Swift ribbon sediments as a consequence of coarser sediment redistribution. Transmissibility is enhanced in sediments containing Chondrites. Chondrites are dendritic feeding burrows with tunnels of uniform thickness branching from a central region near the sediment-water interface. They are thought to be produced by the probing action of a sipiculid worm (Simpson, 1956). These structures penetrate fine-grained sediment at angles oblique to parallel with bedding surfaces. Sediment infilling the burrow is injected from the surface and may differ markedly from the sediment surrounding the burrow. Within the ribbon sediments Chondrites infill generally contains much less clay and organic matter, giving them a relatively "clean" appearance (Plate 8B). This likely is the result of ingestion and subsequent alteration of these compounds by the feeding action of the organism (Pemberton, pers. comm.). The abundance of glauconized pellets contained within burrow filling would support the interpretation.

The sediment of the burrow infill is ususally a coarser sandstone similar in composition and sorting to the sandstones of Facies 6 (Plate 8C). Porosity is greater within infill and presumably permeability has increased as well. The contrast in grain size between the coarser burrow infill and the surrounding sediment (Facies 2,3 or 4) is important in the development of porosity and permeability within the ribbon sediments (Figures 20 and 21).

During periods of high energy storms (such as hurricanes) sediment may be driven seaward in response to wind forcing of surface waters (Figure 8). Once settled, this sediment (Facies 6) becomes subject to biological

reworking. Organisms dispersed by the storm settle as the current energy falls and may penetrate downwards into the safety of the nutrient-rich sediment below the storm-deposited sands. Other organisms buried in the underlying sediment push upwards through the storm deposit in order to utilize the sediment-water interface to feed. Newly-deposited storm-sands then may become partially redistributed as sandy tunnels into the irregularly bedded muds and silts. These sand-rich burrows enhance the transmissibility of the facies by selective grain channelling, providing conduit-like passageways through otherwise low porosity/permeability sediment. Slightly coarser infill for burrows without access to storm sands may be due to burrowing activity by organisms with a preference for firmer substrates. In the case of incomplete shelf blanketing by storm deposits, organisms may have preferentially sought the coarser sediments for stability advantages.

Figure 20: Grain size distributions for framework constituents surrounding Chondrites versus the grain size of particles filling the burrow, for burrows without access to the stringer sandstone Facies 6. Point counts in excess of 100 grains for each analysis, in both charts.

BURROWS WITHOUT ACCESS TO COARSE FACIES 6

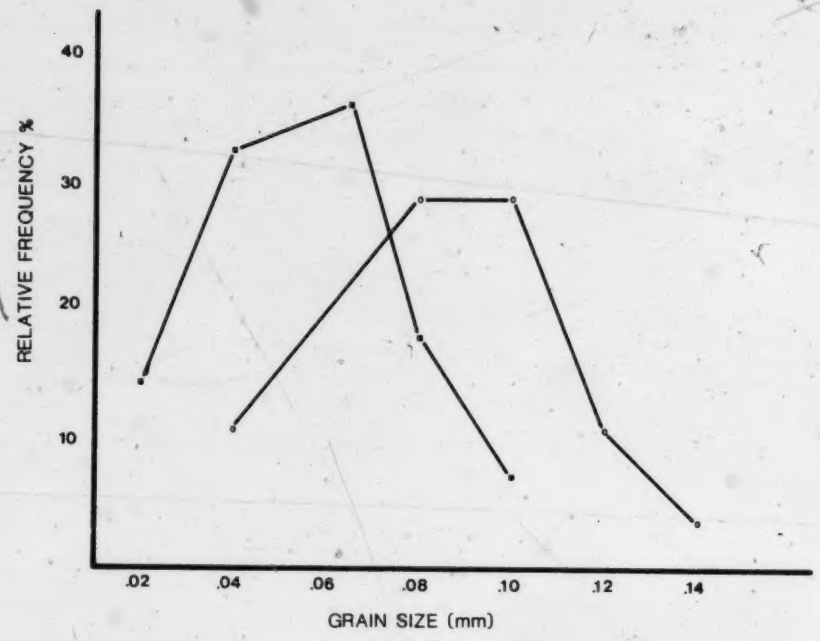

° INFILL SEDIMENT

▪ SURROUNDING SEDIMENT

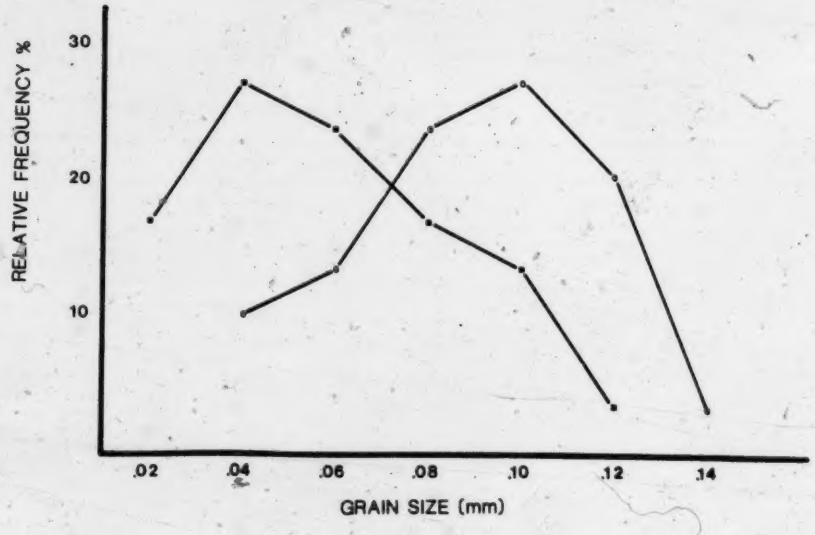

Figure 21: Grain size distributions for framework constituents surrounding Chondrites versus the grain size of particles filling the burrow, for burrows with access to the stringer sandstone Facies 6. Point counts in excess of 100 grains for each analysis, in both charts.

BURROWS WITH ACCESS TO COARSE FACIES **6**

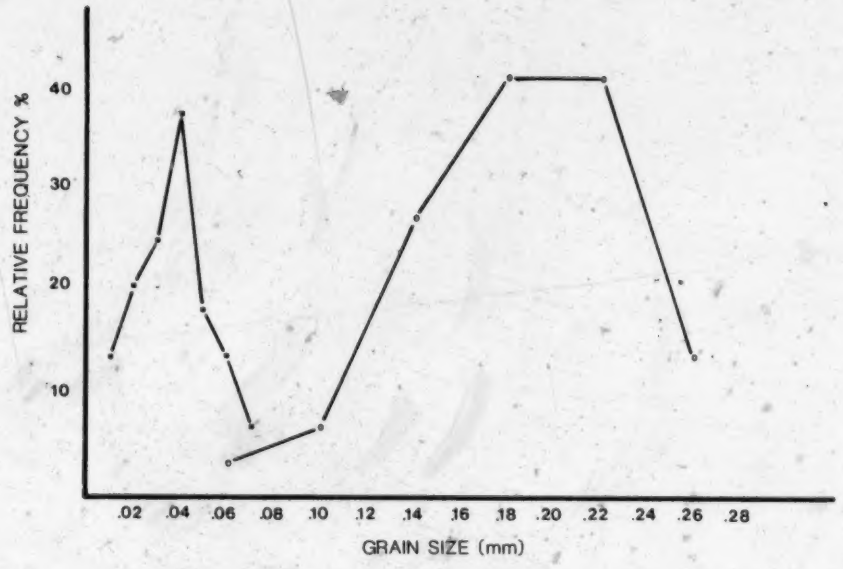

◦ INFILL SEDIMENT

▪ SURROUNDING SEDIMENT

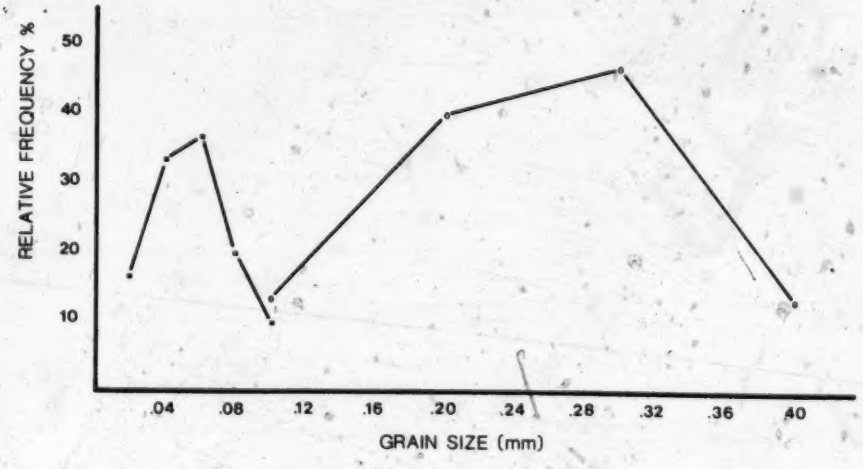

Rock transmissibility is influenced by the macroscopic factors discussed above (stringer sandstone percentage, burrow density and mud percentage)(Figures 22 through 25). Each of these variables was assessed in cored intervals where porosity and permeability had been determined from core analyses. A 35 centimetre by 10 centimetre transparent grid was placed over the core to calculate relative percentages of each component. At each interval the average values from 2-3 measurements were plotted opposite a depth scale with the porosity and permeability. High porosities and permeabilities correspond to an increase in abundance of the stringer sandstone (Facies 6), but are hindered by the presence of mudstone. Rock porosity and permeability also tend to increase with increasing burrow density until burrow density approaches bioturbation levels, at which point porosity and permeability sharply decrease. Upon initial inspection, burrow density appears to increase in zones of stringer sandstone influx, suggesting that the presence of stringer sandstone rather than burrow density is controlling the porosity and permeability. However, in zones lacking significant stringer sandstone, good porosities and permeabilities are found when burrow densities are moderately high, suggesting that both stringer sandstone influx and burrow density are important in the development of porosity and permeability (Figure 25, 1064 metre depth).

Relationships between coarser sandstone, burrow density and mudstone percentages with porosity and permeability are complex (Figure 26). In order to assess the influence of the macroscopic variables or porosity and permeability, statistical analyses were performed on the various wells. A statistically insufficient number of data points within individual wells

required that all data be compiled into one data set to validate analyses. Multiple regression analyses were then performed for both porosity and permeability. The best regression for porosity was found using raw data according to the equation: Porosity = 0.1147 SAND + 0.0302 BURROWS + 0.0320 MUD + 0.0912. The regression coefficient is 0.7378 with a standard deviation of 0.0214. The best regression for permeability was found using transformed data according to the equation: logK = 0.8040 logSAND + 0.9496 logBURROWS - 1.1841 MUD - 0.6688 BURROWS + 2.7077. The regression coefficient is 0.6109 with a standard deviation of 0.499 logK. These regression analyses, however, evaluated the data assuming linear relationships.

Cross-plots of the individual variables plotted against porosity and permeability are not easily understood. This occurs for two reasons: A). lithologic and diagenetic varation between wells, increases scatter; B). the interrelationships of the macroscopic variables. Real trends between porosity and permeability and the factors listed can be seen most effectively when the controlling variables are considered as a group, for individual wells. This problem may be simplified by adding those variables which enhance rock transmissibility and substracting those which hinder rock transmissibility. In this case the stringer sandstone percentage is added to burrow density from which mudstone percentage is then subtracted. The resulting figure can then be plotted against porosity and permeability (Figures 27 to 34).

These cross-plots show real trends. Distinct relationships can be seen between the macroscopic variables and porosity and permeability. Since all variables are expressed as a fraction of one and only the mudstone variable is being subtracted the negative limit an each x-axis is negative 1.

Extrapolation of each curve to this point should predict an approximate minimum porosity and permeability for shale which should approximate zero. Variation in such extrapolation will reflect the influence of additional variables as well as human error in variable percentages calculated. The positive limit along the x-axis is obtained by the summation of the stringer sandstone and burrow density variables; a completely bioturbated sandstone would equal 2.0. A linear function can be applied to the porosity cross-plots while the permeability cross-plots are related by gemetric functions to the macroscopic variables. These relationships illustrate the influence of the designated variables to rock transmissibility. It should be noted that very high burrow densities in the presence of mudstone do not appear to enhance rock transmissibility. This can be noted in well 16-29-5-5W4. Apparently, churning of clay-rich sediment by burrowing organisms results in mud-clogged pore throats upon dewatering. These points were plotted as solid boxes and do not lie on the curves down. Organism burrowing influences rock transmissibility greatest where the rock is 50-80% burrowed, in the presence of some coarser sandstone. The sand-filled burrows provide ideal passageways for fluid migration which become increasingly interconnected with increasing density.

Figure 22: Macroscopic porosity and permeability factors: coarser sandstone, burrowing and mudstone percentages plotted with porosity and permeability at established depth intervals (Porosities and permeabilities taken from core analyses reports provided by Shell Oil).

6-29-5-5W4

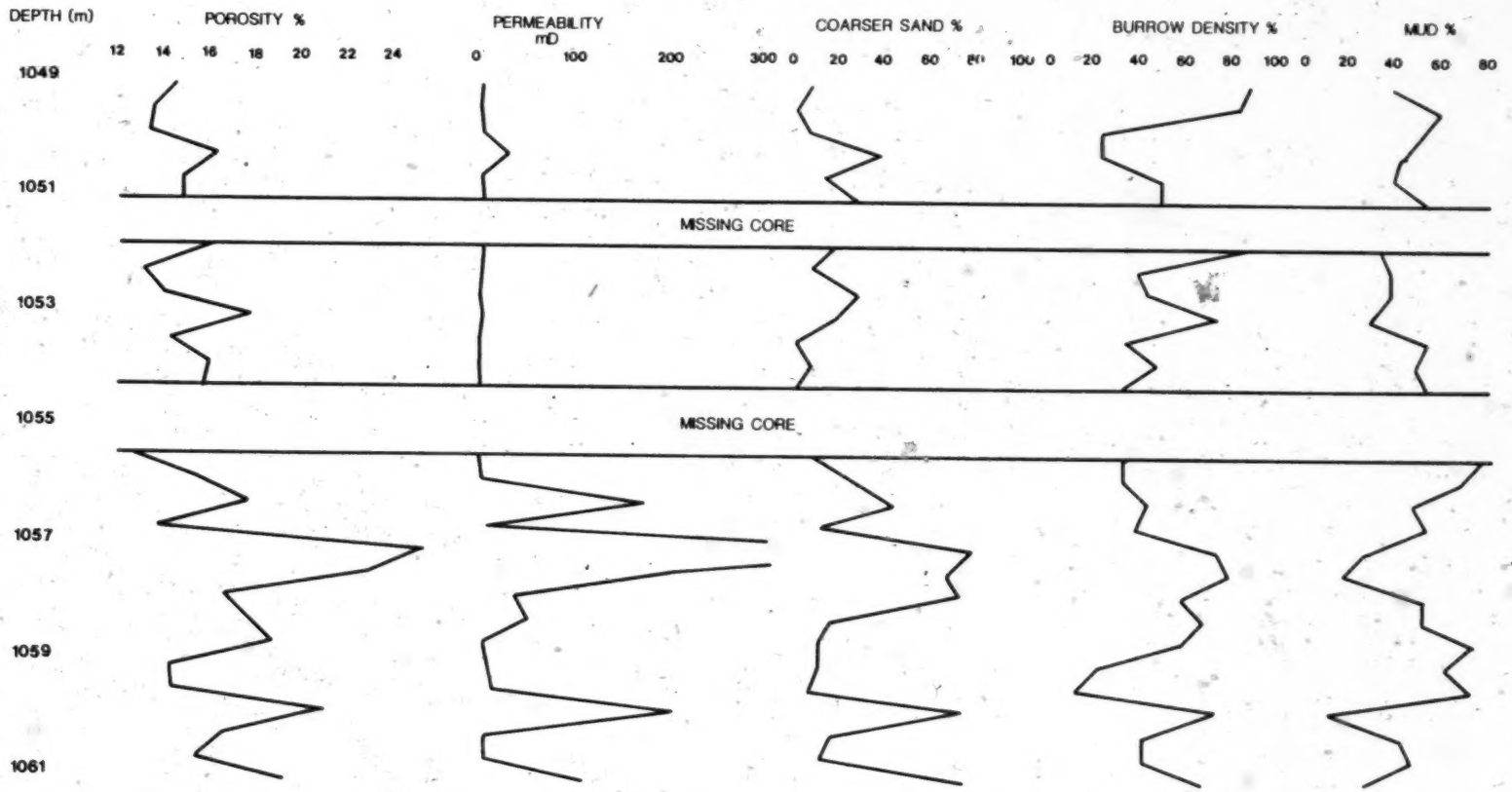
DEPTH (m)
POROSITY %
12 14 16 18 20 22 24
PERMEABILITY mD
0 100 200 300
COARSER SAND %
0 20 40 60 80 100
BURROW DENSITY %
0 20 40 60 80 100
MUD %
0 20 40 60 80
1049
1051
MISSING CORE
1053
1055
MISSING CORE
1057
1059
1061

Figure 23: Macroscopic porosity and permeability factors: coarser sandstone, burrowing and mudstone percentages plotted with porosity and permeability at established depth intervals. (Porosities and permeability taken from core analyses reports provided by Shell Oil).

16-21-5-5W4

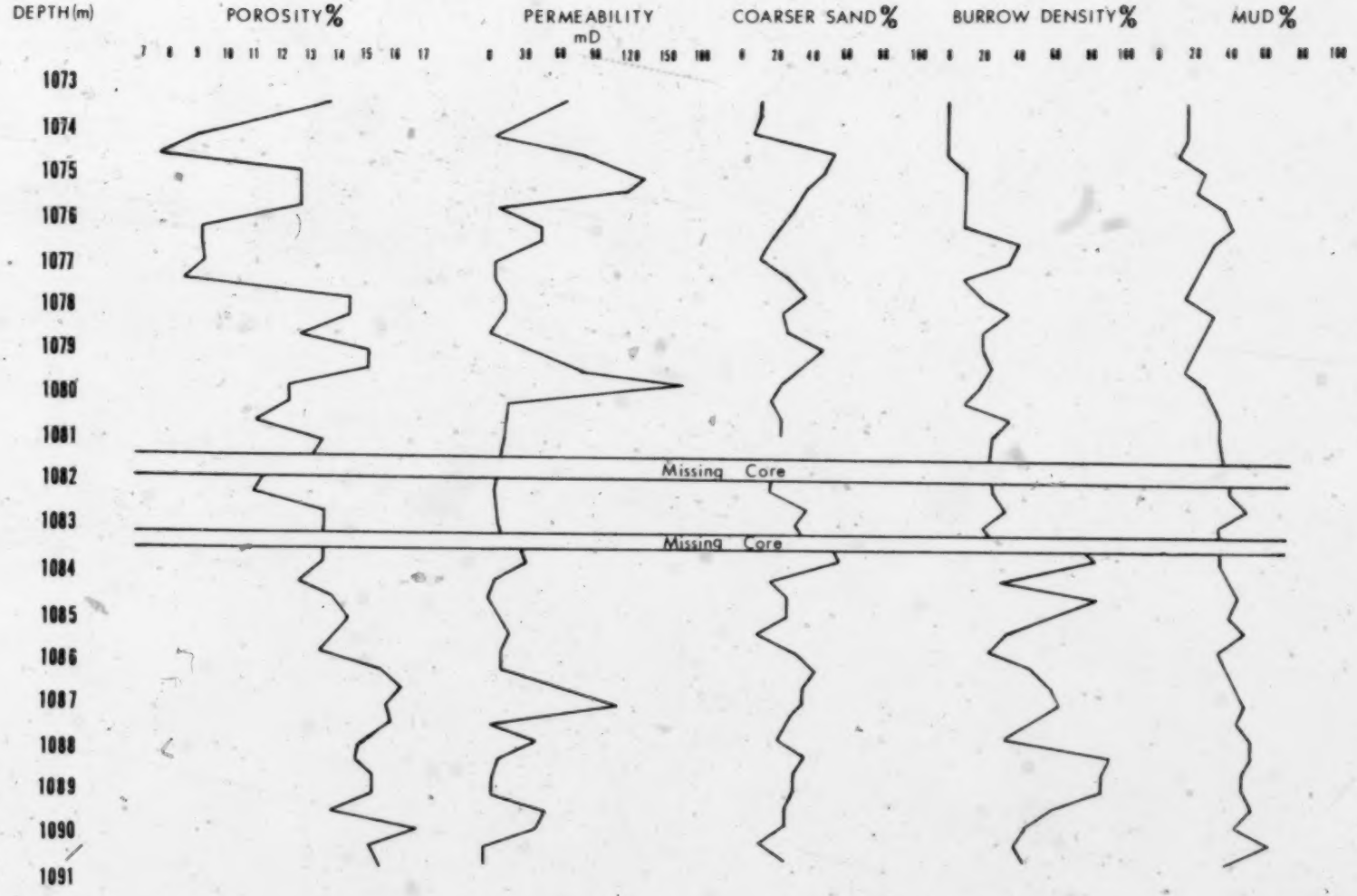
DEPTH(m)
POROSITY %
7 8 9 10 11 12 13 14 15 16 17
PERMEABILITY
mD
0 30 60 90 120 150 180
COARSER SAND %
0 20 40 60 80 100
BURROW DENSITY %
0 20 40 60 80 100
MUD %
0 20 40 60 80 100
1073
1074
1075
1076
1077
1078
1079
1080
1081
1082
1083
1084
1085
1086
1087
1088
1089
1090
1091
Missing Core
Missing Core

Figure 24: Macroscopic porosity and permeability factors: coarser sandstone, burrowing and mudstone percentages plotted with porosity and permeability at established depth intervals. (Porosities and permeabilities taken from core analyses reports provided by Shell Oil).

16-29-5-5W4

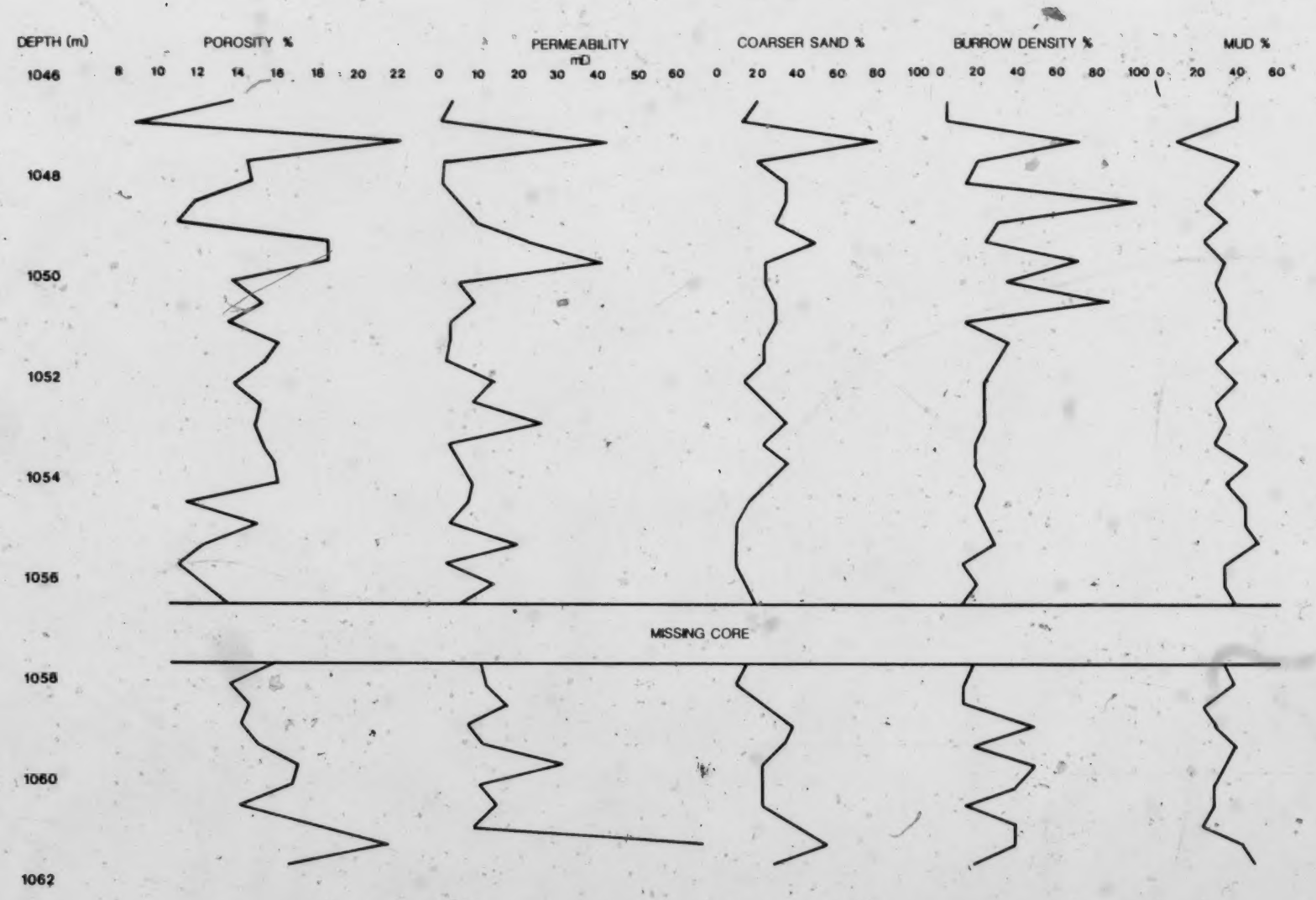
DEPTH (m)
POROSITY %
8 10 12 14 16 18 20 22
PERMEABILITY
mD
0 10 20 30 40 50 60
COARSER SAND %
0 20 40 60 80 100
BURROW DENSITY %
0 20 40 60 80 100
MUD %
0 20 40 60
1046
1048
1050
1052
1054
1056
MISSING CORE
1058
1060
1062

Figure 25: Macroscopic porosity and permeability factors: coarser sandstone, burrowing and mudstone percentages plotted with porosity and permeability at established depth intervals. (Porosities and permeabilities taken from core analyses reports provided by Shell Oil).

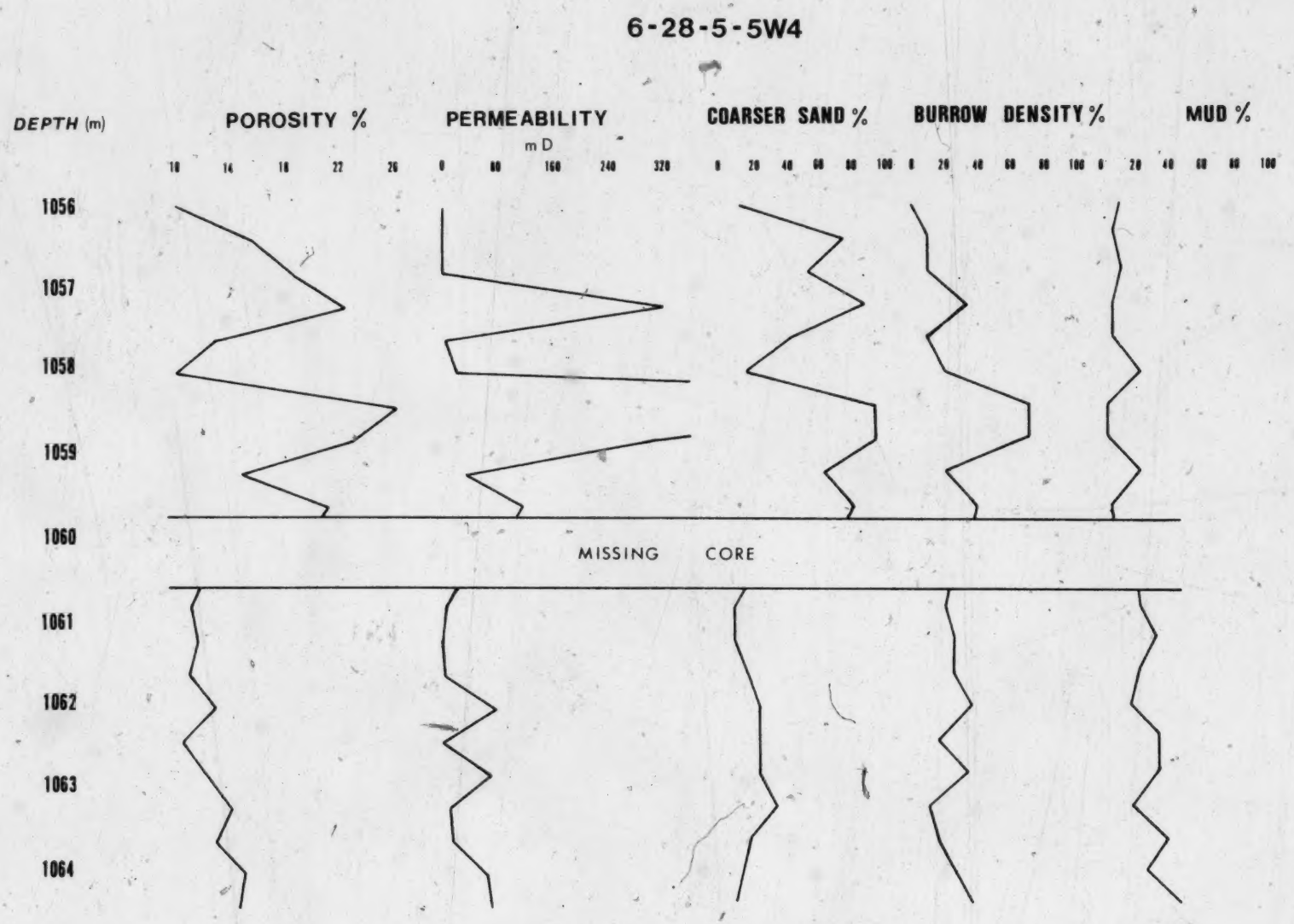
6-28-5-5W4
DEPTH (m)
POROSITY %
PERMEABILITY
mD
COARSER SAND %
BURROW DENSITY %
MUD %
10 14 18 22 26
0 80 160 240 320
0 20 40 60 80 100
0 20 40 60 80 100
0 20 40 60 80 100
1056
1057
1058
1059
1060
MISSING CORE
1061
1062
1063
1064

Figure 26: Crossplots of the macroscopic variables against porosity and permeability.

Independent variables are plotted along the x-axis with the dependent variable porosity plotted along the y-axis. In each of the crossplots the values for both the dependent and independent variables have been scaled between zero and one by the computer, whereby zero define the smallest variable and one the largest. Out of the plane of the diagrams, permeability has been incorporated along the z-axis, with values similarly scaled between zero and one. These permeability axes are subdivided into six equal zones. Points plotted on each of the crossplots are assigned a number which corresponds to the zone along the permeability axis, with permeability systematically increasing from zero to six. Points of lowest permeability values are therefore assigned zero, while highest permeabilities are assigned a six.

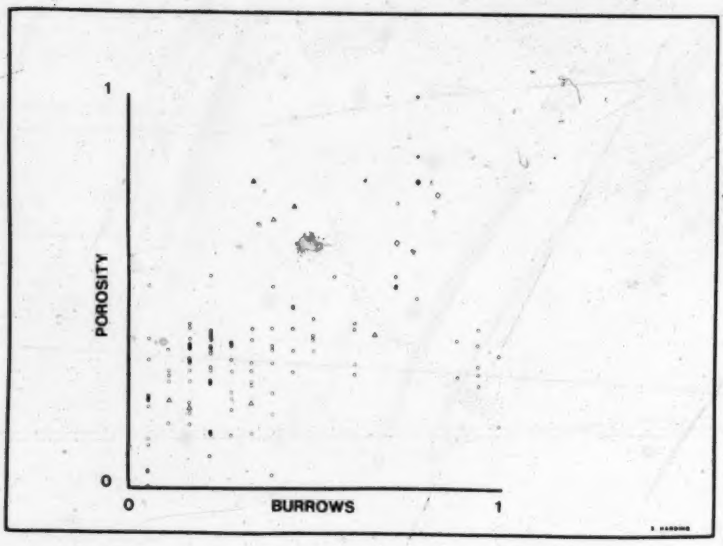
1
POROSITY
0
0
BURROWS
1

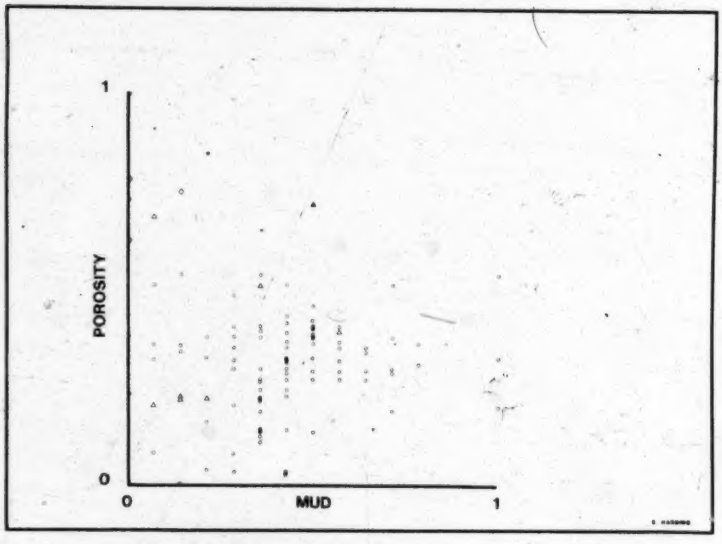
1
POROSITY
0
0
MUD
1

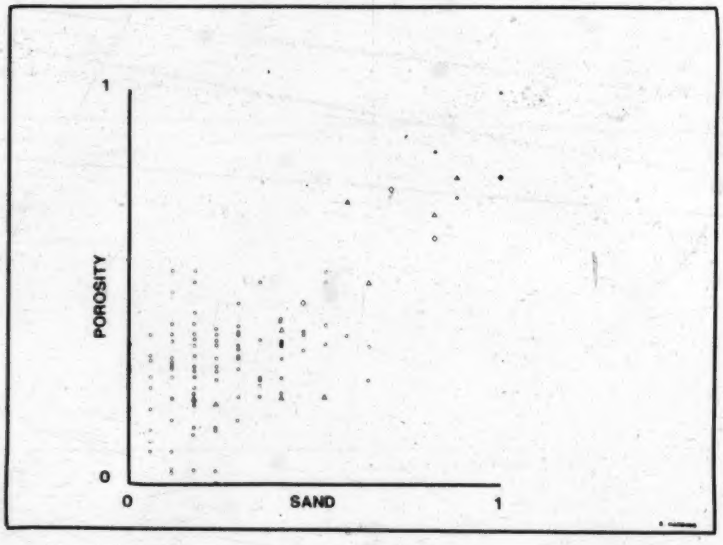
1
POROSITY
0
0
SAND
1

Figure 27: Porosity vs. macroscopic variables cross-plot (6-29-5-5W4) illustrating a linear relationship. (Stringer Sandstone + Burrow Density - Mudstone Percentage)

Note: Solid points designate bioturbated zones and were not considered when constructing the curve.

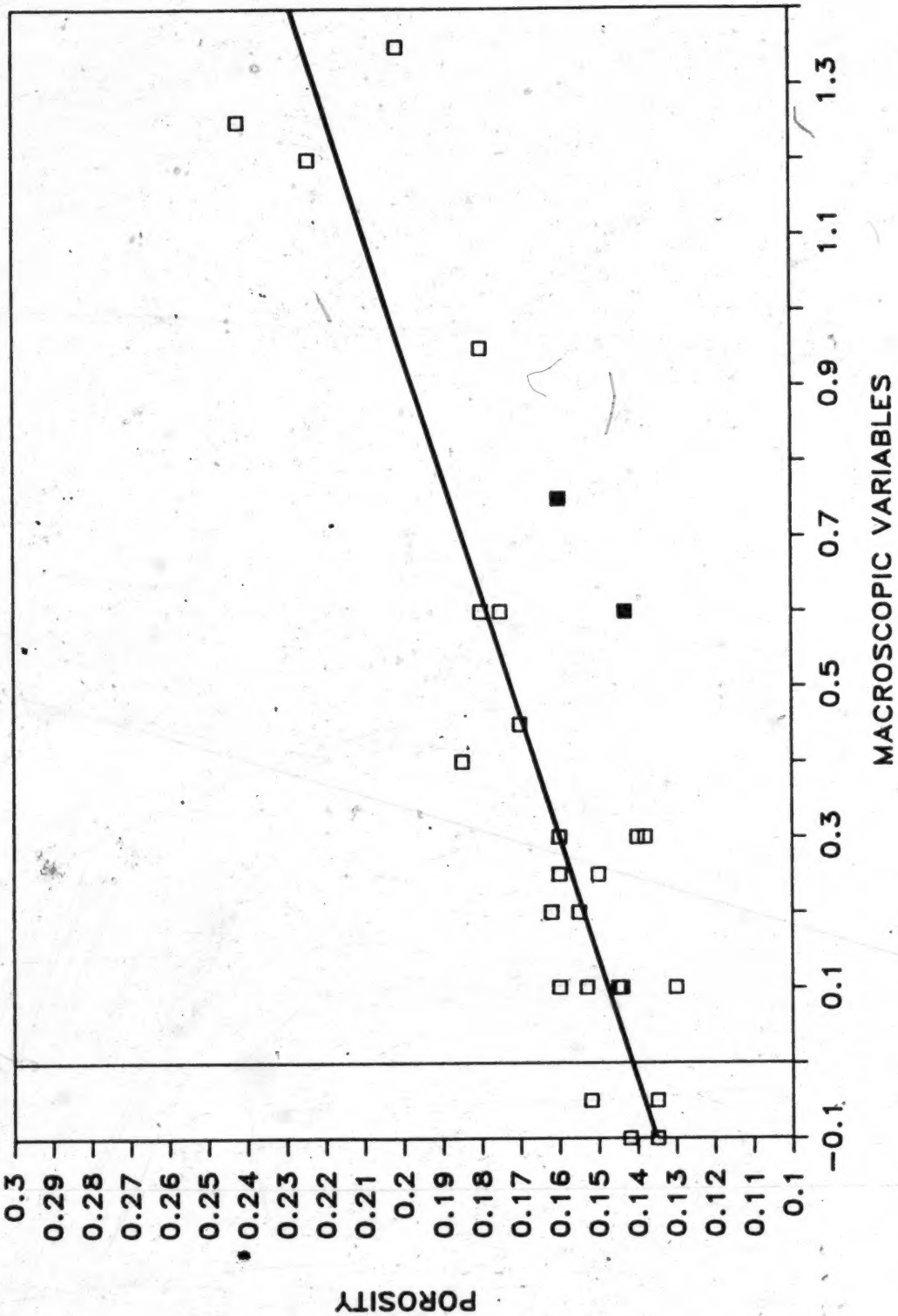
6-29
POROSITY
0.3
0.29
0.28
0.27
0.26
0.25
0.24
0.23
0.22
0.21
0.2
0.19
0.18
0.17
0.16
0.15
0.14
0.13
0.12
0.11
0.1
−0.1
0.1
0.3
0.5
0.7
0.9
1.1
1.3
MACROSCOPIC VARIABLES

Figure 28: Permeability vs. macroscopic variables cross-plot (6-29-5-5W4) illustrating a geometric relationship. (Stringer Sandstone + Burrow Density - Mudstone Percentage)

Note: Solid points designate bioturbated zones and were not considered when constructing the curve.

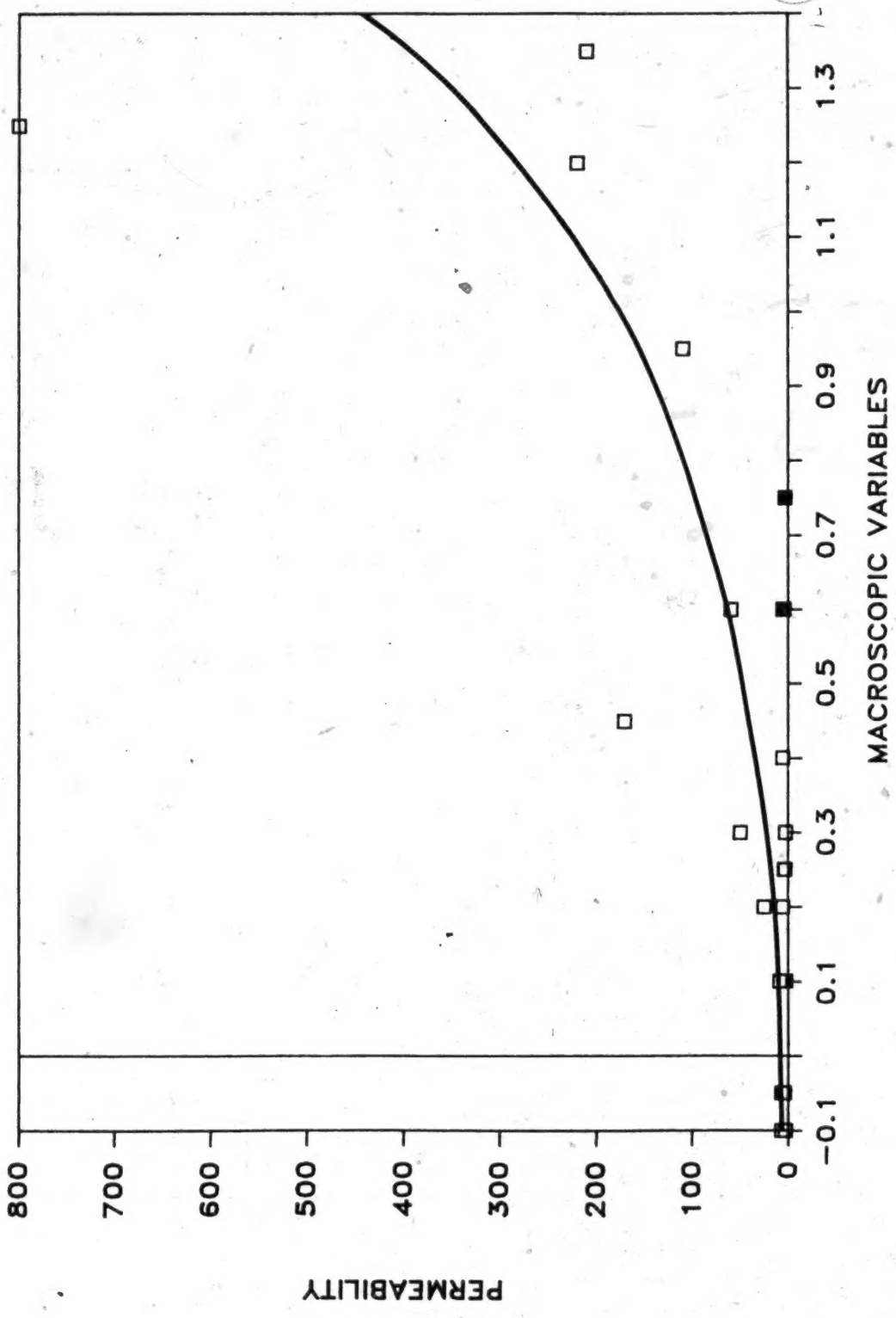
PERMEABILITY
800
700
600
500
400
300
200
100
0
−0.1
0.1
0.3
0.5
0.7
0.9
1.1
1.3
MACROSCOPIC VARIABLES

6−29

Figure 29: Porosity vs. macroscopic variables cross-plot (16-21-5-5W4) illustrating a linear relationship. (Stringer Sandstone + Burrow Density - Mudstone Percentage)

Note: Solid points designate bioturbated zones and were not considered when constructing the curve.

16-21

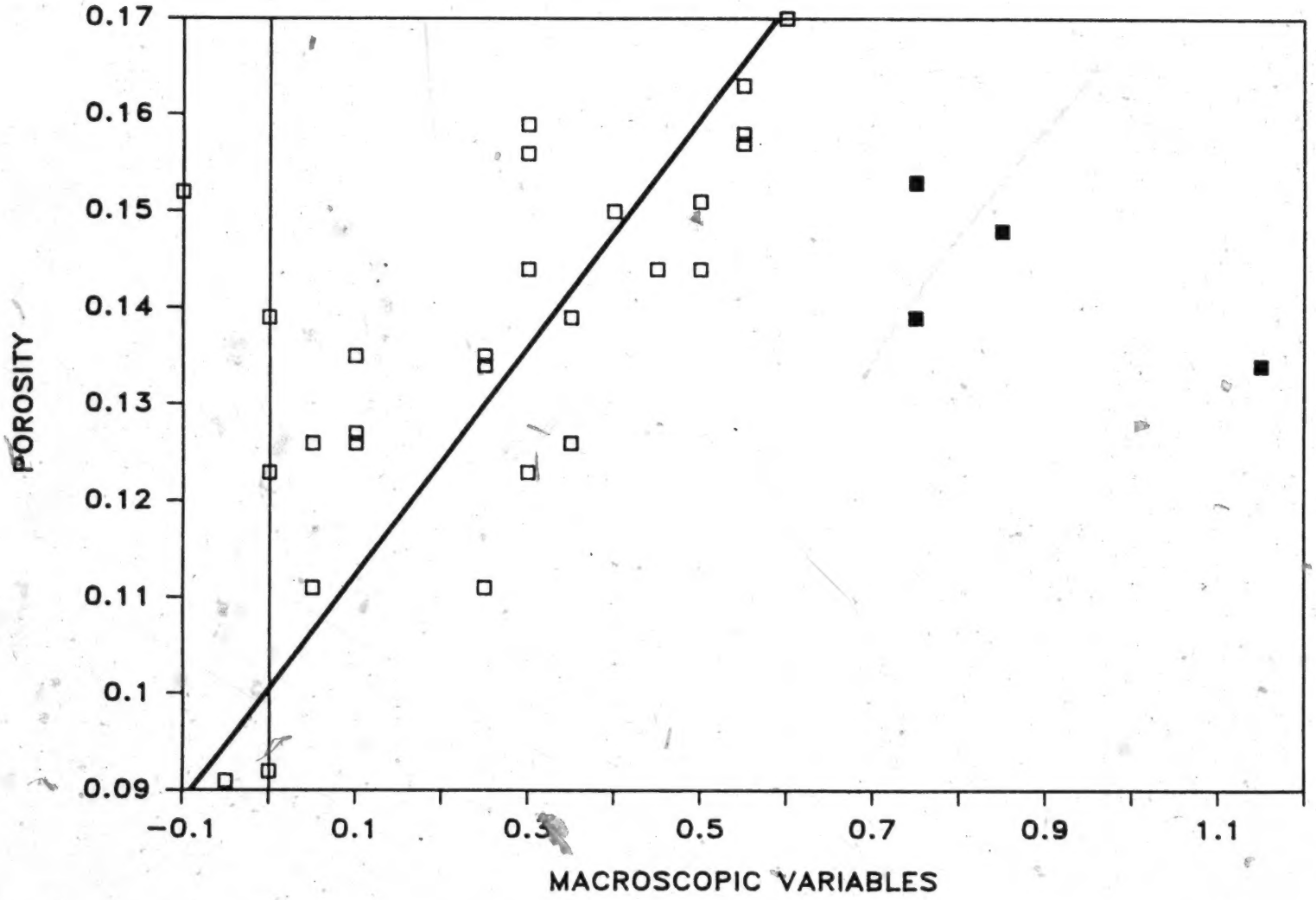
0.17
0.16
0.15
0.14
0.13
0.12
0.11
0.1
0.09
POROSITY
-0.1
0.1
0.3
0.5
0.7
0.9
1.1
MACROSCOPIC VARIABLES

Figure 30: Permeability vs. macroscopic variables cross-plot (16-21-5-5W4) illustrating a geometric relationship. (Stringer Sandstone + Burrow Density - Mudstone Percentage)

Note: Solid points designate bioturbated zones and were not considered when constructing the curve.

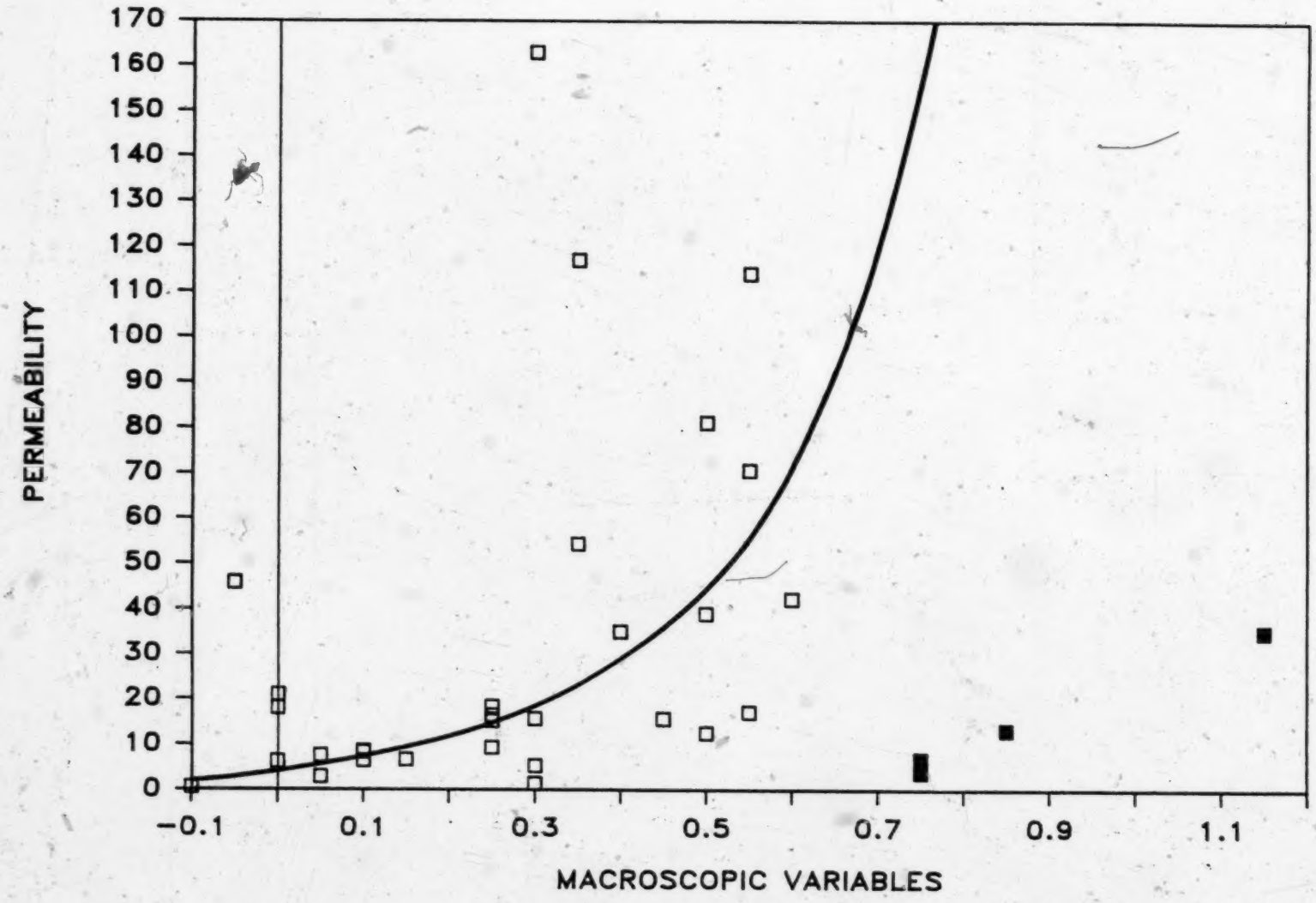
PERMEABILITY
170
160
150
140
130
120
110
100
90
80
70
60
50
40
30
20
10
0
−0.1
0.1
0.3
0.5
0.7
0.9
1.1
MACROSCOPIC VARIABLES

Figure 31: Porosity vs. macroscopic variables cross-plot (16-29-5-5W4) illustrating a linear relationship. (Stringer Sandstone + Burrow Density - Mudstone Percentage)

Note: Solid points designate bioturbated zones and were not considered when constructing the curve.

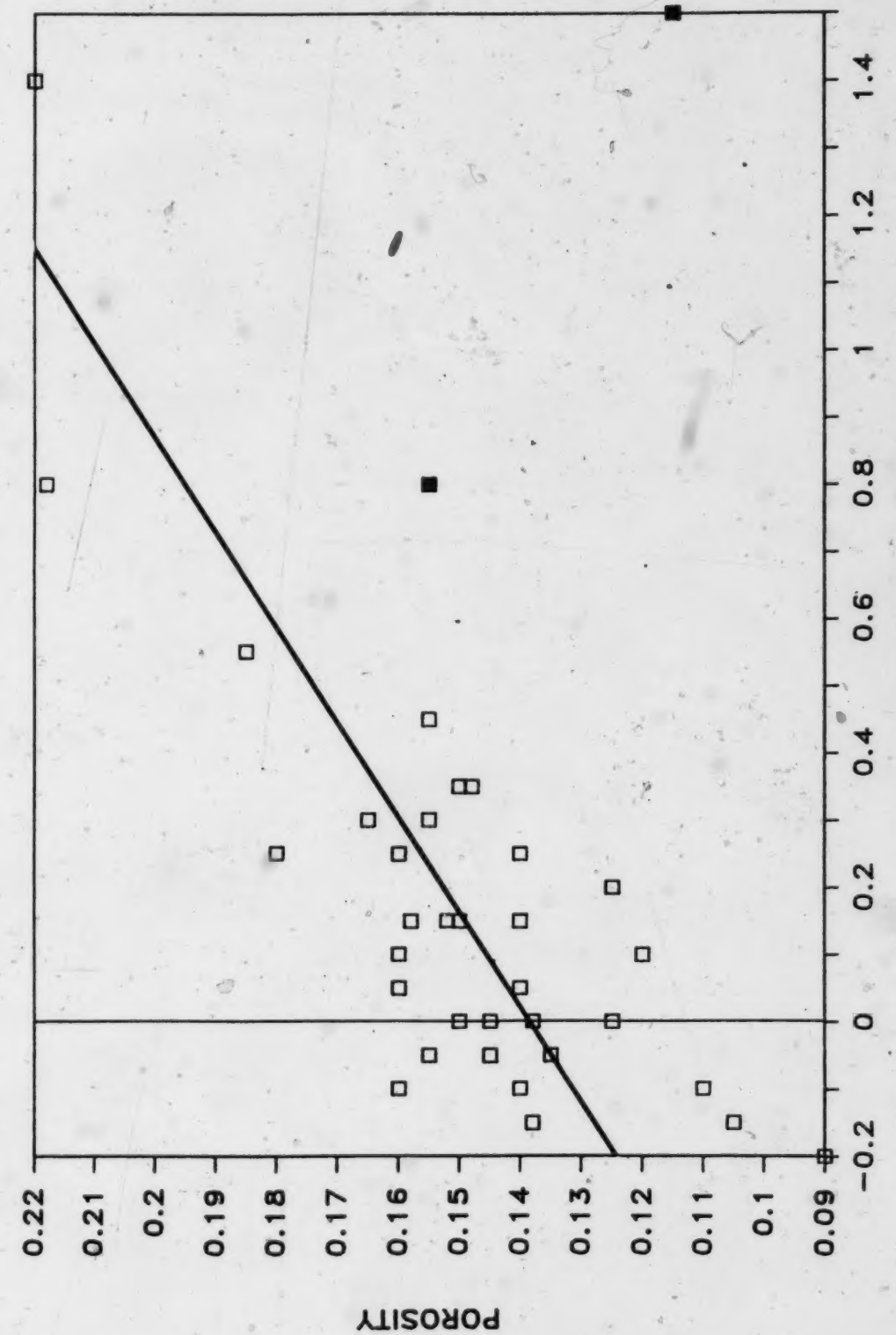
16-29
POROSITY
0.22
0.21
0.2
0.19
0.18
0.17
0.16
0.15
0.14
0.13
0.12
0.11
0.1
0.09
−0.2
0
0.2
0.4
0.6
0.8
1
1.2
1.4
MACROSCOPIC VARIABLES

Figure 32: Permeability vs. macroscopic variables cross-plot (16-29-5-5W4) illustrating a geometric relationship. (Stringer Sandstone + Burrow Density - Mudstone Percentage)

Note: Solid points designate bioturbated zones and were not considered when constructing the curve.

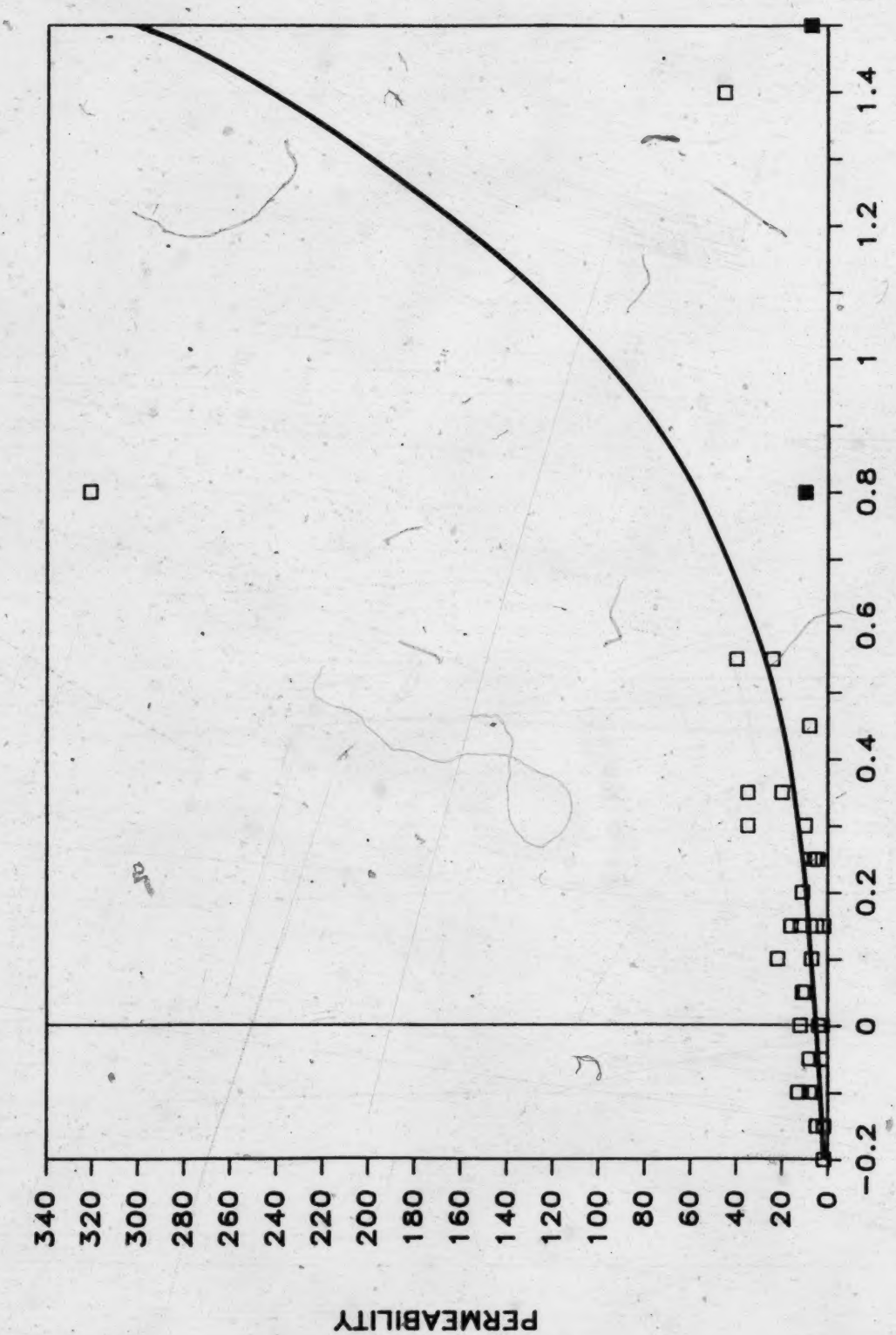
16-29
PERMEABILITY
340
320
300
280
260
240
220
200
180
160
140
120
100
80
60
40
20
0
−0.2
0
0.2
0.4
0.6
0.8
1
1.2
1.4
MACROSCOPIC VARIABLES

Figure 33: Porosity vs. macroscopic variables cross-plot (6-28-5-5W4) illustrating a linear relationship. (Stringer Sandstone + Burrow Density - Mudstone Percentage)

Note: Solid points designate bioturbated zones and were not considered when constructing the curve.

6-28

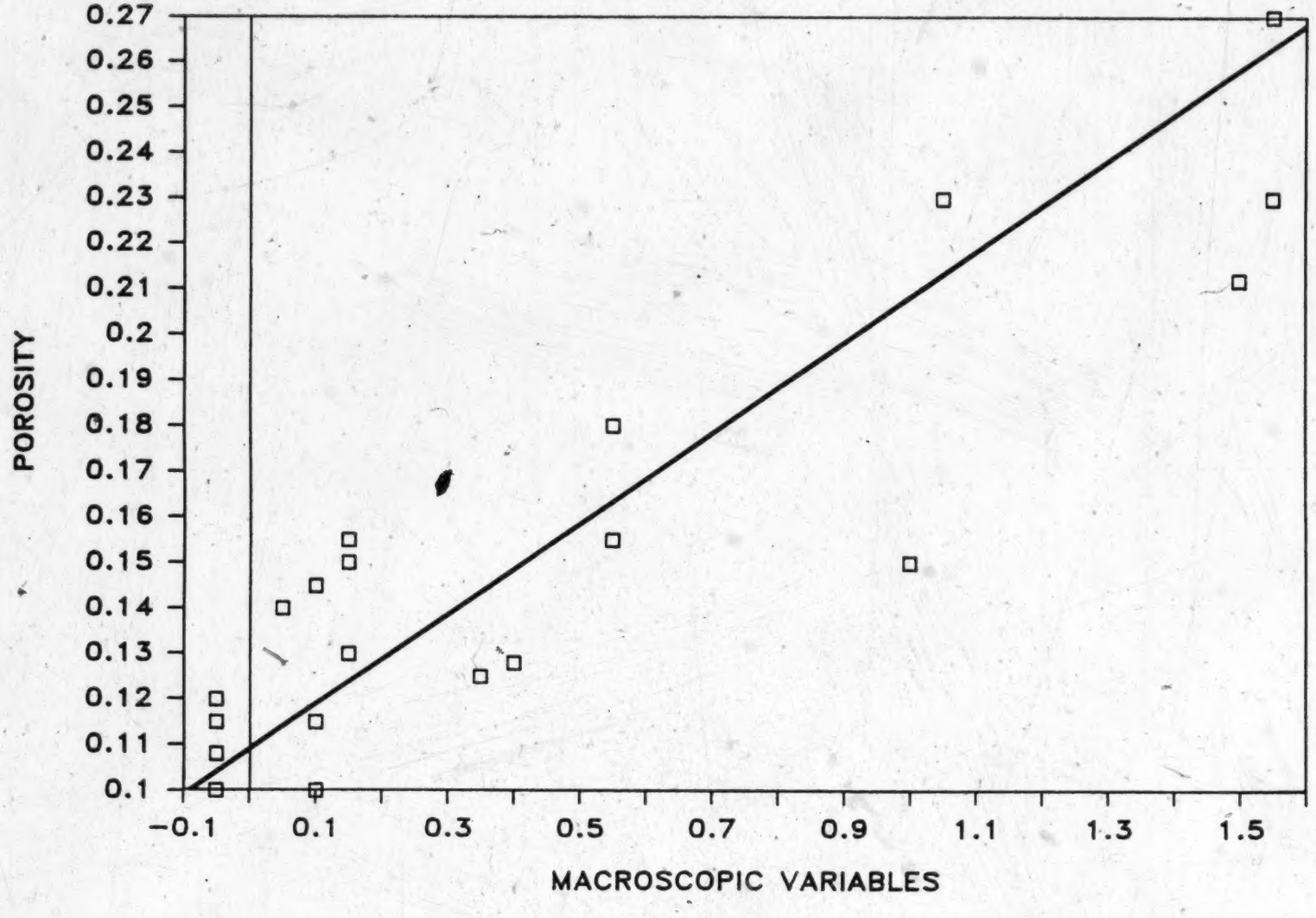
0.27
0.26
0.25
0.24
0.23
0.22
0.21
0.2
0.19
0.18
0.17
0.16
0.15
0.14
0.13
0.12
0.11
0.1
POROSITY
−0.1
0.1
0.3
0.5
0.7
0.9
1.1
1.3
1.5
MACROSCOPIC VARIABLES

Figure 34: Permeability vs. macroscopic variables cross-plot (6-28-5-5W4) illustrating a geometric relationship. (Stringer Sandstone + Burrow Density - Mudstone Percentage)

Note: Solid points designate bioturbated zones and were not considered when constructing the curve.

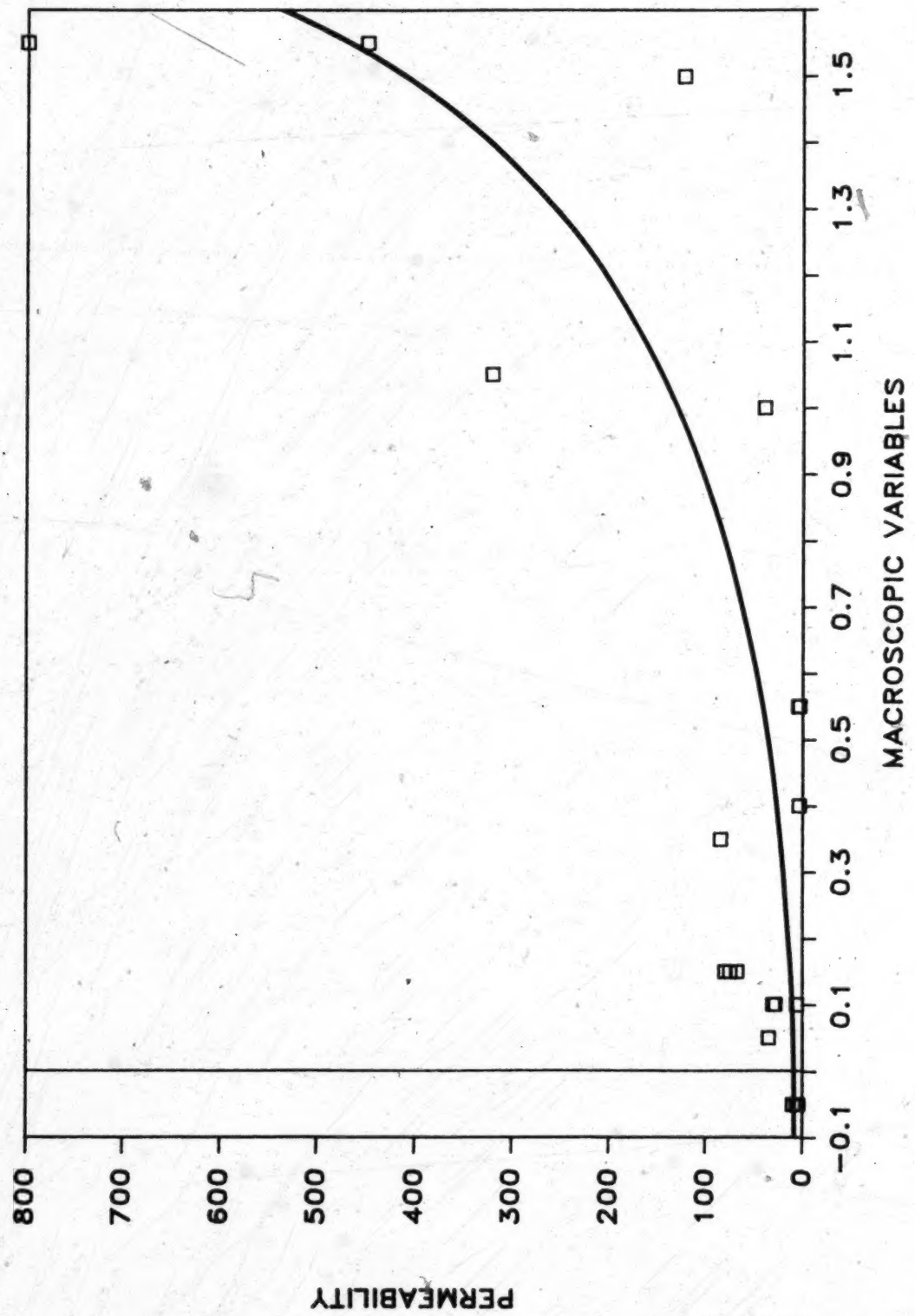
6-28
PERMEABILITY
800
700
600
500
400
300
200
100
0
−0.1
0.1
0.3
0.5
0.7
0.9
1.1
1.3
1.5
MACROSCOPIC VARIABLES

IX. Diagenetic Processes in the Swift Formation

A. Introduction

The Swift Formation is composed of a complex suite of lithologies and the sedimentary particles of a given lithology may display considerable variation. Deposition of abundant clays and organic detritus amidst the framework constituents has greatly complicated the initial chemistry of the sediment. Chemical diagenesis is the product of reactions between minerals and aqueous solutions migrating through the pore network (Hayes, 1979). Pore chemistry constantly changes with increasing pressure and temperature, producing changes in the stable mineral phases within the sedimentary assemblage. Mineral authigenesis and solution provide information about the processes associated with diagenesis and rock transmissibility. The intensity of diagenesis also controls the porosity and permeability of the lithologies.

As sediments become buried and the overlying water no longer readily circulates into them, the chemical system becomes effectively closed. Dapples (1962) recognized closed systems developing in sands at a depth of only a few feet. For interlaminated clay-rich sediments such as those in the Swift Formation, this condition was likely reached at even shallower depths, shortly after burial. By effectively creating a closed system, the sedimentary particles are allowed to equilibrate with the interstitial waters. It is under these conditions that new chemical species may be produced as the result

of pore fluid saturation and precipitation along increasing pressure/temperature gradients. Diagenesis may also occur by oxidation-reduction reactions between mineral constituents, catalyzed by pore fluids. Within the Swift Formation the most important diagenesis minerals are iron compounds and clays. Silica redistribution is also an important process. The chemical and environmental implications of iron compound diagenetic has been discussed at length in Chapter 5 and will not be repeated here.

B. Clay Minerals

The difficulty in recognizing authigenic versus detrital clay in both lithified and unlithified sediments has been alluded to by Powers (1957). Estimation of relative concentrations for sediments exhibiting detrital and diagenetic clays may be further complicated by uneven distributions within a

particular depositional basin. Scanning electron microscopy of the Swift lithologies shows the presence of both authigenic and detrital clay. The origins of individual clay particles cannot always be unequivocally determined.

Authigenic clay minerals may develop in sediments by the processes of neoformation or regeneration (Wilson and Pittman, 1972). Neoformation represents the secondary production of minerals as a direct precipitate, while regeneration accomplishes mineral formation through reactions between precursor materials and the contained waters. The products of both of these processes are observed in the Swift Formation. Kaolinite, the dominant diagenetic clay, is typically present as psuedohexagonal platelets of recrystallized origin. This recrystallized or regenerated variety represents detrital kaolinite which has undergone structural transformation during diagenesis and catagenesis, with the formation of new crystal lattices from primary ones. Kaolinite authigenesis from a feldspar precursor is a second variety of regeneration observed in the Swift ribbon sediments (Plate 9B and 10B).

The majority of authigenic pore-filling kaolinite does not appear to be directly related to mineral regeneration. Instead most of the clay cement has probably precipitated out of formation waters. Reducing conditions during early burial, however, are inferred from the authigenesis of ferrous compounds. Oxidizing waters in the subsurface may be attributed to fresh water infiltration during subaerial exposure between Oxfordian and Aptian times (spanning approximatley 40 million years). Meteoric circulation into the Swift Formation is supported by the presence of hematized biotite and hematite cement throughout much of the ribbon sediments. In some cores, iron oxide "halos" are also observed surrounding siderite concretions.

Illitic coatings appear to be present on some of the quartz grains of Facies 4 and 6; however, the degree of argillaceous film development is difficult to assess. A smectite precipitate is also sporadically observed near the erosional upper contact of Facies 5, but is only a minor component where present. This mineral was likely deposited by the downward percolation of pore waters (illuviation) during subaerial exposure.

C. Quartz

Estimation of the silica budget for the Swift ribbon sediments, is a complicated task. Silica sources will be examined first.

Solution of grain constituents (especially chert fragments) by corrosive pore fluids may have generated substantial amounts of silica. This is best exemplified in the sediments of Facies 6 in which the microcrystalline chert fragments often display extensive diagenetic corroding. The abundance of this mineral, particularly in the coarser sands of Facies 6, may have allowed a substantial influx of silica into the burial environment. The diagenetic leaching of feldspar provides an additional source of silica.

The redistribution of silica within buried sediments is greatly influenced by the clay content, clay composition and the spatial distribution of the clay particles. Development of discrete clay coatings on grains (observed in Facies 6, and to a lesser extent Facies 4) may act as catalysts to enhance the pressure solution of silica (Heald, 1956). Blatt (1980) showed in silica conservation studies that clay coatings probably provide multilayer pathways for fluid migration, otherwise severly restricted by grain to grain contacts. In this way great volumes of silica-rich fluids may escape down

pore throats and supply silica to grain margins (quartz overgrowths). Feldspar overgrowths on partially etched grains are occasionally observed within the ribbon sediments. Throughout the Swift Formation, however, it appears that much of the silicate fluid was incorporated into authigenic kaolinite, as shown in Plate 10B.

X. Diagenetic Controls or Porosity and Permeability

Primary intergranular porosity is typically altered or destroyed during diagenesis (Pittman, 1979). Secondary porosity results from the solution of soluble materials in a sedimentary assemblage under elevated pressures and temperatures. Microporosity, commonly associated with argillaceous sandstones, exists primarily between clay minerals or at pore throat restrictions (Pittman, 1979). The type of porosity, in conjunction with the pore geometry and pore distribution patterns is essential to understanding the reservoir geology (Pittman, 1979).

Within the Swift Formation, solution of sedimentary material during diagenesis is the most important control on porosity and permeability. Secondary porosity is best developed within the stringer sandstones (Facies 6).

Porosity is most readily enhanced by the diagenetic removal of cementing agents (Schmidt and McDonald, 1979). In the coarser sandstone lenses, solution of a calcium carbonate cement is important. In some instances, traces of calcium carbonate are observed bordering grains, which have subsequently become encased in a hematite or clay cement. Less commonly, calcium carbonate cements grains in tight pore spaces, which may have been isolated from leaching fluids. Cement solution is also indicated by oversized

and elongated pore spaces (Plates 11A, B and C). Pore enlargement is commonly accomplished by the additional solution of syntaxial or fringing cement (Schmidt and MacDonald, 1979) however grain boundaries bordering enlarged pores within the Swift sandstones are typically not corroded and may show distinct overgrowths. Solution of intergranular carbonate cement and preferential grain solution is suspected. This process is accomplished by pore fluids migrating through the sediments after lithification. Thermomaturation of organic matter releases carbon dioxide which readily generates carbonic acid in the burial regime (Momper, 1980; Al-Shaieb and Shelton, 1981). Carbonic acid is the primary reagent responsible for leaching the carbonate component and developing secondary porosity (McBride, 1977).

Increasing the concentration of carbon dioxide in the pore fluids also enhances feldspar solution. Corroded and "honeycombed" grains are a useful indicator of secondary porosity (Plate 10A). Honeycombed grains are produced by preferential etching along crystallographic planes. Both orthoclase and plagioclase feldspar display the best examples of this form of diagenetic texture.

Grain molds are also present within the sandstones of the Swift Formation. The resulting pore spaces preserve characteristic outlines of the precursor grain (Plate 11B). The notable absence of calcium carbonate detritus and Fe-Mg rich minerals may suggest their preferential solution during diagenesis. However, the partial solution of feldspar and chert within most of the Swift lithologies, illustrates the potential for the removal of these mineral phases.

Kaolinite is the dominant cementing agent in the Swift Formation. Particles of this mineral are often loosely packed between the framework constituents and do not produce an effective seal to all pore fluids.

Microporosity, although individually not of critical importance to rock transmissibility, may be significant in conjunction with macroporosity (Kieke and Hartmann, 1973; Pittman, 1979). Irreducible water, for example, may be displaced into micropores by hydrocarbons filling intergranular pores (Pittman, 1979). Because of its relatively large size and loose attachment, kaolinite may present additional problems to rock transmissibility; high shear stresses associated with well production may dislodge the kaolinite booklets and squeeze them into pore throats, effectively reducing permeability (Almon and Davis, 1981). This has been a problem with Swift Formation production in some wells (Howard Pitts, Home Oil - pers. comm.; Al Polischuk, Shell Oil - pers. comm.).

Quartz overgrowths do not greatly influence the porosity or permeability of the ribbon sediments. The extent of porosity and permeability reduction due to quartz overgrowths is minor, although some advanced intergrowths are observed within the stringer sandstone reservoirs (Facies 6) (Plate 12).

Microfracturing commonly occurs in the dark ribbon sediments. Passageways so produced undoubtedly enhance the permeability of the Swift ribbon sediments. Oxidation of organic detritus during thermomaturation can generate abnormally high pore pressures, as fluids and gases released from the organic matter are of much greater volume than was the residual organic matter (Momper, 1980). Because organic accumulation is commonly associated with tightly sealed argillaceous laminae, pressure release may only be possible by fracturing the rock. The resulting microfractures provide excellent passageways for fluid migration. In Plate 13, fluid migration through the microfracture is inferred by the development of calcium carbonate rhombs along the inner surface of the microfracture.

XI. Interpretations and Conclusions

The Swift Formation is a coarsening-upwards sequence which records a shallowing-upwards, depositional episode. The sediments were deposited in a predominantly offshore marine setting, with nearshore influence beginning within the uppermost light ribbon sediment. Support for this facies model may be drawn from the observation listed below.

Sedimentation was dominated by settling from suspension. The interstratification of coarse and fine lithologies within the ribbon sediment suggests periodic deposition. Mud was deposited from offshore flowing advective currents, while silts and very fine grained sands were deposited from moderate energy nepheloid flows induced by offshore flowing currents. The depositional energy gradient increases upsection as illustrated by: a) the relative decrease in detrital mudstones b) an increase in the grain size of framework sediment c) an increased percentage and better development of small-scale trough cross-stratification. Medium grained sand stringers were deposited from high energy storm-induced sediment gravity flows.

The transitions in the clay mineral suites suggest a shallowing-upwards sequence. Basal ribbon sediments show assemblages characteristic of an offshore environment, while clay mineral suites higher in the Swift sequences are typically associated with more nearshore to onshore environments. This is further supported by authigenic iron compounds which record an oxidation gradient upsection. Resulting compounds may correspond to the extent of organic matter oxidation prior to deep burial. Glauconite, a typical indicator of marine sediments, persists into the upper regions of the light ribbon sediment facies.

Porosity and permeability may be evaluated using the percentages of a) sandstone stringers b) burrow density and c) mudstone. The transmissibility of the rock was enhanced during diagensis by the development of secondary porosity in the coarser stringer sandstones, and small-scale fractures throughout the Swift ribbon sediments.

Reservoir development within the Swift Formation is predominantly associated with coarser sandstone accumulation (Facies 6). Greatest accumulation of Facies 6 was noted in section 29 of Township 5, Range 5W4M, to the northwest of an apparent offshore shoal. This represents a potential target for future exploration.

PLATES

PLATES

Plate 1: Shell Manyberries 14-5-6-5W4 1083 metres

Lenticular - silt-streaked dark ribbon sediments (Facies 2). This lithofacies is dominated by dark, organic-rich shales.

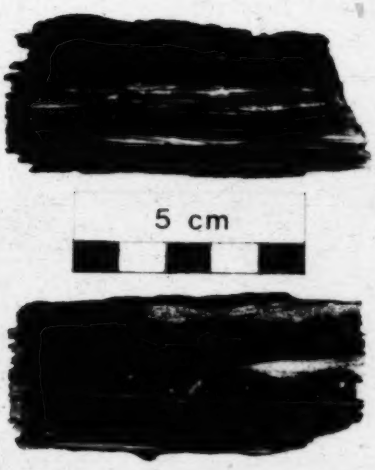
5 cm

Plate 2A: Shell Manyberries 14-5-6-5W4 1075 metres

Wavy-irregular dark ribbon sediments (Facies 3). Low burrow density - note: sand stringer just below the centre of the photograph which is loaded into the ribbon sediments.

Plate 2B: Shell Manyberries 6-29-5-5W4 1052 metres

Facies 3 displaying high burrow density, approaching complete bioturbation and sediment homogenation.

A

B

Plate 3: Shell Manyberries 14-5-6-5W4 1065 metres

Light ribbon sediments (Facies 4). Typical sedimentation patterns with sand stringer near the centre of plate A. Small dark specks are millimetre scale siderite concretions.

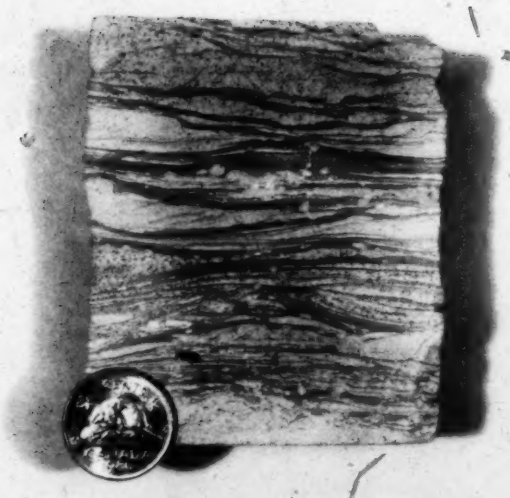

Plate 4: Shell Manyberries 14-5-6-5W4 1059.9 metres

Massive silty-sandstone (Facies 5). Photograph of the primarily structureless lithology of the uppermost lithofacies.

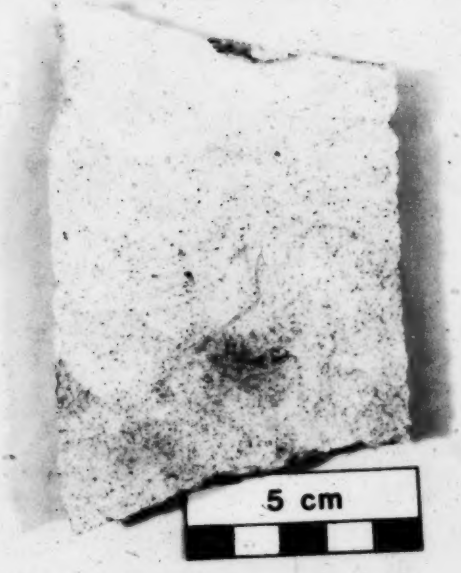
5 cm

Plate 5: Shell Manyberries 16-29-5-5W4 1085 metres

A.) Photomicrograph of thin sandstone stringer (Facies amidst the dark ribbon sediments of Facies 3. B.) Sandstone stringer loaded into the encompassing dark ribbon sediments of Facies 3.

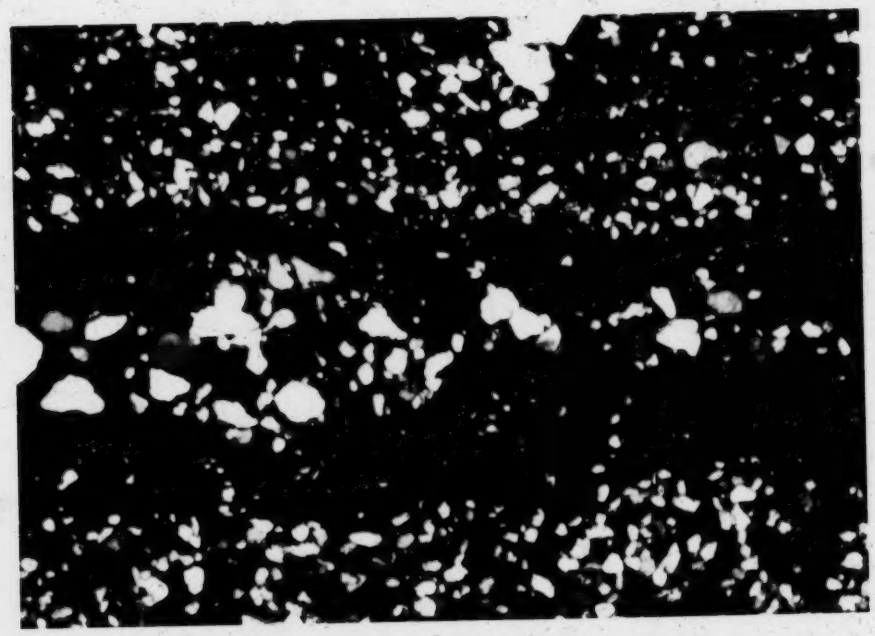

A

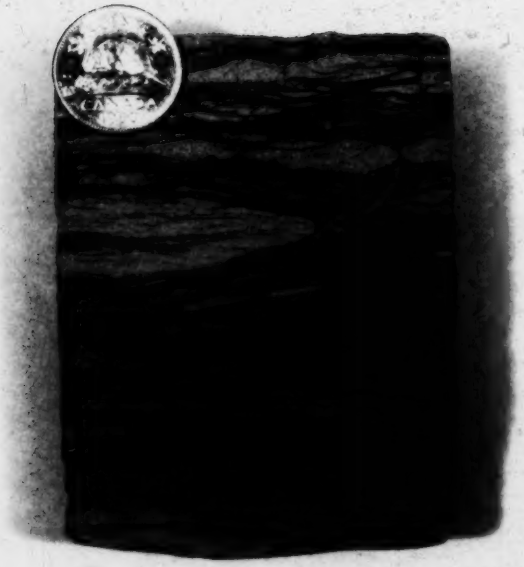

B

Plate 6A: Shell Manyberries 8-29-5-5W4 1052.5 metres

Photomicrograph of the dark ribbon sediments.

Plate 6B: Shell Manyberries 14-5-6-5W4 1076 metres

Photomicrograph of the light ribbon sediments. In both instances the framework appearance displays little porosity or permeability development.

A

B

Plate 7A: Shell Manyberries 14-5-6-5W4 1064.8 metres

Spherulitic siderite observed near the top of Facies 4 (light ribbon sediment).

Plate 7B: Shell Manyberries 6-29-5-5W4 1055.2 metres

Organic detritus observed on the upper surface of a sandstone stringer in Facies 3.

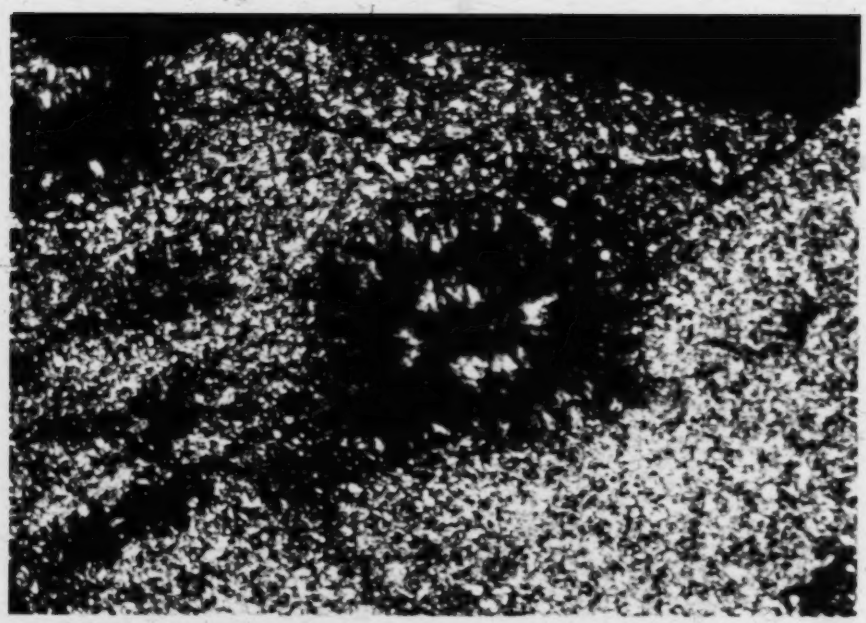

A

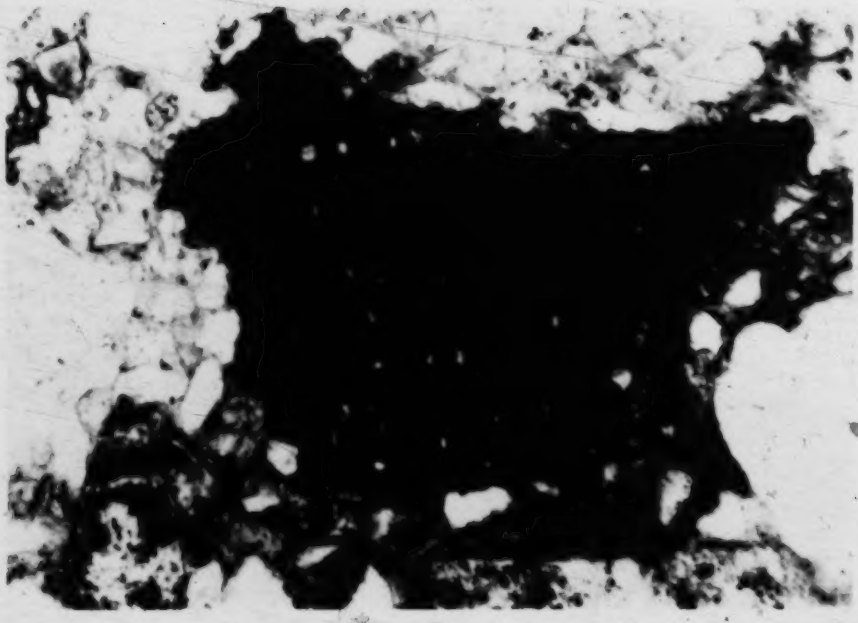

B

Plate 8A: Shell Manyberries 14-5-6-5W4 1083 metres

Glauconite-rich burrow infill observed in Facies 2.

Plate 8B: Shell Manyberries 16-21-5-5W4 1085 metres

Sand infilled Chondrites without access to Facies 6. Note the clean, granular appearance of infill, which markedly differs from the encompassing argillaceous sediments.

Plate 8C: Shell Manyberries 16-29-5-5W4 1058.5 metres

Sand infilled Chondrites with access to Facies 6. Note the dramatic grain size differential of infill to encompassing sediment.

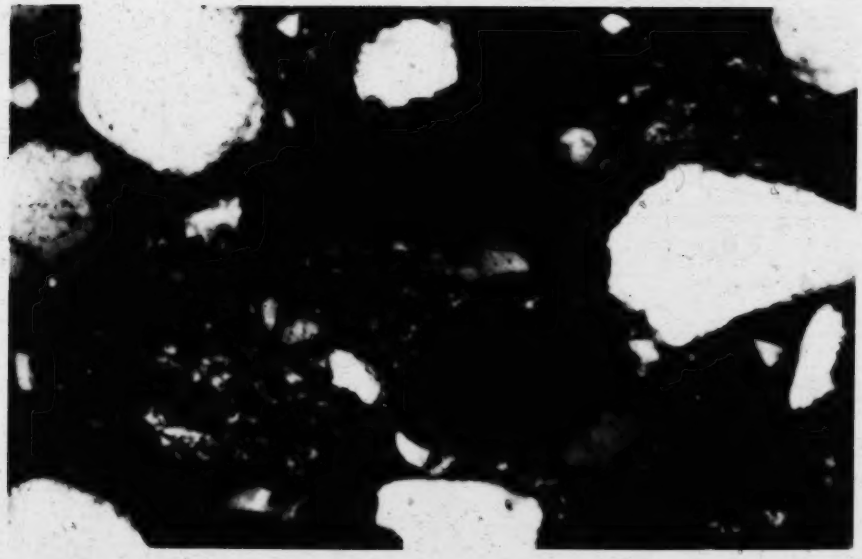

A

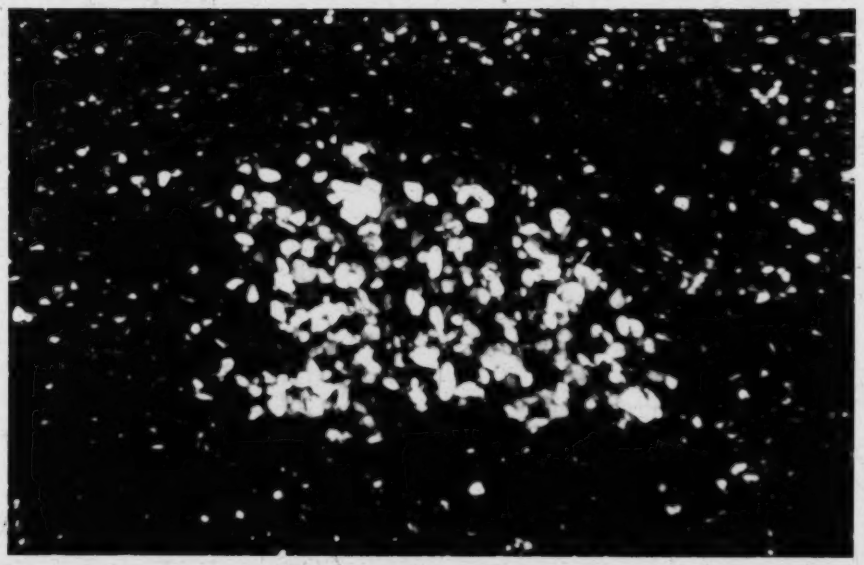

B

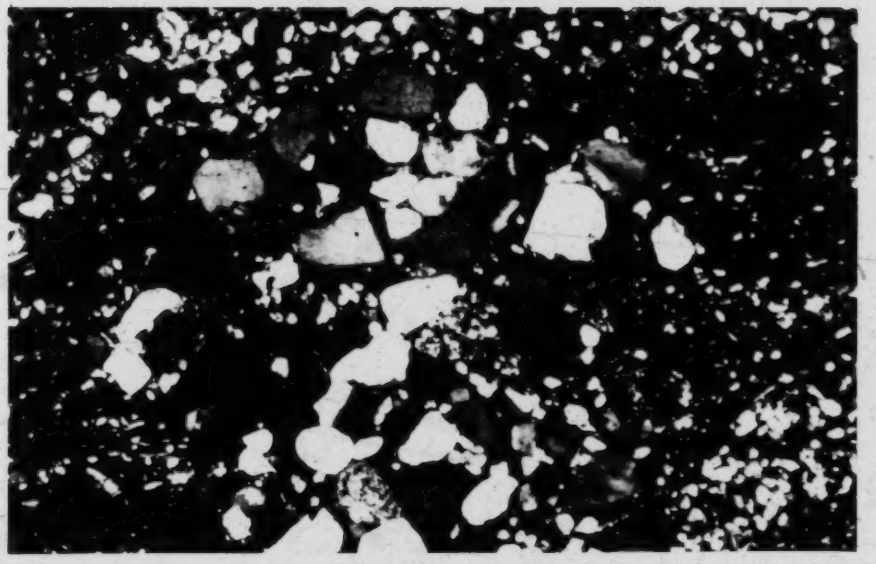

C

Plate 9: Shell Manyberries 14-5-6-5W4 1067.5 metres

Typical example of kaolinite booklets as they commonly occur throughout the ribbon sediments.

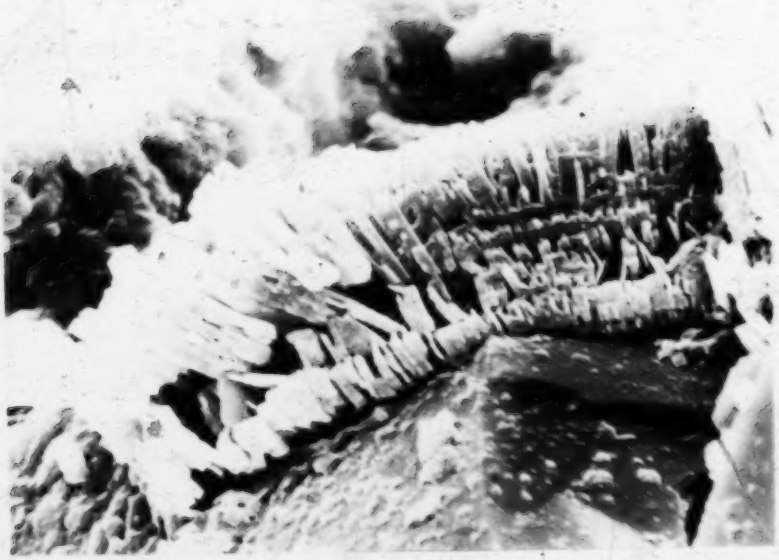

A

B

Plate 10A: Shell Manyberries 16-21-5-5W4 1085 metres

Diagenetic etching in feldspar within the very fine sands of Facies 3. Also illustrates the poorly developed quartz overgrowths in the adjacent pore space.

Plate 10B: Shell Manyberries 14-5-6-5W4 1064.8 metres

Feldspar degradation to kaolinite in Facies 4, subsequently filling the adjacent pore space. Note also the minor development of quartz and feldspar overgrowths.

A

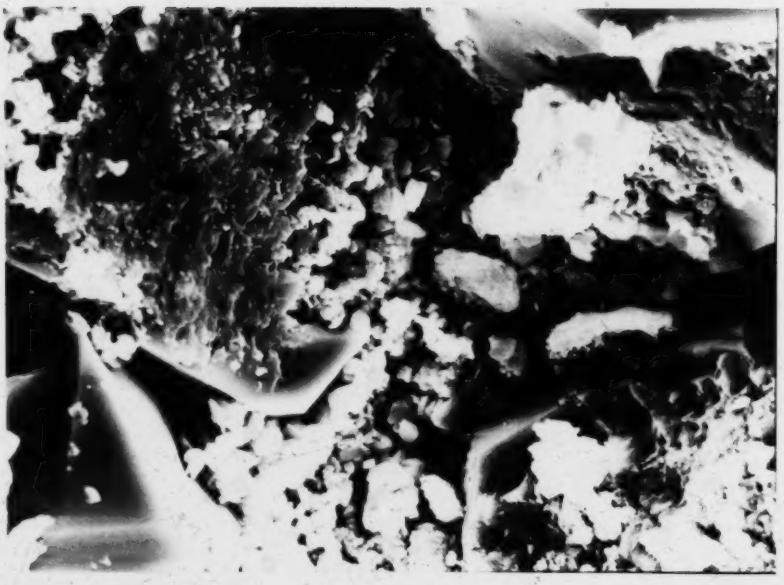

B

Plate 11A,11B, & 11C: Shell Manyberries 6-29-5-5W4 1057.5 metres

A.) Well integrated intergranular porosity (as indicated by blue epoxy). B.) Enlarged pore space in stringer sands, providing evidence for secondary porosity development (leaching of carbonate cement). C.) Grain mold with additional evidence of secondary porosity development.

A

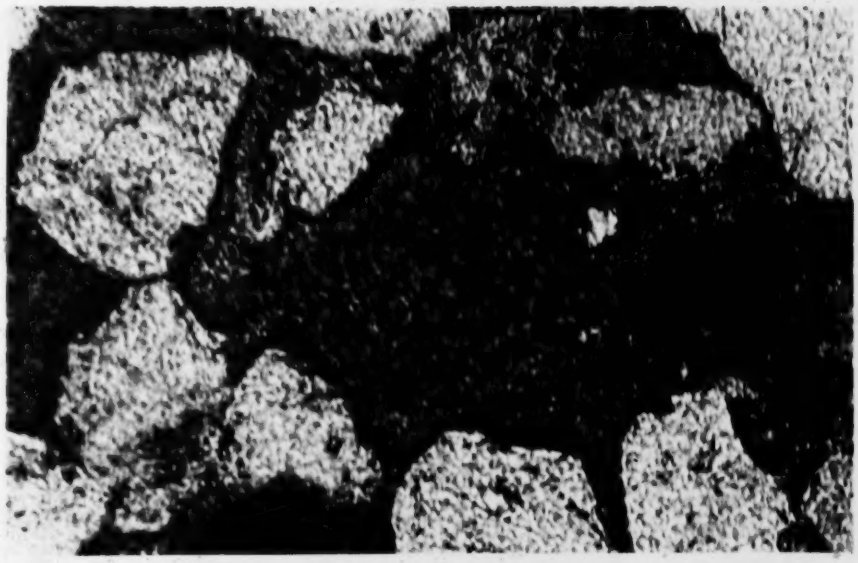

B

C

Plate 12: Shell Manyberries 6-29-5-5W4 1055.2 metres

Crowding of quartz overgrowths in pore space between the medium sands of Facies 6.

Plate 13: Shell Manyberries 6-29-5-5W4 1055.2 metres

Calcium carbonate crystals forming along the inner margin of a microfracture within the dark ribbon sediments.

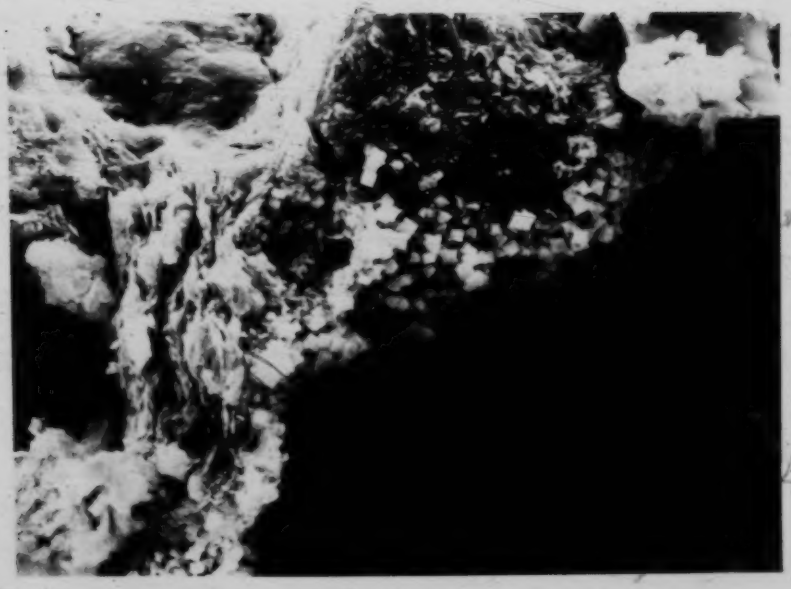

A

B

REFERENCES

Allen, J.R.L., 1970. Physical processes of sedimentation. London, George and Unwin Ltd. 248p.

Almon, W.R., and Davies, D.K., 1981. Formation damage and the crystal chemistry of clays. In Clays and the Resource Geologist, Min. Assoc. Can., F.J. Longstaffe,(ed.). Co-op Press, Edmonton, Alberta.

Al-Shaieb, Z., Shelton, J.W., 1981. Migration of hydrocarbons and secondary porosity in sandstones. Bull. Amer. Assoc. Petrol. Geol., 65, pp. 2433-2436.

van Andel, Tj.H., 1960. Sources and dispersion of Holocene sediment, northern Gulf of Mexico. In: Recent Sediments, Northwest Gulf of Mexico. Shepard, F.P., Phleger, F.B. and van Andel, Tj.H. (eds.), Amer. Assoc. Petrol. Geol., Tulsa, Oklahoma, pp. 34-55.

Beall, A.O., 1968. Sedimentary processes operative along the western Louisiana shoreline. Jour. Sed. Petrol, 38, pp. 869-877.

van den Berg, J.H., 1981. Rhythmic seasonal layering in a mesotidal channel fill sequence, Oostershelde mouth, the Netherlands. In Holocene Marine Sedimentation in the North Sea Basin, Nio, S.D., Shuttenhelm. R.T.E., and van Weering, Tj.C.E. (eds.). Spec. Pub. Int. Assoc. Sediment. 35.

Blatt, H., 1979. Diagenetic processes in sandstones. Soc. Econ. Paleon. Miner. Spec. Paper No. 26, pp. 141-157.

Blatt, H., Middleton, G.V., and Murray, R., 1980. Origin of sedimentary rocks; second edition. New Jersey, Prentice-Hall, 782p.

Brenner, R.L., 1980. Construction of process-response models of ancient epicontinental seaway depositional systems using partial analogs. Bull. Amer. Assoc. Petrol. Geol., 64, pp. 1223-1244.

Brenner, R.L., and Davies, D.K., 1973. Storm-generated conquinoid sandstone: genesis of high-energy marine sediments from the upper Jurassic of Wyoming and Montana. Bull. Geol. Soc. Amer., 84, pp. 1685-1698.

Buss, B.A., Rudolfo, K.S., 1972. Suspended sediments in continental shelf waters off Cape Hatteras, North Carolina. In: Shelf Sediment Transport: Process and Pattern, Swift, D.J.B., Duane, D.B., and Pilkey, O.H. (eds.). Dowden, Hutchinson and Ross, Stroudsberg, Pa. pp. 263-280.

Byrne, I.V., LeRoy, D.O., and Riley, C.M., 1959. The chenier plain and its stratigraphy, southwestern Louisiana. Gulf Coast Assoc. of Geol. Soc. Trans., v.9, pp. 237-259.

Carder, K.L., Beardsley, G.F., and Pak, H., 1971. Particle size distributiions in the eastern equatorial Pacific. J. Geophys. Res. 76, pp. 5070-5077.

Chamberlain, C.K., 1978. Recognition of Trace Fossils in Cores. In: Trace Fossils Concepts, ed. by P.B. Basan, Soc. Econ, Paleon, and Miner. Short Course #5, pp. 119-166.

Christopher, J.E., 1980. The Lower Cretaceous Mannville group of Saskatchewan - a tectonic overview. In: Lloydminster and Beyond: Geology of Mannville Hydrocarbon Reservoirs, ed. by L.S. Beck, J.E. Christopher, and D.M. Kent. Sask. Geol. Soc. Spec. Pub. #5, pp. 3-32.

Clifton, H.E., 1983. Discrimination between subtidal and intertidal facies in Pleistocene deposits, Willapa Bay, Washington. Journ. of Sed. Petrol. Vol. 53, No.2, pp. 353-369.

Cobban, W.A., 1945. Marine Jurassic formations of Sweetgrass Arch, Montana. Bull. Amer. Assoc. Petrol. Geol., 29, pp. 1262-1303.

Collinson, J.D., and Thompson, D.B., 1981. Sedimentary structures. London, George Allen and Unwin Inc., 194p.

Curray, J.R., 1960. Sediments and history of Holocene transgression; continental shelf, northwest Gulf of Mexico. In: Recent Sediments, Northwest Gulf of Mexico. Shepard, F.P., Phleger, F.B., van Andel, Tj.H., (eds.), Amer. Assoc. Petrol. Geol. Tulsa, Oklahoma, pp. 221-266.

Curtis, C.D., and Spears, D.A., 1968. The formation of sedimentary iron minerals. Econ. Geol., 63, pp. 257-270.

Dapples, E.C., 1959. Behavior of silica during diagenesis. In: Silica in Sediments-A Synposium, Ireland, H.A. (ed.), Soc. Econ, Paleon, and Miner. Spec. Pub. #7, 185p.

Dapples, E.C., 1962. Stages of diagenesis in the development of sandstones. Bull. Geol. Soc. Amer., V. 73, pp. 913-934.

Dapples, E.C., 1972. Some concepts of cementation and lithification of sandstones. Bull. Amer. Assoc. Petrol. Geol. 56, pp. 3-25.

Deans, T., 1934. The spherulitic ironstones of West Yorkshire. Geol. Mag. V. L 1, pp. 49-64.

Drake, D.E., 1971. Suspended sediment and thermal stratification in Santa Barbara Channel, California. Deep Sea Res., 18, pp. 763-769.

Drake, D.E., Kolpack, R.L., and Fischer, P.J., 1972. Sediment transport on the Santa Barbara-Oxnard shelf, Santa Barbara Channel, California. In: Shelf Sediment Transport: Process and Pattern, Swift, D.J.B., Duane, D.B., and Pilkey, O.H. (eds.), Dowden, Hutchinson and Ross, Stroudsburg, Pa. pp. 307-332.

Edzwald, J.K., and O'Melia, C.R., 1975. Clay distributions in recent esturine sediments. Clays and Clay Minerals, 23, pp. 39-44.

Forristall, G.Z., Hamilton, R.C., and Cardone, V.J., 1977. Continental shelf currents in tropical storm Delia: observations and theory. J. Phys. Oceanogr. 7, pp. 532-546.

Gibbs, R.J., 1977. Clay mineral segregation in the marine environment. Jour. Sed. Petrol. 47, pp. 237-244.

Glaister, R.P., 1959. Lower Cretaceous of southern Alberta and adjacent areas. Bull. Amer. Assoc. Petrol. Geol., 43, pp. 590-640.

Gould, H.R., and McFarlan, E., Jr., 1959. Geologic history of the chenier plain, southwestern Louisiana. Gulf Coast Assoc. of Geological Societies Trans., V.9, pp. 261-270.

Greensmith, J.T., 1971. Petrology of sedimentary rocks: (rev. fifth edition), New York, Hafner Pub. Co., 502p.

Grim, R.E., 1968. Clay mineralogy, 2nd ed. New York: McGraw Hill Book Co.

Hallimond, A.F., 1925. Iron ores: bedded ores of England and Wales. Petrography and Chemistry. Mem. Geol. Surv.: Spec. Min. Repts., XXIX.

Hayes, B.J.R., 1982. Upper Jurassic and lower cretaceous stratigraphy of southern Alberta and north-central Montana. Unpub. Ph.D. thesis, University of Alberta, 303p.

Hayes, B.J.R., 1983. Stratigraphy and petroleum potential of the Swift Formation (upper Jurassic), southern Alberta and north-central Montana, Bull. Can. Jour. Petrol. Geol., Vol 31, No.1, pp. 37-52.

Hayes, J.B., 1979. Sandstone diagenesis: the hole truth. In: Aspects of Diagenesis: Soc. Econ. Paleon, and Miner. Spec. Pub. #26, pp. 127-139.

Hayes, M.O., 1967. Hurricanes as geological agents: case studies of hurricanes Carla and Cindy, 1963. Texas Bur. Econ. Geol. Rept. Invest. 61.

Heald, M.T., 1956. Cementation of Simpson and St. Peter sandstones in parts of Oklahoma, Arkansas and Missouri. Jour. Geol. 64, pp. 16-30.

Heald, M.T. and Larese, R.E., 1973. The significance of solution of feldspar in porosity development. Jour. Sed. Petrol., 43, pp. 458-460.

Hedberg, H.D., 1976. International stratigraphic guide - a guide to stratigraphic classification, terminology, and procedure. International Subcommission on Stratigraphic Classification. New York, John Wiley and Sons, 200p.

Herbaly, E.L., 1974. Petroleum geology of Sweetgrass Arch, Alberta. Bull. Amer. Assoc. Petrol. Geol., 58, pp. 2227-2244.

Hill, G.W., 1985. Ichnofacies of a modern size-graded shelf, Northwestern Gulf of Mexico. The Society of Economic Paleontologists and Mineralogists. Spec. Pub. No.35, Ed. H. Allen Curran, pp. 195-210.

Howard, J.D., and Reineck, H.E., 1972. Georgia coastal region, Sapelo Island, U.S.A.: Sedimentology and biology, IV. Physical and biogenic sedimentary structures of the near-shore shelf: Senckenbergiana marit., V.4, pp. 81-123.

Howard, J.D., and Reineck, H.E., 1981. Depositional facies of high-energy beach-to-offshore sequence: comparison with low-energy sequence. Bull. Amer. Assoc. Pet. Geol. Vol. 65, pp. 807-830.

Imlay, R.W., 1957. Paleoecology of Jurassic seas in the western interior of the United States. In: Treatise on Marine Ecology and Paleoecology, Part II, ed. by H.S. Ladd. Geol. Soc. Amer. Mem. 67, chpt. 17, pp 469-503.

Inman, D.L., 1952. Measures for describing the size distribution of sediments. Jour. Sed. Petrol., 22, pp. 125-145.

Jago, C.F., 1981. Sediment response to waves and currents, North Yorkshire Shelf, North Sea. In: Holocene Marine Sedimentation in the North Sea Basin, Nio, S.D., Shuttenhelm, R.T.E., and Weering, Tj.C.E. (eds.). Spec. Pub. Int. Assoc. Sediment. #5, pp. 105-117.

Kieke, E.M., and Hartmann, D.J., 1973. Scanning electron microscope application to formation evaluation. Gulf Coast Assoc. Geol. Soc. Trans. V.23, pp. 60-67.

Kulm, L.D., roush, R.C., Harlett, J.C., and Neudeck, R.H., 1975. Oregon continental shelf sedimentation: interrelationships of facies distribution and sedimentary processes. Jour. Geol., 83, pp. 145-175.

McBride, E.F., 1977. Secondary porosity-importance in sandstone reservoirs in Texas. Gulf Coast Assoc. Geol. Soc. Trans., 27, pp. 121-122.

McCave, I.N., 1972. Transport and escape of fine-grained sediment from shelf areas. In: Shelf Sediment Transport: Process and Pattern, Swift, D.J.B., Duane, D.B., and Pilkey, O.H. (eds.). Dowden, Hutchinson and Ross, Stroudsburg, Pa. pp. 225-248.

Malouta, J.L., Thornton, T.S., Gorsline, A.M., 1981. Processes and rates of recent (Holocene) basin filling in an active transform maring: Santa Monica Basin, Califonia continental borderland. Jour. Sed. Petrol., 51, pp. 1077-1095.

Meade, R.H., 1966. Factors influencing the early stages of the compaction of clays and sands-review. Jour. Sed. Petrol., 36, pp. 1085-1101.

Momper, J.A., 1980. Generation of abnormal pressures through organic matter transformation (abs.). Amer. Assoc. Petrol. Geol. 64, p. 753.

Morton, R.A., 1981. Formation of storm deposits by wind forced currents in the Gulf of Mexico and the North Sea. Spec. Pub. Int. Assoc. Sediment. #5. In: Holocene Marine Sedimentation in the North Sea Basin, Nio, S.D., Shuttenhelm, R.T.E., and Weering, Tj.C.E. (eds.), pp. 385-396.

Murray, S.P., 1970. Bottom currents near the coast during hurricane Camille. Jour. Geophys. Res. 75, pp. 4579-4582.

Nair, R.R., 1976. Unique mud banks, Kerala, Southwest India. Bull. Amer. Assoc. Petrol. Geol 60, pp. 616-621.

Nelson, B.W., 1960. Clay mineralogy of the bottom sediments of the Rappahannock river, Virginia: seventh nat. Conf. Clays and Clay Minerals, pp. 135-147.

Peterson, J.A., 1958. Marine Jurassic of northern Rocky Mountains and Williston basin. Bull. Amer. Assoc. Petrol. Geol., 41, pp. 399-440.

Peterson, J.A., 1972. Jurassic system. In Geologic atlas of the Rocky Mountains Region, U.S.A., ed. by W.W. Mallory. Rocky Mountain Assoc. Geol., pp. 177-189.

Pittman, E.D., 1972. Diagenesis of quartz in sandstones as revealed by scanning electron microscopy. Jour. Sed. Petrol., 42, pp. 1383-1389.

Pittman, E.D., 1979. Porosity, diagenesis and productive capability of sandstone reservoirs, In: Aspects of Diagenesis, Soc. Eco Paleon. Miner. Spec. Pub. #26, pp. 159-173.

Pocock, S.A.J., 1962. Microfloral analysis and age determination of strata at the Jurassic-Cretaceous boundary in the Western Canada Plains. Palaeontographica Abt. B,Bd. 111, pp. 1-95.

Pocock, S.A.J., 1970. Palynology of the Jurassic sediments of Western Canada (pt. II). Palaeontographica Abt. B,Bd. 137, pp. 85-153.

Polasek, T.L., and Hutchinson, C.A. Jr., 1967. Characterization of non-uniformities within a sandstone reservoir from a fluid mechanics standpoint. In: Seventh World Petroleum Cong. Proc., V.2, Elsevier Pub. Co. Ltd., Barking, pp. 397-407.

Porrenga, D.H., 1966. Clay minerals in recent sediments off the Niger Delta. Clays and Clay Minerals, 14, pp. 221-223.

Postma, H., 1961. Transport and accumulation of suspended matter in the Dutch Wadden Sea. Netherlands Jour. of Sea Res. 1, 1/2, pp. 148-190.

Powers, M.C., 1953. A new roundness scale for sedimentary particles. Jour. Sed. Petrol. 23, pp. 117-119.

Powers, M.C., 1957. Adjustment of land derived clays to the marine environment. Journ. Sed. Petrol. 27, pp. 355-372.

Reimer, J.D., 1982. Geological and petrophysical study of the Sunburst and Swift sandstones, Manyberries area, Alberta. Company report, Home Oil, Calgary.

Reineck, H.E., and Singh, I.B., 1972. Genesis of laminated sand and graded rhythmites in storm sand layers of shelf mud. Sedimentology, 18, pp. 123-128.

Schmidt, V., and McDonald, D.A., 1979. Texture and recognition of secondary porosity in sandstones. In: Aspects of Diagenesis, Soc. Econ. Paleon. Miner. Spec. Pub. #26, pp. 209-225.

Seilacher, A., 1955. Spuren und fazies im unterkambrium. In: Schindewolf, O.H., and Seilacher, A., (eds.), Beitrage zur Kennthis des Kambriums in der Salt Range (Pakistan). Akademie der Wissenschaften und der Literature, Mainz, Abhandlungen der Mathematisch-Naturwissenschattlichen Klasse, V.10, pp. 11-143.

Siever, R., 1962. Silica solubility, 0-200 degrees celcius, and the diagenesis of silica sediments. Jour. Geol. 70, pp. 127-150.

Smith, J.D., and Hopkins, T.S., 1972. Sediment transport on the continental shelf off of Washington and Oregon in light of recent current measurements. In: Shelf Sediment Transport Process and Patter, Swift, D.J.B., Duane, D.B., and Pilkey, O.H. (eds.). Dowden, Hutchinson and Ross, Stroudsburg, Pa. pp. 143-180.

Spencer, E., 1925. On some occurrences of spherulitic siderite and other carbonates in sediments. Quart. Journ. Geol. Soc., LXXXI, pp. 667-705.

van Straaten, L.M.J.U., and Kuenen, P., 1957. Accumulation of fine-grained sediments in the Dutch Wadden Sea. Geol. en Mijnbouw (ns. ser.), 193, pp. 329-354.

Stubblefield, W.L., Lavelle, J.W., Swift D.J.P., and McKinney T.F., 1975. Sediment response to the present hydraulic regime on the central New Jersey shelf. Journ. Sed. Petrol. 45, pp, 337-358

Subramanian, V., 1975. Origin of surface pits on quartz as revealed in scanning electron microscopy. Jour. Sed. Petrol. 45, pp. 530-534.

Swift, D.J.P., Ludwick, J.C., and Boehmer, W.R., 1972. Shelf sediment transport: a probability model. In: Shelf Sediment Transport: Process and Pattern, Swift, D.J.B., Duane, D.B., and Pilkey, O.H. (eds.). Dowden, Hutchinson and Ross, Stroudsburg, Pa. pp. 195-223.

Towe, K.M., 1962. Clay mineral diagenesis as a possible source of silica cement in sedimentary rocks. Jour. Sed. Petrol. 32, pp. 26-28.

Udden, J.A., 1898. Mechanical composition of wind deposits. Augustana Library Publ., No.1.

Walker, R.G., 1984 Facies models. Geoscience Canada Reprint Series 1. Toronto, Geological Association of Canada, 317p.

Weaver, C.E., 1959. The clay petrology of sediments. Proc. Sixth Natl. Conf. on Clays and Clay Mierals, pp. 154-187.

Weaver, C.E., 1960. Possible uses of clay minerals in search for oil. Bull. Amer. Assoc. Petrol. Geol., 44, pp.1505-1518.

Weir, J.D., 1949. Marine Jurassic formations of southern Alberta plains. Bull. Amer. Assoc. Petrol. Geol. 33, pp. 547-563.

Wells, J.T., and Coleman, J.M., 1977. Nearshore suspended sediment variations, central Surinam Coast. Marine Geology, 24, pp. M47-M54.

Wells, J.T., and Coleman, J.M., 1981. Physical processes and fine-grained sediment dynamics, Coast of Surinam, South America. Jour. Sed. Petrol., 51, pp. 1053-1068.

Wentworth, C.K., 1922. A scale of grade and class terms for clastic sediments. Jour. Geol., 30, pp. 377-392.

Whitehouse, U.G., Jeffrey, L.M., and Debbrecht, J.D., 1960. Differential settling tendencies of clay minerals in saline waters. Proc. Seventh Nat. Conf. Clays and Clay Minerals, pp. 1-79.

Wilson, M.D., and Pittman, E.D., 1977. Authigenic clays in sandstones: recognition and influence on reservoir properties and paleoenvironmental analysis. Jour. Sed. Petrol., 47, pp. 3-31.

APPENDIX

16-29-1-9W4M

(911 - 912.5m)
Lithofacies 4: Ribbon sediment-light colour. Silty-V.F. grained sublitharenite; framework constituents 65-75% very light grey, wavy to irregularly interlaminated with mudstone-light grey. Additionally contains centimetre-scale M. grained sand stringers. Low burrow density, small scale, low-angle trough cross-stratification; reactivation surfaces are frequently observed. Erosional upper contact and gradational lower contact.

(912.5 - 942.0m)
Lithofacies 3: Ribbon sediment-dark colour. Silt-V.F. grained sublitharenite. Framework constituents decreasing downsection 70%-30% - very light grey. Irregularly interlaminated with an organic-rich mudstone, grey black to black; minor occurrence of M. grained sand stringers (always less than 5 centimetres in thickness). Moderate to high burrow density (predominantly Chondrites); minor small scale low-angle cross-stratification; nodular and disseminated pyrite; glauconite abundant. Thin lenses of lithofacies 2 near base. Gradational upper contact, sharp base with underlying Rierdon Formation.

3-13-1-13W4M

(787 - 801m)
Lithofacies 5: Sandstone. V.F.-M. grained litharenite. A few chalky-white shale lenses, yet predominantly massively bedded coarsening upwards lithofacies. Sharp grain/colour transition at 797.8m - depositional not erosional, as soft sediment deformation and liquifaction are observed at the boundary. Carbonized rootlets towards the base, clay clasts observed randomly. Authigenic siderite increasing towards base. Erosional upper contact, gradational lower contact.

(801.0 - 806.5m)
Lithofacies 4: Ribbon sediment-light colour. Silt-F. grained sublitharenite; framework constituents 45-65% - very light grey, wavy to irregularly interlaminated with mudstone-light grey. Additionally contains centimetre-scale M. grained sand stringers. Low burrow density. Very mud-rich zone at 802m, appears to be rooted. Minor small scale, low-angle trough cross-stratification. Sideritic at top, glauconite increases downsection. Gradational upper and lower contacts.

10-34-2-7W4M

(925.8 - 926.5m)

Lithofacies 4: Ribbon sediment-light colour. Silt-V.F. grained sublitharenite; framework constituents 65-75% - very light grey, wavy to irregularly interlaminated with mudstone-light grey. Additionally contains centimetre-scale M. grained sand stringers. Moderate burrowing, predominantly Chondrites, minor bioturbation zones. Very sideritic. Gradational lower contact.

(926.5 - 931m)
Lithofacies 3: Ribbon sediment-dark colour. Silt-V.F. grained sublitharenite. Framework constituents decreasing downsection 70%-30% - very light grey. Irregularly interlaminated with an organic-rich mudstone, grey black to black; containing also centimetre-scale F. grained sand stringers, often loaded into the ribbon sediment. Moderate to high burrow density (predominantly Chondrites); minor small scale low-angle cross-stratification; nodular and disseminated pyrite; glauconite abundant. Gradational upper contact, particularly shaley base - almost structureless.

(931 - 933m)
Lithofacies 2: Ribbon sediment-dark colour (lenticular-silt-streaked). Predominantly siltstone sublitharenite. Framework constituents below 35%, very light grey; encompassed in an organic-rich shale-grey black to black. Low burrow density, Chondrites dominant; very minor small scale, low-angle trough cross-stratification; pyrite common nodular and disseminated; glauconite abundant. Lensing upper contact.

6-31-2-8W4M

(803.7 - 809.2m)
Lithofacies 4: Ribbon sediment-light colour. Silt-V.F. grained sublitharenite; framework constituents 65-75% very light grey, wavy to irregularly interlaminated with mudstone-light grey (darkening towards base). M. grained sand stringers also noted. Moderate burrowing, predominantly Chondrites, increasing downsection; minor small scale, low-angle trough cross-stratification. Siderite decreasing downsection. Very distorted bedding at top, possibly gradational with the overlying unit (Gladstone Formation?).

14-25-2-10W4M

(789.2 - 794.6m)
Lithofacies 5: Sandstone V.F.-M. grained litharenite. Light grey to buff with abundant silt and matrix mud. Predominantly massively bedded, coarsening upwards lithofacies; minor soft sediment deformation, authigenic siderite increasing towards base. Gradational lower contact.

(794.6 - 804.3m)
Lithofacies 4: Ribbon sediment-light colour. Silt-V.F. grained sublitharenite; framework constituents 70-85% very light grey, wavy to irregularly interlaminated with mudstone-light grey. Additionally contains centimetre-scale M. grained sand stringers. Moderate burrowing, predominantly Chondrites, minor bioturbation zones; minor small scale, low-angle trough cross-stratification. Sideritic at top, glauconite increases downsection. Gradational upper and lower contacts.

(804.3 - 804.9m)
Lithofacies 3: Ribbon sediment-dark colour. Silt-V.F. grained sublitharentie. Framework constituents decreasing downsection 65-35% - very light grey. Irregularly interlaminated with an organic-rich mudstone. grey black to black; containing also centimetre-scale M. grained sand stringers, often loaded into the ribbon sediment. Moderate to high burrow density (predominantly Chondrites); minor small scale low-angle cross-stratification; nodular and disseminated pyrite; glauconite abundant. Gradational upper contact, and possibly lower contact also.

(804.9 - 809.2m)
Lithofacies 1: Shale - pred. massive, m. grey. Minor silt lenses; carbonaceous detritus common; pyrite and glauconite observed. Upper contact gradational, lower contact not observed.

10-28-3-7W4M

(897.7 - 901.5m)
Lithofacies 3: Ribbon sediment-dark colour. Silt-V.F. grained sublitharenite. Framework constituents increasing to 898m (v. shaley top), then decreasing downsection 55%-30% - very light grey. Irregularly interlaminated with an organic-rich mudstone, grey black to black; containing also centimetre-scale M. grained sand stringers, often loaded into the ribbon sediment. Low burrow density (predominantly Chondrites); minor small scale low-angle cross-stratification; nodular and disseminated pyrite; glauconite abundant. Small high angle fractures observed. Contacts not distinguishable.

11-4-3-8W4M

(861.5 - 870m)
Lithofacies 3: Ribbon sediment-dark colour. Silt-V.F. grained sublitharenite. Framework constituents decreasing downsection 55-40% - very light grey. Irregularly interlaminated with an organic-rich mudstone, grey black to black; containing also centimetre-scale M. grained sand stringers, often loaded into the ribbon sediment; the abundance of lithofacies increases downsection. Low to moderate burrow density (predominantly Chondrites); minor small scale low angle cross-stratification; nodular and disseminated pyrite; glauconite abundant. Upper contact shows gradational colour to light ribbon sediment.

9-22-3-8W4M

(878.0 - 892.4m)
Lithofacies 3: Ribbon sediment-dark colour. Silt-V.F. grained sublitharenite. Framework constituents decreasing downsection 90%-70% - very light grey. Irregularly interlamined with an organic-rich mudstone, grey black to black; containing also centimetre-scale M. grained sand stringers, often loaded into the ribbon sediment. Moderate to high burrow density (predominantly Chondrites); burrow density markedly increasing downsection; good small scale low-angle cross-stratification; nodular and disseminated pyrite; glauconite abundant. Gradational upper contact (appears to be transitional with light ribbon sediment (core missing from 881.8 - 884.2).

(892.4 - 898.2m)
Lithofacies 2: Ribbon sediment-dark colour (lenticular-silt-streaked). Predominantly siltstone sublitharenite. Framework constituents below 35%, very light grey; encompassed in an organic-rich shale-grey black to black. Low burrow density, Chondrites dominant; very minor small scale, low-angle trough cross-stratification; pyrite common nodular and disseminated; glauconite abundant. Lensing upper contact, sharp based.

(893.2 - 898.2m)
Lithofacies 1: Shale - predominantly massive. Silty top, minor silt lenses throughout; carbonaceous detritus common; pyrite and glauconite observed. Upper contact sharp, lower contact abrupt with pebble conglomerate.

(898.2 - 898.4m)
Conglomerate - chert-belemnite (dark grey shale matrix). Unique lithology with an study area, observed at base of shale member in Type locality.

6-19-3-9W4M

(853.0 - 853.9m)
Lithofacies 5: Sandstone. V.F.-M. grained litharenite. Light grey to buff with abundant silt and matrix mud. Predominantly massively bedded, coarsening upwards lithofacies; minor soft sediment deformation, questionable slumping at the top - very chaotic; mnr. low angle cross-beds near base. Authigenic siderite increasing towards base. Erosional upper contact, gradational lower contact.

(853.9 - 856.3m)
Lithofacies 4: Ribbon sediment-light colour. Silt-V.F. grained sublitharenite; framework constituents 65-75% - very light grey, wavy to irregularly interlaminated with mudstone, mud laminae thinning upsection, and darkening towards the base; contains centimetre-scale sand stringers; very low burrow density, predominantly Chondrites; minor small scale, low-angle trough cross-stratification. Sideritic at top, glauconite increases downsection. Gradational upper and lower contacts.

7-8-4-4W4M

(1128.5 - 1134.3m)
Lithofacies 4: Ribbon sediment-light colour. Silt-V.F. grained sublitharenite; framework constituents 50-75%, increasing in abundance downsection, as does bed definition increase - very light grey, wavy to irregularly interlaminated with mudstone-light grey. Additionally contains centimetre-scale M. grained sand stringers. Moderate burrowing, predominanly Chondrites, minor bioturbation zones; minor small scale, low-angle trough cross-stratification. Sideritic at top, glauconite increases downsection. Gradational upper and lower contacts.

(1134.3 - 1142.8m)
Lithofacies 3: Ribbon sediment-dark colour. Silt-V.F. grained sublitharenite. Framework constituents decreasing downsection 50-30% - very light grey. Irregularly interlaminated with an organic-rich mudstone, grey black to blak; containing also centimetre-scale M. grained sand stringers, often loaded into the ribbon sediment. Moderate to high burrow density (predominantly Chondrites); minor small scale low-angle cross-stratification; nodular and disseminated pyrite; glauconite abundant. Gradational upper contact, disturbed lower contact.

(1142.8 - 1149.0m)
Lithofacies 1: Shale - prodominantly massive; med-grey. Minor silt lenses; carbonaceous detritus common; pyrite and glauconite observed. Upper contact disturbed, lower contact not observed.

6-22-4-4W4M

(1066.2 - 1071.3m)
Lithofacies 4: Ribbon sediment-light colour. Silt-V.F. grained sublitharenite; framework constituents 65-75% - very light grey wavy to irregularly interlaminated with mudstone-light grey. Additionally contains centimetre-scale M. grained sand stringers. Moderate burrowing, predominantly Chondrites, minor bioturbation zones; minor small scale, low-angle trough cross-stratification. Sideritic at top, glauconite increases downsection. Lower contact very gradational - mud ribbons darkening gradually to 1071m.

(1071.4 - 1076.3m)
Lithofacies 3: Ribbon sediment-dark colour. Silt-V.F. grained sublitharenite. Framework constituents decreasing downsection 70%-40% - very light grey. Irregularly interlaminated withan organic-rich mudstone, grey black to black; containing also centimetre-scale M. grained sand stringers, often loaded into the ribbon sediment. Moderate to high burrow density (predominantly Chondrites); minor small scale low-angle cross-stratification; nodular and disseminated pyrite; glauconite abundant. Gradational upper contact.

15-15-4-15W4

(873.6 - 874.0m)
Lithofacies 5: Argillaceous siltstone. Very light brown. Predominantly massively bedded, with minor silty shale lamination; minor soft sediment deformatioon, carbonized rootlets towards the top, abundent plant material. Authigenic siderite increasing towards base. Erosional upper contact, gradational lower contact.

(874.0 - 874.6m)
Lithofacies 4: Ribbon sediment-light colour. Silt-V.F. grained sublitharenite; framework constituents 65-75% - very light grey, wavy to irregularly interlaminated with mudstone-light grey. Minor burrowing; slightly calcareous and sideritic; good reactivation surfaces, minor small scale, low-angle trough cross-stratification. Gradational upper contact, abrupt lower contact.

(874.6 - 880.1m)
Lithofacies 1: Shale - predominantly massive. Minor silt lenses; carbonaceous detritus common; pyrite observed and abundant glauconite (increasing downsection). Thin bentonitic layers noted; relatively sideritic base, abrupt upper contact, lower contact not observed.

10-3-5-4W4M

(1076.0 - 1078.2m)
Lithofacies 4: Ribbon sediment-light colour. Silt-V.F. grained sublitharenite; framework constituents 65-75% - very light grey, wavy to irregularly interlaminated with mudstone-light grey. Additionally contains centimetre scaleM. grained sand stringers. Moderate burrowing, predominantly Chondrites, minor bioturbation zones; minor small scale, low-angle trough cross-stratification. Sideritic at top, glauconite increases downsection. Gradational lower contact, shale laminae darkening towards the contact.

(1078.2 - 1202.0m)
Lithofacies 3: Ribbon sediment-dark colour. Silt-V.F. grained sublitharentie. Framework constituents decreasing downsection 70%-30% - very light grey. Irregularly interlaminated with an organic-rich mudstone, grey black to black, containing also centimetre-scale M. grained sand stringers, often loaded into the ribbon sediment, increased abundance and thickness of coarser lenses downsection; ;mud clasts around 1091.5m. Moderate to high burrow density (predominantly Chondrites); minor small scale low-angle cross-stratification; nodular and disseminated pyrite; glauconite abundant. Gradational upper contact, lower contact not preserved.

(1202.0 - 1202.2m)
Lithofacies 1: Shale - predominantly massive. Minor silt lenses; carbonaceous detritus common; pyrite and minor siderite observed. Contacts not preserved.

15-12-5-5W4M

(1111.0 - 1112.1m)
Lithofacies 5: Argillaceous siltstone - siltier to base. Light brown to med. brown, appears to be a slightly fining-upwards sequence; minor soft sediment deformation; very carbonaceous throughout, caarbonized rootlets towards top. Erosional upper contact, lower contact unclear.

(1112.1 - 1118.4m)
Lithofacies 4: Ribbon sediment-light colour. Silt-V.F. grained sublitharenite; framework constituents 65-85% - very light grey, wavy to irregularly interlaminated with mudstone-light grey. Additionally contains centimetre-scale M. grained sand stringers. Moderate burrowing, predominantly Chondrites, minor bioturbation zones; minor and good reactivation surfaces in spots. Sideritic at top, glauconite increases downsection. Gradational lower contact.

(1114.4 - 1125.8m)
Lithofacies 3: Ribbon sediment-dark colour. Silt-V.F. grained sublitharenite. Framework constituents decreasing downsection 70%-40% - very light grey. Irregularly interlaminated with an organic-rich mudstone, grey black to black; containing also centimetre-scale M. grained sand stringers, often loaded into the ribbon sediment. Moderate to high burrow density (predominantly Chondrites); minor small scale low-angle cross-stratification, good reactivation surfaces; nodular and disseminated pyrite; glauconite abundant. Gradational upper and lower contacts.

(1025.8 - 1026.5m)
Lithofacies 2: Ribbon sediment-dark colour (lenticular-silt-streaked). Predominantly siltstone sublitharenite. Framework constituents below 35%, very light grey; encompassed in an organic-rich shale-grey black to black. Low burrow density, Chondrites dominant; very minor small scale, low-angle trough cross-stratification; pyrite common nodular and disseminated; glauconite abundant. Gradational upper and lower contacts.

(1126.5 - 1133.0m)
Lithofacies 3: Ribbon sediment-dark colour. Silt-V.F. grained sublitharenite. Framework constituents decreasing downsection 65%-30% - very light grey, irregularly interlaminated with an organic-rich mudstone, grey black to black; abundant centimetre-scale F.-M. grained sand stringers, often loaded into the ribbon sediment, greater grain size variation between sand stringers than is typically observed (alos get colour variation). Moderate to high burrow density (predominantly Chondrites); minor small scale low-angle cross-stratification; nodular and disseminated pyrite; glauconite abundant. Gradational upper contact, facies 2 lenses in and out towards base.

3-13-5-5W4M

(1135.7 - 1139.6m)
Lithofacies 5: Sandston. V.F.-M. grained litharenite. Light grey to buff with abundant silt and matrix mud. Predominantly massively bedded, coarsening upwards lithofaces; minor soft sediment deformation towards the base, and minor low-angle crossbeds observed; carbonized rootlets towards the top, clay clasts observed prodominantly at top. Authigenic siderite increasing towards base. Erosional upper contact, gradational lower contact.

(1139.6 - 1142.0m)
Lithofacies 4: Ribbon sediment-light colour. Silt-V.F. grained sublitharenite; framework constituents 65-75% - very silty top, matrix mud percentage increases downsection irregularly interlaminated with shale-light grey. Additionally contains cm. scale M. grained sand stringers; minor small scale, lwo-angle trough cross-stratification. Sideritic throughout. Gradational upper contact.

16-21-5-5W4M

(1076.0 - 1076.8m)
Lithofacies 5: Sandston. V.F.-M. grained litharenite. Light grey to buff with abundant silt and matrix mud. Predominantly massively bedded units, with minor soft sediment deofrmation, towards base; carbonized rootlets towards the top, authigenic siderite throughout. Erosional upper contact, gradational lower contact.

(1076.8 - 1084.5m)
Lithofacies 4: Ribbon sediment-light colour. Silt-V.F. grained sublitharenite; framework constituents 65-75% - very light grey, wavy to irregularly interlaminated with mudstone-light-med grey. Contains abundant centimetre-scale M. grained sand stringers. Moderate burrowing, predominantly Chondrites, minor bioturbation zones; minor small scale, low-angle trough cross-stratification. Sideritic at top, glauconite increases downsection. Gradational upper contact not present.

(1053.5 - 1054.4m) - MISSING CORE
Lithofacies 3: Ribbon sediment-dark colour. Silt-V.F. grained sublitharenite. Framework constituents decreasing downsection 70%-50% - very light grey. Irregularly interlaminated with an organic-rich mudstone - black; occasionally lenticularly bedded with shales; containing also centimetres scale M. grained sand stringers, often loaded into the ribbon sediment. Moderate to high burrow density (predominantly Chondrites); minor small scale low-angle cross-stratification; nodular and disseminated pyrite; glauconite abundant. Gradational upper contact, lower contact not observed.

6-28-5-5W4M

(1053.0 - 1062.0m)
Lithofacies 5: Sandstone. V.F.-M. grained litharenite. Light grey to buff with varying silt and matrix mud. Stratification varies from poorly defined parallel bedding, to low-angle cross-bedding, to massive bedding. Cross-bedding appears restricted to sub-units within the facies which containn the coarsest grain sizes; minor 18 centimetre shale lense near base. Carbonized rootlets towards the top, additional veinlets infilled with calcium carbonate and kaolinite are present which may represent diagenetically infilled root systems. Clay clasts (1-3cm) in length are observed throughout the unit. Sideritic is present predominantly near base. Erosional upper contact, gradational lower contact.

(1062.0 - 1066.1m)
Lithofacies 4: Ribbon sediment-light colour. Silt-V.F. grained sublitharenite; framework constituents 70-30% - systematically decrease towards the base of the unit, with a well developed mud-rich lense at 1065.4m. Colour of framework constituents is predominantly very light grey; wavy to irregularly interlaminated with mudstone-light grey. Additionally contains centimetre-scale M. grained sand stringers. Moderate burrowing, predominantly Chondrites, minor bioturbation zones; minor small scale, low-angle trough cross-stratification. Sideritic at top, glauconite increases downsection. Gradational upper contact and sharp basal contact.

(1066.1 - 1067.0m)
Lithofacies 1: Shale - predominantly massive. Minor silt lenses; carbonaceous detritus common; pyrite and glauconite observed. Upper contact sharp, lower contact not observed.

6-29-5-5W4M

(1040.0 - 1047.8m)
Lithofacies 4: Ribbon sediment-light colour. Silt-V.F. grained sublitharenite; framework constituents 65-75% - very light grey, wavy to irregularly interlaminated with mudstone-light grey. Additionally contains centimetre-scale M. grained sand stringers. Moderate burrowing predominantly Chondrites, minor bioturbation zones minor small scale, low-angle trough cross-stratification. Siderite not observed; minor glauconite visible. Gradational lower contact (upper contact not present).

(1047.8 - 1053.0m)
Lithofacies 3: Ribbon sediment-dark colour. Silt-V.F. grained sublitharenite. Framework constituents decreasing slightly downsection 70%-55% - very light grey. Irregularly interlaminated with an orgainic-rich mudstone, grey black to black; containing abundant centimetre-scale M. grained sand stringers, often loaded into the ribbon sediment. Intervals 1055-1056.8m and 1058.6-1061m are dominated by the medium sand component. These thicker intervals contain some good planar cross-stratification. Some intervals near the top of facies 3 contain low-angle sand/shale lamination, which may represent slumped surfaces. Minor fractures (2-10cm) in length are present. Moderate to high burrow density (predominantly Chondrites); minor small scale low-angle cross-stratification; nodular and disseminated pyrite; glauconite abundant. Gradational upper contact, lower contact not observed, but thin 8-10cm lenses of lithofacies 2 are observed near the base of the core.

8-29-5-5W4M

(1050.0 - 1053.0m)
Lithofacies 5: Sandstone. V.F.-F. grained litharenite. Light grey to buff with abundant silt and matrix mud. Predominantly massively bedded, possibly fining - upwards lithofacies; minor soft sediment deformation, extensive carbonized rootlets towards the top, clay clasts observed sporadically throughout, increasing towards base. Erosional upper contact, sharp lower contact.

(1053.0 - 1054.7m)
Lithofacies 4: Ribbon sediment-light colour. Silt-V.F. grained sublitharenite; framework constituents 70-80% - very light grey, wavy to irregularly interlaminated with mudstone-light grey. Relatively low burrow density; small scale, low-angle trough cross-stratification. Sideritic at top, glauconite increases downsection. Sharp upper and lower contacts.

(1054.7 - 1061.0m)
Lithofacies 1: Shale - predominantly massive. Unit possesses a very silty top, as well as, a silty base; additional small-scale (0.5cm) silt lenses are observed throughout Chondrites burrowing observed near top. Carbonaceous detritus common; pyrite and glauconite observed. Upper and lower contacts sharp.

16-29-5-5W4M

(1047.0 - 1050.8m)
Lithofacies 5: Sandstone, V.F.-M. grained litharenite. Light grey to buff with abundant silt and matrix mud. Predominantly massively bedded, coarsening upwards lithofacies; minor soft sediment deformation, carbonized rootlets predominantly in silty base, clasts in coarsening transition. Authigenic siderite increasing towards base. Erosional upper contact, gradational lower contact.

(1050.8 - 1059.0m)
Lithofacies 4: Ribbon sediment-light colour. Silt-V.F. grained sublitharenite; framework constituents 65-75% - very light grey, wavy to irregularly interlaminated with mudstone-light grey. Additionally contains centimetre-scale M. grained sand stringers. Moderate burrowing, predominantly Chondrites, minor bioturbation zones; minor small scale, low-angle trough cross-stratification. Sideritic at top, glauconite increases downsection. Gradational upper and lower contacts.

(1059.0 - 1052.7m)
Lithofacies 3: Ribbon sediment-dark colour. Silt-V.F. grained sublitharenite. Framework constituents decreasing downsection 70%-30% - very light grey. Irregularly interlaminated with an organic-rich mudstone, grey black to black - shale increasing towards base, minor lenticular bedding; containing also centimetre-scale M. grained sand stringers, often loaded into the ribbon sediment. Moderate to high burrow density (predominantly Chondrites); minor small scale low-angle cross-stratification; nodular and disseminated pyrite; glauconite abundant. Gradational upper contact, debatable lower contact.

14-34-8-7W4M

(1043.4 - 1049.0m)
Lithofacies 1: Shale - predominantly massive. Minor silt lenses; carbonaceous detritus common; predominantly quite structureless and very crumbly; small pyrite blebs and glauconite observed. Upper contact unclear, lower contact not observed.

14-5-6-5W4M

(1059.0 - 1060.5m)
Lithofacies 5: Sandstone. V.F.-M. grained litharenite. Light grey to buff with abundant silt and matrix mud. Predominantly massively bedded, coarsening upwards lithofacies; minor soft sediment deformation, carbonized rootlets towards the top, clay clasts observed predominantly near base. Authigenic siderite increasing towards base. Erosional upper contact, gradational lower contact.

(1060.5 - 1073.6m)
Lithofacies 4: Ribbon sediment-light colour. Silt-V.F. grained sublitharenite; framework constituents 65-75% - very light grey, wavy to irregularly interlaminated with mudstone-light grey. Additionally contains centimetre-scale M. grained sand stringers. Moderate burrowing, predominantly Chondrites, minor bioturbation zones; minor small scale, low-angle trough cross-stratification. Sideritic at top, glauconite increases downsection. Gradational upper and lower contacts.

(1073.6 - 1081.0m)
Lithofacies 3: Ribbon sediment-dark colour. Silt-V.F. grained sublitharenite. Framework constituents decreasing downsection 70%-30% - very light grey. Irregularly interlaminated with an organic-rich mudstone, grey black to black; containing also centimetre-scale M. grained sand stringers, often loaded into the ribbon sediment. Moderate to high burrow density (predominantly Chondrites); minor small scale low-angle cross-stratification; nodular and disseminated pyrite, glauconite abundant. Gradational upper and lower contact.

(1081.0 - 1034.0m)
Lithofacies 2: Ribbon sediment-dark colour (lenticular-silt-streaked). Predominantly siltstone sublitharentie. Framework constituents below 35%, very light grey; encompassed in an organic-rich shale-grey black to black. Low burrow density, Chondrites dominant; very minor small scale, low-angle trough cross-stratification; pyrite common nodular and disseminate; glauconite abundant. Lensing upper contact, sharp based.

4-2-1-16W4M

(740.3 - 744.9m)
Lithofacies 1: Shale - predominantly massive. Abundant silt lenses; carbonaceous detritus common; pyrite observed in small nodules and disseminated; glauconite abundant, predominantly concentrated in thin lenses; very micaceous. Both contacts appear to be quite sharp.

7-31-6-12W4M

(889.5 - 890.7m)
Lithofacies 5?: Sandstone. F.-C. grained litharenite. Light grey to buff with abundant silt and matrix mud. Unit also contains lenses of "cleaner" medium sand. Predominantly massively bedded, however, coarse-grained base has varying angles of cross-stratification dip. Authigenic siderite increasing in basal region. Upper contact not present, lower contact quite sharp.

(890.7 - 894.2m)
Lithofacies 4: Ribbon sediment-light colour. Silt-V.F. grained sublitharenite; framework constituents 55-40% - very light grey, wavy to irregularly interlaminated with mudstone-light grey. Additionally contains centimetre-scale M. grained sand stringers. Very low burrow density, predominantly Chondrites, minor Skolithos; minor small scale, low-angle trough cross-stratification, becoming distinctly bimodal in some regions. Sideritic at top, glauconite increases downsection, becoming concentrated in thin laminae near base. Sharp upper and lower contacts.

(894.2 - 895.5m)
Lithofacies 2: Ribbon sediment-dark colour (lenticular-silt-streaked). Predominantly siltstone sublitharenite. Framework constituents below 35%, very light grey; encompassed in an organic-rich shale-grey black to black. Sand stringer Facies 6 very rarely observed. Extremely shaley unit with predominantly poker-chip fracturing habit. Low burrow density, Chondrites dominant; very minor small scale, low-angle trough cross-stratification; pyrite common nodular and disseminate; glauconite abundant. Lensing upper contact, sharp based.

10-5-6-13W4M

(913.1 - 914.6m)
Lithofacies 5: Sandstone. V.F.-F. grained litharenite. Light grey to buff with abundant silt and matrix mud. Predominantly massively bedded, coarsening upwards lithofacies; minor soft sediment deformation, authigenic siderite increasing towards base. Upper contact unclear, gradational lower contact.

(914.6 - 919.0m)
Lithofacies 4: Ribbon sediment-light colour. Silt-V.F. grained sublitharenite; framework constituents 65-75% - grain size systematically decreasing downsection from V.F. sand to silt; wavy to irregularly interlaminated with mudstone-light grey. Additionally contains centimetre-scale M. grained sand stringers, with a 35cm thick unit observed at 917.6m. Low burrow density. Minor small scale, low-angle trough cross-stratification. Sideritic at top, glauconite increases downsection, pyrite observed slightly above the dark/light ribbon transition. Gradational upper and lower contacts.

(919.0 - 920.3m)
Lithofacies 3: Ribbon sediment-dark colour. Silt-V.F. grained sublitharenite. Framework constituents approximatley 45% - very light grey. Irregularly interlaminated with an organic-rich mudstone, grey black to black; containing also centimetre-scale M. grained sand stringers, often loaded into the ribbon sediment. Moderate to high burrow density (predominantly Chondrites); minor small scale low-angle cross-stratification, appears to be undirectional. Nodular and disseminated pyrite present, glauconite abundant. Gradational upper contact, lower contact not observed.

6-23-7-3W4M

(1430.8 - 1434.0m)
Lithofacies 4: Ribbon sediment-light colour. Silt-V.F. grained sublitharenite; framework constituents 65-85% - very light grey, wavy to irregularly interlaminated with mudstone-light grey. Additionally contains centimetre-scale M. grained sand stringers. Low burrow density, predominantly Chondrites, where present; minor small scale, low-angle trough cross-stratification, reactivation usrfaces observed. Siderite and glauconite present. Upper contact not observed, lower contact unclear.

(1434.0 - 1446m)
Lithofacies 3: Ribbon sediment-dark colour. Silt-V.F. grained sublitharenite. Framework constituents decreasing downsection 70%-40% - very light grey. Irregularly interlaminated with an organic-rich mudstone, grey black to black; containing also centimetre-scale M. grained sand stringers, often loaded into the ribbon sediment; from 1440.5 to 1442 metres, zone of predominantly coarser sand (Facies 6). Moderate to high burrow density, abundant bioturbation zones (predominantly Chondrites); minor small scale low-angle cross-stratification; nodular and disseminated pyrite; glauconite abundant, often upper contact, lower contact not observed.

2-21-8-16W4M

(980.8 - 984.3m)
Lithofacies 5: Sandstone. V.F.-M. grained litharenite. Light grey to buff with abundant silt and matrix mud, as well as, silty/argillaceous zones (10-15cm thicknesses). Very carbonaceous. Predominantly massively bedded, coarsening upwards lithofacies; minor soft sediment deformation, carbonized rootlets towards the top, clay clasts observed lower in the unit. Minor authigenic siderite. Contacts do not appear to be present.

6-1-8-4W4M

(1261.0 - 1261.3m)
Lithofacies 4: Ribbon sediment-light colour. Silt-V.F. grained sublitharenite; framework constituents 75-85% - very light grey, wavy to irregulaly interlaminated with mudstone-light grey. Additionally contains centimetre-scale M. grained sand stringers. Moderate burrowing, predominantly Chondrites, minor bioturbation zones. Erosional upper contact, lower contact gradational.

(1261.3 - 1262.2m)
Lithofacies 3: Ribbon sediment-dark colour. Silt-V.F. grained sublitharenite. Framework constituents decreasing downsection 60-45% - very light grey. Irregularly interlaminated with an organic-rich mudstone, grey black to black; containing also centimetre-scale M. grained sand stringers, often loaded into the ribbon sediment. Moderate to high burrow density (predominantly Chondrites); minor small scale low-angle cross-stratification; nodular and disseminated pyrite; glauconite abundant. Gradational upper contact, lower contact not observed.

14-20-7-16W4M

(1019.0 - 1019.7m)
Lithofacies 5: Silty-Mudstone, very carbonaceous. Predominantly massively bedded, may be rooted. Upper contact not observed, sharp lower contact.

(1019.7 - 1021.2m)
Lithofacies 4: Ribbon sediment-light colour. Silt-F. grained sublitharenite; framework constituents 65-75% - very light grey, wavy to irregularly interlaminated with mudstone-light grey, good small scale cross-stratification. Very low burrow density, minor pyrite in thin laminae towards base. Sharp upper contact, gradational lower contact.

(1021.2 - 1028.5m)
Lithofacies 1: Shale - predominantly massive. Minor silt lenses; very silty top - grey-green. Upper 2-3 metres not calcareous; becoming both calcareous and more cohesive towards the base. Gradational upper contact, lower contact not observed.

7-29-2-8W4M

(858.0 - 861.0m)
Lithofacies 4: Ribbon sediment-light colour. Silt-V.F. grained sublitharenite; framework constituents 75-85% - very light grey, wavy to irregularly interlaminated with mudstone-light grey. Additionally contains centimetre-scale M. grained sand stringers. Moderate burrowing, predominantly Chondrites, minor bioturbation zones; minor small scale, low-angle trough cross-stratification. Sideritic at top. Erosional upper contact, gradational lower contact.

(861.0 - 867.4m)
Lithofacies 3: Ribbon sediment-dark colour. Silt-V.F. grained sublatharenite. Framework constituents decreasing downsection 50-35% - very light grey. Irregularly interlaminated with an organic-rich mudstone, grey black to black; containing also centimetre-scale M. grained sand stringers, often loaded into the ribbon sediment. Low to moderate burrow density (predominantly Chondrites); excellent small scale low-angle cross-stratification; nodular and disseminated pyrite, minor siderite; glauconite abundant. Gradational upper contact, lithofacies 2 appearing in thin lenses towards base (yet base not observed).

6-36-1-10W4M

(864.8 - 871.4m)
Lithofacies 4: Ribbon sediment-light colour. Silt-V.F. grained sublitharenite; framework constituents 45-60% - very light grey, wavy to irregularly interlaminated with mudstone-light grey. Additionally contains centimetre-scale M. grained sand stringers. Low burrow density. Minor small scale, low-angle trough cross-stratification. Sideritic near top, glauconite increases downsection. Upper contact not observed, mud laminae darkening downsection, yet lower contact not present.

6-1-4-9W4M

(878.5 - 884.1m)
Lithofacies 4: Ribbon sediment-light colour. Silt-V.F. grained sublitharenite; framework constituents 40-80% - very light grey, wavy to irregularly interlaminated with mudstone-light grey. Additionally contains centimetre-scale M. grained sand stringers. Moderate burrowing, predominantly Chondrites, minor bioturbation zones; minor small scale, low-angle trough cross-stratification. Sideritic at top, slightly pyritic near base. Erosional upper contact, very gradational lower contact; darkening downsection from 882.5m.

(884.1 - 887.0m)
Lithofacies 3: Ribbon sediment-dark colour. Silt-V.F. grained sublitharenite. Framework constituents increasing downsection 40-55% - very light grey. Irregularly interlaminated with an organic-rich mudstone, grey black to black, containing also centimetre-scale M. grained sand stringers, often loaded into the ribbon sediment, greater percentage of sand stringers towards base conc. at 886m. Moderate to high burrow density (predominantly Chondrites); increasing markedly downsection, closely related to sand in flux. Minor small scale low-angle cross-stratification; nodular and disseminated pyrite; glauconite abundant. Gradational upper contact, lower contact not observed.